# THE REGENERATION OF DEACTIVATED HYDROTREATING CATALYSTS

*BY*

**MEENA ABDUL-NABI MARAFI**

**Master of Philosophy**

M.Phil.

**THE UNIVERSITY OF ASTON IN BIRMINGHAM**

**1988**

The University of Aston in Birmingham

# REGENERATION OF DEACTIVATED HYDROTREATING CATALYSTS

Meena Abdul-Nabi Marafi

Master of Philosophy 1988

## SUMMARY

The literature relating to the characterization of hydroprocessing catalysts, their deactivation due to deposition of metal contaminant (mainly Ni and V salts), and regeneration processes has been reviewed.

Leaching of spent atmospheric residue hydrodesulphurization (ARDS) catalysts and of pure metal sulphides using oxalic, malonic or acetic acid was studied experimentally. The influence of promoters, was investigated. A comparitive study was made of the selectivity of V removal from pure metal sulphides, and from spent catalyst samples. Catalysts were characterised using X-ray diffraction (XRD), electron microprobe analysis, elemental analysis by ICAP spectroscopy, surface area and porosity measurements and activity tests.

Deposition of large concentrations of metals (15% V and 4% Ni) on the catalyst surface, associated with a considerable loss of surface area (from 203 to 44 $m^2/g$) and pore volume (from 0.7 to 0.14 ml/g) led to catalyst deactivation. Fresh catalyst had a large proportion of the pore volume distributed mainly in two ranges of pore diameter, 60-150 Å and > 10000 Å. In spent catalyst the majority of pores were narrowed and plugged by the deposits and the concentration of vanadium sulphides deposits was highest near the exterior surface and a minimum at the center of the pellet.

An increase in temperature in the range 25°C to 75°C increased the extent of leaching. The order of efficiency of the acids for V extraction was oxalic acid > malonic acid > acetic acid. The selectivity of the reagents for metals removal depended upon the stability constant of complex formation and the ionization constant of the acid. Acid concentration in the range 0.33 to 1 M had little effect on the degree of metals leaching but extraction was more effective when aluminium nitrate was added. Selected alternative salts, did not enhance leaching activity. The kinetics of leaching of pure metal sulphides by oxalic acid appeared to be controlled by a chemical reaction, the rate determining step being the formation of metal ions from sulphides. Conversely with spent catalyst, mass transfer in the carbon matrix deposits appeared to be rate controlling. Build-up of a passivating layer of product was observed after some leaching; subsequent leaching was dictated by the slow removal of this film followed by relatively fast attack on exposed sulphides.

Metals leaching resulted in substantial increases in the surface area and pore volume of the catalysts. A significant improvement of HDS activity (up to 83% of that for the fresh catalyst) followed metals leaching although carbon deposits were retained. Thus catalyst is deactivated primarily by blocking of the pores and by fouling of the surface by contaminant metals.

Key words: Hydrotreating Catalyst Rejuvenation
Metal Sulphides Leaching

*DEDICATED*

*TO*

*MY BELOVED COUNTRY, KUWAIT*

*MY FAMILY*

*AND*

*MY BEAUTIFUL CHILDREN*

*TARIK AND MONA*

# ACKNOWLEDGEMENTS

I wish to express my deepest thanks to Dr. C. J. Mumford, Dr. A. Stanislaus and Professor M. A. Fahim for their help and supervision throughout this study.

I also wish to express my appreciation to Dr. Saed Akashah for initiating this work and for his continuous encouragement, and also a special thanks to Professor D. L. Trimm for his valuable comments.

The author thanks the Central Analytical Laboratory and the Catalysis group at KISR.

Special thanks to my friend Ms. Huda Al-Zaid for her valuable instruction in computing.

CONTENTS

# LIST OF TABLES

# LIST OF FIGURES

## 1.0 INTRODUCTION

Catalysts are widely used in different petroleum refinery processes such as hydrotreating, reforming, catalytic cracking, hydrocracking etc. One of the most important roles that catalysts play is in the up-grading of heavy oil and residue to more valuable and economic products. Although the major components of petroleum are hydrocarbons, other substances exist in small quantities. These include molecules contained nitrogen, sulfur, copper and parts per million (ppm) of metallo-organic compounds such as vanadium, arsenic and nickel. Sulphur, nitrogen and metals are undesirable in refinery operations because of their corrosive and poisonous effect. Hydrotreating processes such as hydrodesulphurization, hydrodenitrogenetion, hydroxygenation and hydrodemetallization are widely used to remove the undesirable elements.

The catalysts most commonly used in hydrotreating processes are derived from alumina-supported sulphides of cobalt-molybdenum or nickel-molybdenum. However, catalysts used in such petroleum refining processes will lose catalytic activity with time due to various causes, such as fouling resulting from the deposition of carbonaceous deposits on the active sites of catalyst surfaces and deposits of heavy metals from the feedstock (such as nickel and vanadium) on the catalyst pellets, thereby reducing the effective surface area and pore size for catalytic activity. Poisoning and sintering are another cause of catalyst deactivation: the former is caused by strong chemisorption of reactants, products or impurities on the active catalytic sites. Sintering on the other hand results from decreasing catalyst surface area and porosity, usually favoured by high temperature. High temperature may also lead to changes in the phase transformation of catalytic components and the support.

Catalyst deactivation is seen to be a complex problem and undesirable. Accordingly regeneration or replacement of catalysts will be required. Regeneration is possible only if deactivation is a reversible process. Thus, coked and metal-deposited catalysts could be regenerated while poisoned or sintered catalysts may have to be rejected.

Disposal of the deactivated catalysts presents serious problems. As mentioned earlier most hydrotreating catalysts contain catalytically active transition metals and accumulated poisons such as nickel or vanadium salts. Dumping of such material may lead to environmentally unacceptable leaching of metals from the catalysts, while metals recovery may be uneconomic. Often it is more desirable to regenerate the spent catalyst for re-use.

As deactivation of catalyst is considered a serious problem worldwide, Kuwait refineries also suffer from this problem; in hydroprocessing refineries the amount of catalyst consumed is reported to be about 7000 ton/year. So regeneration processes can be shown to be economically feasible by a simple analysis; if only 25% of spent catalyst is regenerated, 1,750 ton will be reused. At a price of $5.00/kg of catalyst, there are potential annual savings of $8,750,000.

Different methods have been proposed for catalyst regeneration. Coke may be removed by reaction with steam and/or oxygen

$$C + O_2 \longrightarrow CO_2$$

$$C + H_2O \longrightarrow CO + H_2$$

Another proposed approach is to selectively remove the contaminated metals such as vanadium and nickel by chemical techniques (132-135). This method is not yet well-developed and requires more study.

The present study is mainly concerned with the regeneration of deactivated hydrodesulphurization catalyst used at Kuwait National Petroleum Company by selectively removing the undesirable metal deposits using chemical treatment techniques. Although a few processes for the removal of metal and coke deposits have been reported in patents, information on selective removal of these deposits have yet to be published. The present research program therefore involved studies on the kinetics and mechanisms of metal removal from spent catalysts together with the characterization of the physico-chemical properties of the spent and treated samples. The main objective was to be able to propose possible regeneration procedures based upon the assessment of catalyst properties.

Several workers have attempted to regenerate/rejuvenate the metals-fouled spent residue hydroprocessing catalysts by selective removal of vanadium by chemical treatment, using different acids such as oxalic acid, citric acid, and oxalic acid with promoters such as aluminium nitrate. As a result the main program concentrated on metals recovery by selective leaching using oxalic acid, malonic acid or acetic acid both with, and without, promoter. A comparative study of these reagents was initiated, based on the amount of metal leached, and the nature of metal leached.

## 2.0 THE ROLE OF CATALYSTS IN PETROLEUM REFINING

Catalysts are used extensively in the refining of petroleum crude oils. Figure 2.1 shows the various catalytic units in a modern refinery. Crude oils are complex mixtures, mostly of hydrocarbons which range from associated gases up to non-distillable residue. The first refinery operation is distillation which is carried out to separate the crude oil into different boiling range fractions typically shown in Table 2.1.

Table 2.1. Boiling Ranges of Typical Crude Oil Fractions

| Fraction | ASTM Boiling Range (°C) |
|---|---|
| Butanes and lighter | |
| Light straight-run gasoline (LSR) | 32.2 - 104.4 |
| Naphtha (heavy straight-run gasoline) | 82.0 - 204 |
| Kerosine | 176.6 - 282 |
| Light gas oil (LGO) | 215.5 - 338 |
| Atmospheric gas oil | 288.0 - 443 |
| Vacuum gas oil (VGO) | 398.8 - 565.5 |
| Vacuum reduced crude | 538 and above |

The distillation products are further refined to yield the desired products by catalytic processes such as hydrotreating, isomerization, reforming, catalytic cracking, hydrocracking, etc. Figure 2.1.

Heavy oils and residues which have low economic values are upgraded by conversion into lighter products such as transportation fuels (gasoline, kerosene, diesel, etc.) and petrochemical feedstocks. Catalytic processes such as hydrotreating, hydrocracking, catalytic cracking, etc. have been widely used to remove undesirable elements such as S, N and metals (Ni and V) from the residue and to convert them to valuable lighter products Table 2.2.

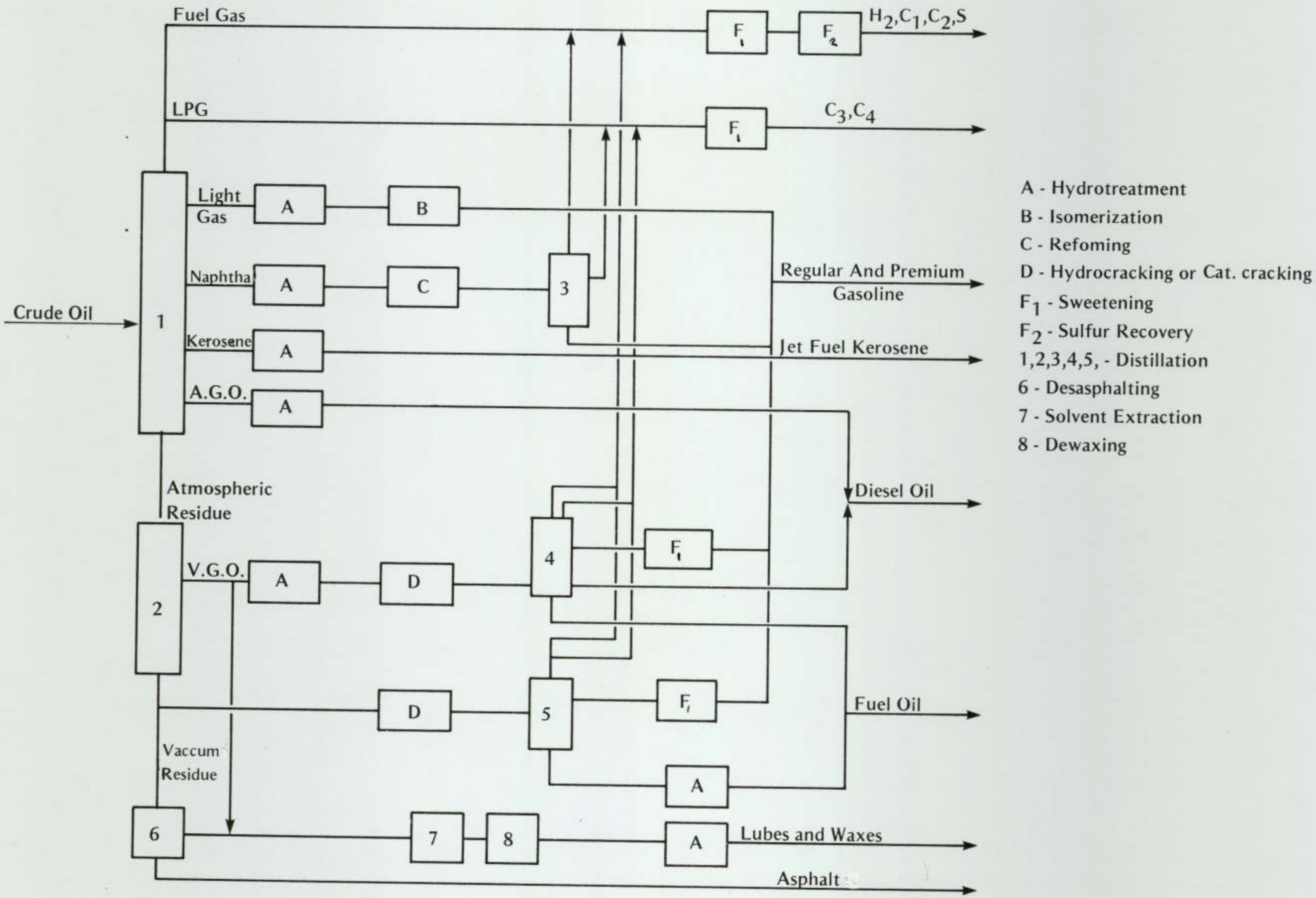

Figure 2.1. Catalytic units in a refinery scheme

Table 2.2. Catalysts Used in Various Refinery Processes

| Process | Reason for Operation | Catalyst |
|---|---|---|
| Cat-reforming | To increase octane in gasoline | Pt on $Al_2O_3$<br>Pt-Re on $Al_2O_3$ |
| Cat-cracking | To convert large petroleum molecules into smaller hydrocarbon mainly for high octane gasoline | Silica alumina<br>Zeolite |
| Hydrotreating | To remove S, N and metals and to produce valuable lighter products | $Co\text{-}Mo\text{-}Al_2O_3$<br>$Ni\text{-}Mo\text{-}Al_2O_3$ |
| Isomerization | To increase the quality and the quantity of gasoline | Friedel Craft $AlCl_3$, HCl Pt on alumina silica or zeolite |
| Hydrocracking<br>(Hydroconversion) | To convert residual oil to high octane gasoline | $Ni\text{-}Mo\text{-}Al_2O_3$<br>$Ni\text{-}W\text{-}Al_2O_3$ |

## 2.1 Catalyst Deactivation

### 2.1.1 Introduction to Catalyst Deactivation

The catalysts used in petroleum refining processes may lose their activity with time due to poisoning, fouling, sintering, phase transformations or loss of active catalyst components through chemical reaction with the support or vapour transport. It is the purpose of this section to review briefly the causes and basic mechanisms of various modes of catalyst deactivation.

The rate of catalytic reaction can be expressed in terms of the equation:

$$\frac{dc}{dt} = k.\ s.\ (\text{concentration of adsorbed species})^{\alpha}.\ \eta$$

where k is the chemical rate constant, s is the surface area, $\alpha$ is the order of reaction and $\eta$ is the effectiveness factor. Changes in any of the factors on the right-hand side of the equation will cause changes in the rate, dc/dt, and it is easy to show how various causes of catalyst deactivation affect different factors and, as a result, reduce the rate of reaction.

Thus for example, catalyst deactivation may result from adsorption of a poison such as sulphur on metals or alkali on stoichometric acidic oxide catalysts. In this case, the nature of the catalytic surface changes and the chemical rate constant is altered. Alternatively, the catalyst may sinter, causing a loss of surface area, s, and a reduction in rate. Coke formation, or the deposition of any unreactive material on the surface masks the surface (and reduces the concentration of adsorbed species) and also blocks pores, reducing surface area and increasing resistance to mass transfer (decreased values of $\eta$). Although the net effect is the same i.e., the rate is reduced, the causes of deactivation obviously differ and may, or may not, be minimized or reversed. Therefore, it is necessary to consider various modes of catalyst deactivation as separate effects which may, or may not, be related.

### 2.1.2 Poisoning

Catalyst poisoning is one of the most severe problems associated with the commercial application of catalyst. Poisoning involves the strong chemisorption of reactants, products or impurities on the active catalytic sites. A poison blocks the active sites as a result of very strong adsorption (1). Catalyst poisons tend to be selective, i.e., a certain species may be a poison in some reactions but not in others, depending on its adsorption strength relative to that of other species which compete for catalytic sites. Some of the most severe poisoning encountered in catalytic systems is that induced by sulphur, nitrogen or metals on metal catalysts. Sulphur apparently bonds so strongly to metal surfaces that the presence of only ppm quantities of sulphur contaminants in the feed is significant. Because of the essentially irreversible adsorption of sulphur compounds on metal, regeneration is usually impossible. Sulphur compounds include $H_2S$, $CS_2$, MeSH, $Et_2SH$, $Me_2S$, EtS, thiophene, COS, $SO_2$ and $SO_3$.

In general, catalyst poisons can be classified according to chemical species, the types of reaction poisoned, and the selectivity for active catalyst sites. For example, organic bases and ammonia are poisons for acidic oxide catalysts used in cracking and hydrocracking reactions; sulphur and arsenic compounds are poisons for metals (e.g., Pt, Ni) in hydrogenation, dehydrogenation and steam reforming reactions (2). A selective poisoning process is one that initially poisons the most active sites.

### 2.1.3 Fouling

Fouling involves physical deposition of species from the fluid or gas phase on the catalyst surface resulting in blockage of reaction sites or pores. Deposition of coke or carbon on porous catalysts is considered as fouling. The coke covers the active surface and reduces the contact between the reactants and the catalytic sites and reduces the reaction rate. The mechanisms of carbon and of coke deposition on catalysts have been detailed in several reviews (3, 4).

Coke is a general term which describes carbonaceous deposits on catalysts. These can include high molecular weight polycyclic aromatics and carbons, which may be formed in the gas phase or on a surface. Coke deposition on catalysts is a complex process affected by several factors. The net accumulation of coke is usually a balance between coke formation, which occurs as a result of adsorption, dehydrogenation and polymerization of carboneous residues, and coke removal which occurs from gasification. The balance depends on the operating conditions and on the nature of the catalyst. Possible routes of carbon formation are shown in Figure 2.2. Coke accumulation can be minimized by adjusting reaction conditions, or mass and heat transfer effects and controlling the catalyst chemistry.

Deposition of metal sulphides on the catalyst pores during hydroprocessing of heavy residues is also an example of fouling. The heavy residues contain high concentrations of large-sized (M.Wt. 20,000 g/mole), organometallic compounds of e.g. vanadium or nickel present predominantly in the asphaltenes, which decompose by hydrodemetallization (HDM) reactions during hydroprocessing to give metal sulphides and hydrocarbons. Due to diffusion limitations the metal sulphides tend to concentrate on the outer edges of the catalyst pellets and particularly in the pore mouths of the catalyst. Deposition of metal sulphides in large amounts at the pore mouths plugs the pores and physically restricts access of the reactant molecules to the active sites on the catalyst surface within the pores. As a result it leads to catalyst deactivation (5). Extensive fouling by coke and metal deposition may also plug the reactor void space and result in high pressure drop across the catalyst bed.

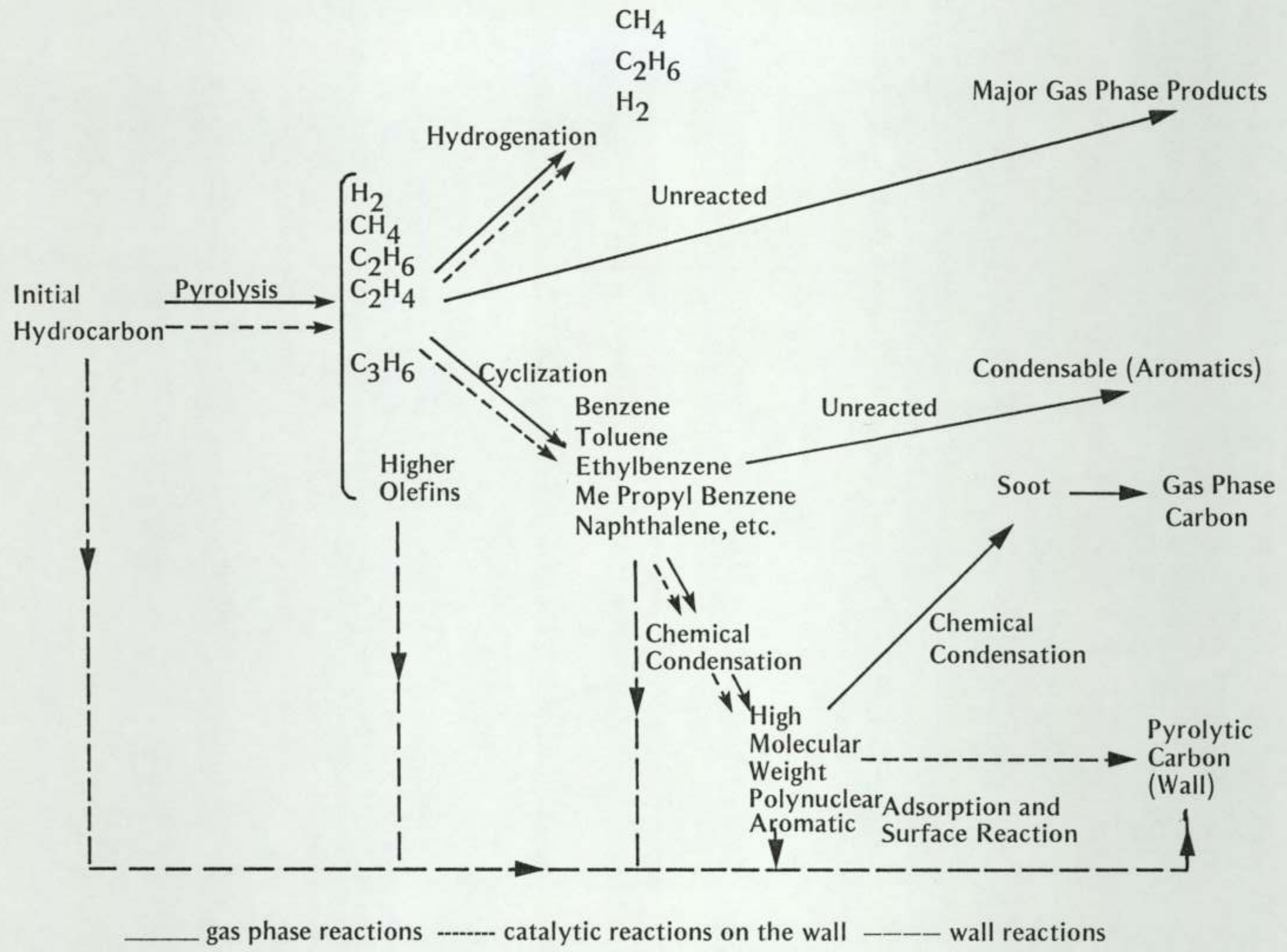

Figure 2.2. Possible routes of carbon formation.

### 2.1.4 Sintering

Sintering is a major factor determining catalyst life, since it involves loss of surface area and porosity that can be reversed only with considerable difficulty - if at all. It arises because, in order to obtain maximum gas - solid contact, catalysts are usually prepared with high surface areas. Thus, there is always a thermodynamic driving force to minimise surface free energy, a force resisted only by an activation barrier. As the temperature increases, this barrier is overcome, and the catalyst sinters.

The mechanism of sintering can differ widely. As the temperature of the solid increases, atoms on the surface first become mobile (surface diffusion). This leads to the smoothing of very unstable surfaces and to the development of faceted or spherical particles, a process which may be enhanced by the gases present. Huttig (6) proposed that in theory surface diffusion - related sintering should become important at about one-third of the melting point of the solid, a prediction which has been borne out by some experimental measurements. However the influence of gases, or of trace impurities in the surface, can have a major effect on the temperature at which sintering starts (7, 8).

At higher temperatures, volume diffusion of material starts to become important, and gross changes in the structure of the solid can occur. Eventually, and usually at very high temperatures, evaporation-condensation processes can also lead to gross sintering or to loss of solid.

Some success has been achieved in stablising materials against sintering by the addition of small amounts of a second component. For example in the case of alumina sintering can be enhanced, or inhibited, by the addition of small ($\leqq$ 3 wt%) amounts of appropriate additives (9). The addition of metal, necessarily present as the catalyst, retards sintering slightly in small amounts and enhances sintering in higher amounts. The addition of very small amounts (ca 0.1 wt %) of rare earth oxides (either Ce, Nd, Sm, Eu, Dy, Er, Y or Yb) was found to affect the temperature at which sintering occurred without deleterious effects on the catalytic activity. The mode of action of these stabilising oxides or of the metals is often open to considerable question.

The sintering of metals on a support is a process of particular industrial importance, and considerable attention has been devoted to establishing empirical relationships and models which describe the process (10). Two mechanisms have been advanced for metal sintering in supported metal catalysts.

- Crystallite migration: Entire metal crystallites move over the support surface, collide and coalesce.
- Atomic migration: Metal atoms detach from the crystallites, migrate over the surface and are captured by larger crystallites.

Crystallite migration is important in the early stages of sintering, where crystallites are small. Atomic migration becomes important and influences sintering at higher temperatures in the later stages where the crystallites are larger.

Sintering of catalysts and supports is clearly very undesirable, since it is usually very difficult or impossible to reverse. As a result, there is considerable interest in the prevention of sintering. The obvious way to do this is to keep the temperature low, (less than 500°C) and particular care should be taken if the catalyst is to be regenerated by burning-off coke deposits.

### 2.1.5 Phase Transformations and Solid State Reactions

Migration of atoms in a crystal lattice can also result in changes of phase. Thus, in the case of alumina it is well known that various crystal forms can exist, even though the alpha phase is thermodynamically most stable. As a result, as temperature is increased, phase changes occur, and Gitzen (9) has produced a very useful guide to the temperature stability of the various phases. That these phase changes result in a loss of surface area and porosity is obvious from the dimensions of the unit cells of the crystal forms, Table 2.3.

High temperatures can also cause interaction between the catalyst components and the support leading to the transformation of the active catalytic phases to non-catalytic ones (11). For example in alumina based steam reforming catalysts, reaction between nickel oxide and the alumina support can occur under reforming conditions resulting in the formation of nickel aluminate spinel (12).

$$NiO + Al_2O_3 \text{ -----> } Ni\,Al_2O_4$$

Table 2.3. Unit Cell Dimensions of Alumina Phases

| Alumina | Crystallinity | a(Å) | b(Å) | c(Å) |
|---|---|---|---|---|
| η | Cubic | 7.90 | | |
| θ | Monoclinic | 5.62 | 2.86 | 11.74 |
| γ | Cubic | 7.90 | | |
| δ | Tetragonal | 7.96 | 7.96 | 11.74 |
| α | Rhombohedral-hexagonal | 5.13 | | |

Nickel bound in nickel aluminate spinel does not contribute to catalyst activity; consequently, the activity of the catalyst declines. In alumina based cobalt-molybdenum or nickel-molybdenum hydrotreating catalysts the reaction between $MoO_3$ and $Al_2O_3$ can occur, resulting in the formation of a catalytically inactive aluminium molybdate phase.

Another thermal effect is the volatilization of the catalytic materials. In hydrotreating catalysts, loss of active molybdena phase has been observed on heating at temperatures above 700°C (13). Loss of catalytic metals is also possible through formation of compounds such as carbonyls, sulphides, halides, etc. in environments containing Co, $H_2S$, HCl or halogens.

Catalyst deactivation is clearly a complex problem which may result from many causes. Deactivation may be reversible or irreversible. Catalyst sintering, for example, is irreversible, whereas deactivation by coke formation can be reversed by gasification of the coke. Care must be taken to avoid high temperatures during carbon combustion regeneration. Catalyst foulants involving metal deposits are usually difficult to remove. In general, the nature of deactivation and regeneration depends on the individual process. In Chapter 4 the nature of deactivation of catalysts used in the hydroprocessing of heavy residues and the problems associated with the regeneration of the deactivated catalysts are reviewed in detail.

## 2.2 Catalyst Regeneration

Catalyst deactivation is undesirable but, despite careful process control to prevent it, a catalyst inevitably loses activity with time. The deactivated catalysts can be regenerated in some processes. Regeneration is possible only if the deactivation is a reversible type. For example, formations of coke or carbon are fairly easily removed by gasification with oxygen, steam, carbon dioxide or hydrogen (14).

$$C + O_2 \longrightarrow CO_2$$
$$C + H_2O \longrightarrow CO + H_2$$
$$C + CO_2 \longrightarrow 2CO$$
$$C + 2H_2 \longrightarrow CH_4$$

The rate of gasification depends strongly on the structure of the carbon and on the degree of contact between carbon and the catalyst.

Sintering, on the other hand, is generally irreversible, though certain noble metal catalysts (e.g., $Pt/Al_2O_3$) can be redispersed.

Regeneration of catalysts deactivated by poisoning depends on the nature of the poison. For example, with sulphur poisoned Ni steam reforming catalysts it is reported that up to 80% of the surface sulphur could be removed by treatment with steam at 700°C. The following reactions occur.

$$NiS + H_2O \longrightarrow NiO + H_2S$$

$$H_2S + 2H_2O \longrightarrow SO_2 + 3H_2$$

Sulphur poisoned Pt catalysts can be regenerated by treatment with hydrogen at 400-500°C.

Catalysts deactivated by fouling by metal deposits in the pores (e.g., residue hydrotreating catalysts) are usually difficult to regenerate. Such deposited metal foulants can be removed by chemical washing, but care must be taken to avoid dissolution of support or catalytic metals during such chemical treatments. The problems associated with the regeneration of coke and metals fouled residue hydrotreating catalysts are reviewed in detail in Chapter 4. The deactivation causes and possible regeneration procedures for different types of catalysts are summarized in Table 2.4.

Table 2.4. Catalyst Deactivation Causes and Re-activation Procedures

| Catalyst | Deactivation | As a Result of | Possible Remedy |
|---|---|---|---|
| Metals | Sintering | High temperatures possibly enhanced by excessive gas flow | Redistribution may be possible. Addition of stabilizer, control of gas flow. |
| | Poisoning | Compounds of elements of Groups VB & VIB. | By oxidation or reduction. |
| | | Metals ions of 5 or more d electrons | Regeneration difficult. Change to a more poison-resistant catalyst |
| | Fouling | Coke | Burn off.<br>Adjust size of surface ensemble |
| | | Dusting/metals deposition | May be difficult to remove |
| Metal oxides (stoichiometric) | Sintering | High temperatures possibly enhanced by excessive gas flow | Addition of stabilizers<br>Control of gas flow. |
| | Poisoning | Alkali | Re-acidification |
| | Fouling | Coke | Burn-off |
| | | Metals (e.g., Ni) | Add a metal passivator |
| | | Metal deposits | Difficult to remove |
| Metal oxides (non-stolchiometric) | Sintering | High temperatures | Add stabilizers |
| | Poisoning | Valency stabilizing poison | May be difficult to regenerate |
| | Fouling | Less likely | Oxidation of coke<br>Inorganic foulants may be difficult to remove. |

# 3.0 RESIDUE UPGRADING

## 3.1 Introduction

Upgrading of heavy petroleum oils and residues to more valuable lighter products, such as transportation fuels and petrochemical feedstocks, has attracted increased attention world-wide. Several factors have contributed to the necessity for heavy residue conversion. These include economic and environmental pressures. The demand for heavy fuel oils has declined whilst the transportation fuels and petrochemical feedstocks are in increasing market demand. The heavy feedstocks contain high concentrations of metals (Ni and V) and asphaltenes which pose severe catalyst deactivation problems.

## 3.2 Established Technologies for Residue Upgrading

A range of processes has been developed and commercialized for residual oil upgrading. Available technologies have been reported in several papers and reviews (15-20). In general, residue conversion can be described as a reduction in molecular weight by cracking the heavy molecules and an increase of the H/C ratio. Two different ways are commonly used to increase the hydrogen to carbon (H/C) ratio: (a) the carbon rejection technology (b) the hydrogen addition process. A list of the available technologies is presented in Table 3.1.

Table 3.1. Residue Upgrading Technologies

| Non Catalytic | | Catalytic | |
|---|---|---|---|
| C. Rejection Process | Reference | H. Addition Process | Reference |
| Visbreaking | (21-24) | Gulf-HDS | (39, 40) |
| | | Shell-HDM/HDS | (41) |
| Delayed coking | (25-27) | Chevron-RDS | (42, 43) |
| Deasphalting | (28-31) | Exxon-Residi-fining | (44) |
| Fluid coking | (32) | UOP-RCD Unibon | (45, 46) |
| Flexicoking | (33) | Union Oil Unicracking HDS | (47, 48) |
| Heavy Oil Cracking (HOC) | (34-35) | IFP-BASF | (27, 49) |
| | | Haldor-Topsoe | (50) |
| | | Dynacracking | (53) |
| Asphalt Residual Treatment (ART) | (36-38) | H-Oil | (51, 52) |
| | | LC-fining | (54, 55) |
| | | UOP-Aurabon | (56, 57) |
| | | CANMET | (58, 59) |
| | | M-coke | (60) |

## Carbon Rejection Technology

The carbon rejection processes are predominantly thermal and non-catalytic. They involve the breakdown of molecules into a complete range of products from solid to gas by heat in the absence of catalyst or externally added hydrogen. The thermal cracking operations are strongly dependent upon feed stock properties, cracking temperature and residence time. Features of the most important thermal processes are summarised below:

### Delayed Coking

Delayed coking is one of the best established processes for heavy residue upgrading. It is a low-pressure (2-3 bars) thermal process in which the feedstock is raised to a temperature above its coking point (400-500°C) and introduced into a coking drum in which the coke and vapor are formed.

### Flexicoking

This is an integrated fluid coking and coke gasification process which converts heavy feed stocks to 99% of fuel gas, naphtha, middle distillates, heavy gas oil and a low sulfur coke gas (61). A fluidized bed reactor is used and temperature is raised to 550°C at atmospheric pressure to crack the heavy residue to vaporized products and coke. The coke is then reacted with steam and oxygen to form coke-gas rich in hydrogen and carbon oxides.

### Visbreaking

This process involves a mild thermal cracking of heavy residue to produce middle distillates and a stable heavy fuel oil (62). The feed is raised to a temperature between 450-490°C and subjected to residence times in the range of minutes. Operating pressures can be as high as 50 atm. for liquid phase visbreaking and as low as 7 atm. for partial vaporization. Two basic types of reactor are used (63), coil reactors and soaking-drum reactors. However, the severity of operation is highly dependent on the nature of the charged stocks and the product specification. The principles of the hydrotreating processes and the types of catalyst used are reviewed in the following section.

## 3.3 Hydrogen Addition Technology: Hydrotreating Processes

Hydrotreating processes usually involve contacting the petroleum feed stocks with hydrogen in the presence of a suitable catalyst under specific operating conditions to remove impurities such as S, N, O and metals (Ni, V, etc.) and/or to effect conversion to lower molecular weight hydrocarbons. These processes are considered the dominant product line up-grading processes, as they are capable of removing metals (V, Ni), sulphur, nitrogen and asphaltenes by a series of processes such as hydrodesulphurization, hydrodemetalization, hydrodenitrogenation and hydocracking. All the processes operate in the presence of hydrogen and may occur simultaneously.

## Hydrodesulphurization

The most important hydroprocessing application is the hydrodesulphurization process which involves reactions leading to removal of sulfur from petroleum compounds by their conversion into $H_2S$ and hydrocarbon products. Typical operating conditions for commercial HDS units are shown in Table 3.2. Hydrodesulphurization catalysts are usually composed of (64) a mixture of transition-metal compounds (Co-Mo, Ni-Mo, Co-W and/or Ni-W) on an alumina carrier. The catalysts are produced in the oxide form and are sulphided before, or during, use in the reactor (65).

Table 3.2. Typical Operating Conditions for Commercial HDS Units

| | Distillates | Residuals |
|---|---|---|
| Temperature, °C | 300-400 | 340-425 |
| Pressure, atm. | 35-75 | 55-170 |
| LHSV, vol F/vol cat-hr | 2-10 | 0.2-1 |
| $H_2$ recycle rate, scf/bbl | 300-2,000 | 2,000-10,000 |
| Catalyst life, years | 10 | 0.5-1 |

Some sulphur containing compounds present in petroleum fractions are shown in Table 3.3.

Table 3.3. Some sulfur-containing compounds in petroleum

| Compound Class | Structure |
|---|---|
| Thiols (mercaptans) | RSH |
| Disulfides | $RSSR'$ |
| Sulfides | $RSR'$ |
| Thiophenes |  , 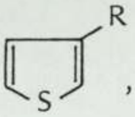 , etc. |
| Benzothiophenes | 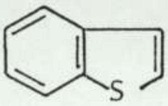 , 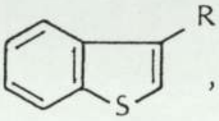 , etc. |
| Dibenzothiophenes | 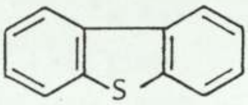 , 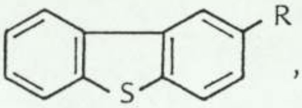 , etc. |
| Benzonaphthothiophenes | 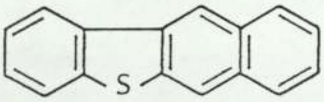 , 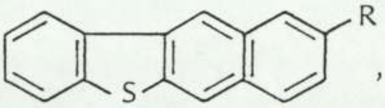 , etc. |
| Benzo dibenzothiophenes | 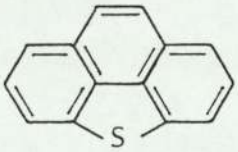 , 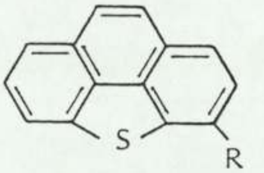 , etc. |

It has been shown that the thiols are more reactive than the compounds in the class of thiophenes.

The most important classes of reactions occurring in hydrodesulphurization processes (64) are.

### 1 – Hydrodesulphurization:

Mercaptans $RSH + H_2 \longrightarrow RH + H_2S$

Sulphides $R_4SR_2 + H_2 \longrightarrow R_4H + R_2H + H_2S$

Disulphides $R_4SSR_2 + H_2 \longrightarrow R_4H + R_2H + 2H_2S$

Thiophenes

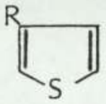

$+ 4H_2 \longrightarrow RCH(CH_3)\ CH_2CH_3 + H_2S$

Benzothiophenes

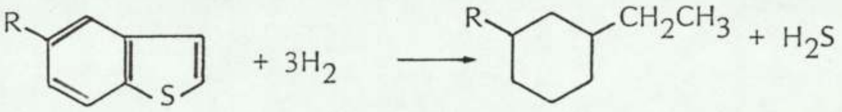

### Hydrodemetallization

Nickel and vanadium are the major metals usually found in petroleum residues (66). They are mainly concentrated in the asphaltenes and have complex organic structures termed porphyrins. Figure 3.1 shows two examples of Ni and V containing porphyrin-type structures. During catalytic hydrotreating the metal containing organometallic complexes are hydrogenated and cracked with the removal of the metals (often as lower molecular weight complexes) from the complex hydrocarbon structures. The metals are subsequently deposited on the catalyst surface causing catalyst deactivation by pore mouth plugging.

e.g., $RM + H_2 + nH_2S \dashrightarrow RH + MS_n$

Hydrodemetallization is influenced more by the catalyst texture than by the catalytic sites. The rate of hydrodemetallizaton reaction is limited by the rate of diffusion of the organometallic compounds through catalyst pores.

## Hydrodenitrogenation

Removal of nitrogen from petroleum streams is important, since the basic nitrogen compounds tend to poison the acidic sites of the catalysts responsible for cracking. Some examples of typical denitrogenation reactions are shown below.

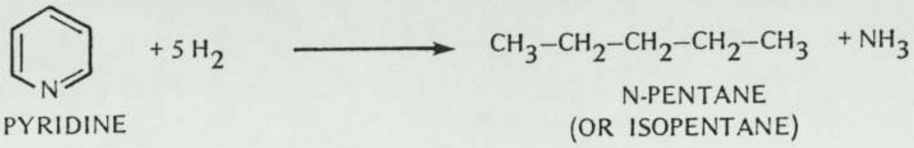

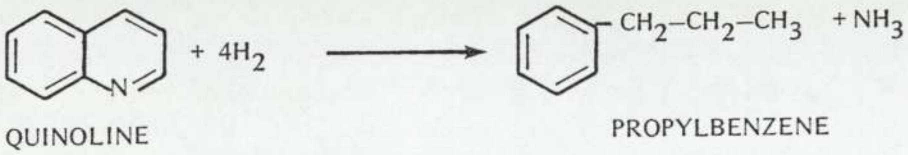

## Hydrocracking

Hydrocracking involves cracking of the large hydrocarbon molecules to lighter products followed by hydrogenation of the lighter fragments. The reaction becomes significant under severe processing conditions such as high temperature and low space velocity. One example of a hydrocracking reaction is,

$$R - CH_2 - CH_2 - R' + H_2 \text{------>} RCH_3 + R'CH_3$$

Polycyclic aromatic structures such as asphaltenes are converted to smaller molecular size products by hydrocracking reactions.

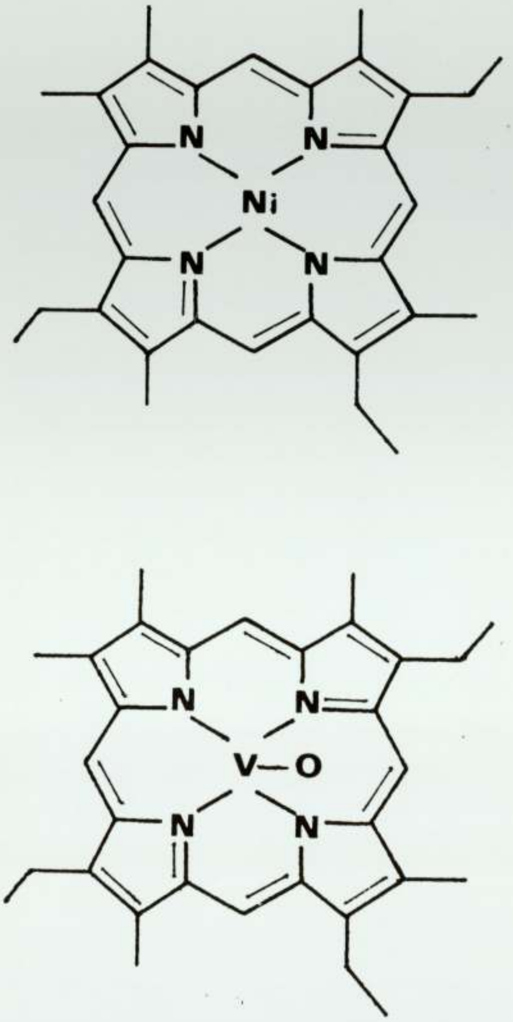

Figure 3.1. Nickel and vanadyl etioporphyrins.

Hydrogenation of Olefins and Aromatics

Examples of typical hydrogenation reactions are,

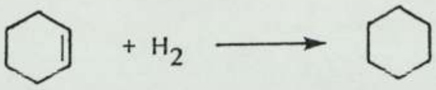

$$CH_3 - CH = CH - CH_2 - CH_3 + H_2 \longrightarrow CH_3 - CH_2 - CH_2 - CH_2 - CH_3$$

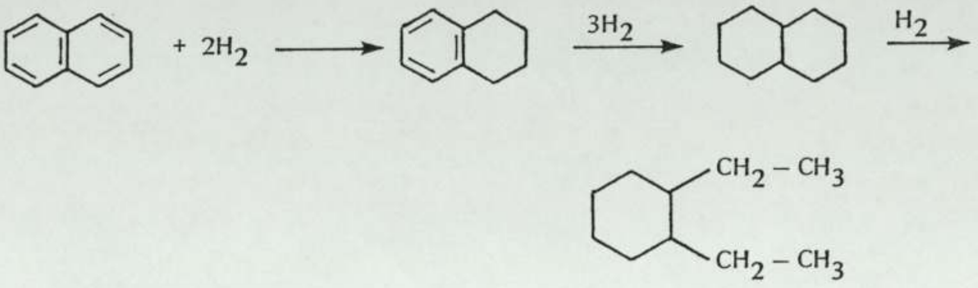

Such reactions play an important role in catalytic hydrotreating, especially in reducing coke formation by saturating the olefinic coke precursors.

Hydroprocessing (Hydrogen addition) Technologies

Several commercial reactors have been introduced for hydroprocessing (HDS, HDN, HDM, HC, etc.) of heavy residues. These include (1) fixed bed reactors, (2) trickle bed reactors, and (3) ebullating-bed reactors. The design and application of these reactors depends on the nature of feedstocks, operating conditions, catalyst types and structure, and the reactions occurring during the hydrodesulphurization processes. A simplified diagram of a fixed bed hydrodesulphurization process is shown in Figure 3.2.

Even distribution of hydrogen gas and liquid are of great importance in fixed bed or trickle bed reactors. With heavy feedstocks, bed plugging can occur in these reactor systems leading to high pressure drop across the reactor.

In ebullating bed reactors (such as in the H-Oil or the LC fining processes), catalyst particles are held in suspension by the upward velocity of the liquid feedstock and hydrogen gas. The oil, hydrogen and the catalyst are well mixed in the process. Relatively small catalyst particles can be used in this process without the pressure drop constraint of fixed bed or trickle bed reactors.

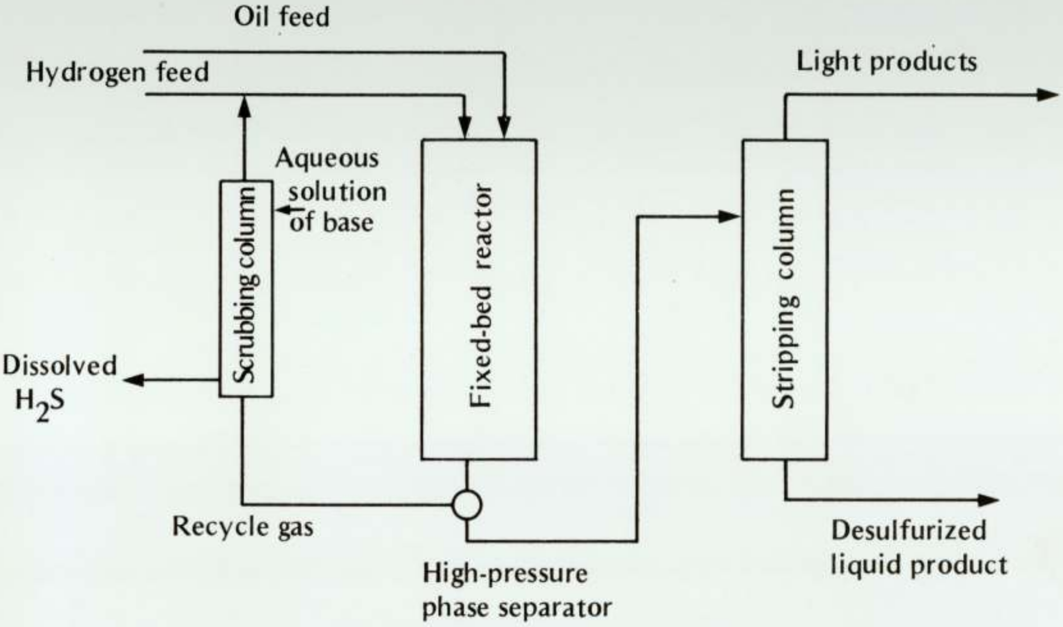

**Figure 3.2. Simplified diagram of a hydrodesulfurization process.**

Commercial processes presently available for hydroprocessing are summarized in Table 3.1. The processes licensed by companies such as Gulf, Shell, Exxon, Haldor-Topsoe, Chevron, etc. apply fixed bed trickle reactor technology. H-Oil and LC fining processes use ebullating bed reactors. CANMET, M-Coke, and VOP-Auroban processes apply slurry phase technologies.

The hydrogen addition processes have several advantages over the carbon rejection processes. In carbon rejection processes such as visbreaking, solvent deasphalting and delayed coking, a substantial part of the fuel is rejected as coke resulting in the loss of valuable liquid hydrocarbon. Production of lesser amounts of undesirable gaseous products, increased distillates in the desired boiling ranges (middle range oil), significant removal of heteroatoms (S, N, and metals), relatively high reduction of Conradson carbon and higher liquid yields are the major advantages of the hydrogen addition processes.

The use of catalysts in hydrogen addition processes (hydroprocessing) has some disadvantages. The most important of these are (1) the catalyst cost, (2) the complexity of the reactions system, and (3) the rapid rate of catalyst deactivation.

## 3.4 Hydrotreating Catalysts

### 3.4.1 Catalyst Type

Catalysts consisting of molybdenum supported on γ-alumina and promoted by cobalt or nickel (Co-Mo/$\gamma$-$Al_2O_3$ or Ni-Mo/$\gamma$-$Al_2O_3$) are commonly used for hydrotreating heavy and residual oils (67). The nickel-molybdenum system is generally agreed to be less active for hydrodesulphurization (HDS) than the Co-Mo system, though it appears to have a better activity for hydrodenitrogenation (HDN) and hydrocracking (HC) reactions (68, 69). These catalysts are manufactured by impregnation of the γ-alumina support by solutions containing the active metal ions, followed by drying and calcining. After calcining, the catalyst precursors are present in their oxidic form. Catalysts are then converted to sulphides using $H_2S$ or organo-sulphur compounds in hydrogen. Table 3.4 shows different catalysts for hydrotreating of residuums (70, 71).

### 3.4.2 Structural Features

The structural and catalytic properties of hydrotreating catalysts have been the subject of extensive investigation (72-76). These researches have yielded valuable information on the nature of active phases and the role of promoters.

In the oxidic precursor state, the Mo phase is present in 'monolayer' type structures (77) bonded via oxygen bridges to the alumina support, Figure 3.3. One picture of the oxidic form involves a layer structure in which $Mo^{6+}$ is incorporated in an epitaxial monolayer of $MoO_3$ (77). An additional layer of oxygen ions, termed the capping layer', is located on top of the monolayer to maintain charge neutrality. Some of the promoter (Co or Ni) remains on the surface of an oxide while a portion penetrates the bulk (78). The various species likely to be found on $Co\text{-}Mo/\gamma\text{-}Al_2O_3$ oxidic catalysts are $MoO_3$ monolayer, $CoAl_2O_4$, $CoMoO_4$, $Co_3O_4$, $Al(MoO_4)_3$ and CoMo active complex (79). A bi-layer model Figure 3.4 has been proposed by Delmon et al. (80) to describe the structure of the oxidic form of the $Co\text{-}Mo/\gamma\text{-}Al_2O_3$ system. According to this model, the Co-Mo bi-layer in the oxidic catalyst comprises a monolayer of octahedral $Co^{II}$ superimposed on a monolayer of tetrahedral $Mo^{VI}$ which is in turn bound to $\gamma\text{-}Al_2O_3$. All of the Mo in the catalyst is in the bi-layer, but part of the cobalt enters the $Al_2O_3$ lattice giving inactive $CoAl_2O_4$. Molybdenum improves the dispersion of cobalt and so facilitates entry of Co to the alumina lattice especially at calcination temperatures above 467°C (80). The HDS activities of the catalysts have been found to relate to the proportion of octahedral (Co or Ni) in the oxide form of the catalyst (81). Sulphiding the catalyst converts the oxide precursors to the active sulphide phases (e.g., $MoS_2$ and $Co_9S_8$).

Many different structural models have been proposed to describe the active phase of $Co\text{-}Mo\text{-}Al_2O_3$ and related catalysts in the operating sulphided catalyst. Some of the models most often referred to are:

i) the "monolayer model" (67, 77);

ii) the contact synergy model (73, 82, 83);

iii) the intercalation model (84-85).

The monolayer model is simply an extension of the monolayer theory outlined above for the precursor oxide phases, in which the oxygen ions of the capping layer are replaced by sulphur ions. In the contact synergy

Table 3.4. Different Catalysts Used for Hydrotreating Residue

| Firm | Preferred Metals | $SiO_2$ % wt on Si, Al, and other Components | Catalyst bulk density, g/cc | Average pore volume, cc/g | Pore diameter, Å | Specific surface, $m^2/g$ |
|---|---|---|---|---|---|---|
| **Catalysts for Hydrotreating of Residuums** | | | | | | |
| Esso | Ni + Mo or Co + Mo | 1-6 | <0.70 | >0.25 | Mainly 30-70 | >150 |
| UOP | Ni + Mo | 2-60 | 0.4-0.9 | <0.15 | 40-150 | 100-300 |
| Standard Oil of Indiana | CoMo | Prefer 1-10, may contain zeolites | - | >0.5 | 100-200 | 150-500. Prefer 300-350 |
| Gulf | Mo +Co + Ni | 0 | - | 0.46 | Regular distribution 0-240 Å. Average diameter 140-180 Å. | 165-220 |
| Texaco | Ni or Co + Mo or Ni + W | 2-30 | 0.5-0.7 | 0.6-0.1 | - | 300-800 |
| UOP | Ni + Mo | 10-90 | - | - | - | - |
| Shell | NiCo-WoMo | Prefer 70-90 | 0.71 | - | 90 | 292 |
| Chevron | Group VI + VII | $SiO_2$, practically no metal phosphates | - | Porosity >60% | >60 | >100 |
| Nippon Oil Co. | CoMo or NiW | No $SiO_2$ | - | 0.3 of pores >75 Å | Many pores of 1,000-50,000 Å | - |
| Hydrocarbon research | CoMo (+Ni) | 0-100 | - | 0.45-0.5 | 60-70 Å plus channels 100-1000 Å plus channels >1000 Å | 260-355 |

Table 3.4 (Cont'd)

| Firm | Preferred Metals | $SiO_2$ % wt on Si, Al, and other Components | Catalyst bulk density, g/cc | Average pore volume, cc/g | Pore diameter, Å | Specific surface, $m^2/g$ |
|---|---|---|---|---|---|---|
| | | Analysis of Commercial Samples of Catalysts | | | | |
| Girdler G-35B (G) | CoMo<br>Co 3%<br>Mo 5.6% | - | 0.96 | 0.22 | Mainly <200 Å | 270 |
| Pro Catalyse Co. (F) IFD HR 304 | CoMo<br>Co 1.76%<br>Mo 7.86% | - | 0.5 | 0.78 | Regular distribution up to 5000 Å plus larger pores | 283 |
| Davison Chemical Co. (N) NiCoMo-I | NiCoMo<br>Ni 0.34%<br>Co 0.65%<br>Mo 8.0% | - | 0.64 | 0.39 | Peak at 250 Å | 222 |

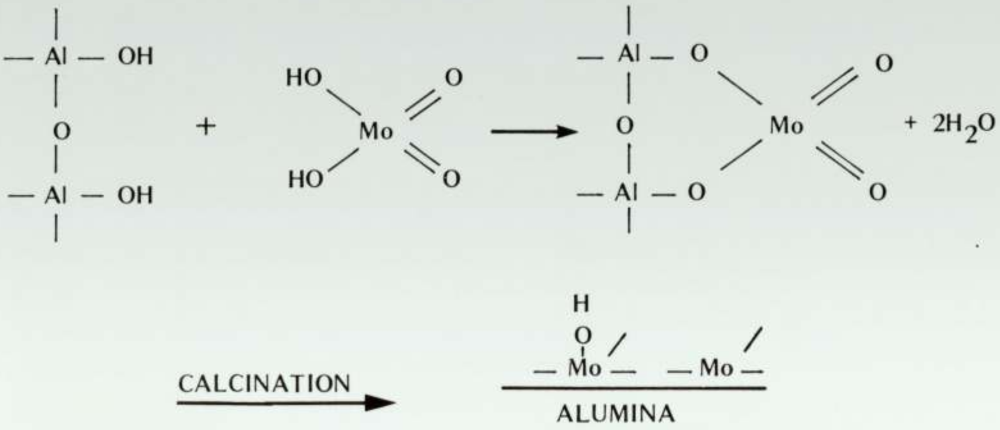

Figure 3.3. Molybdate monolayer on alumina surface.

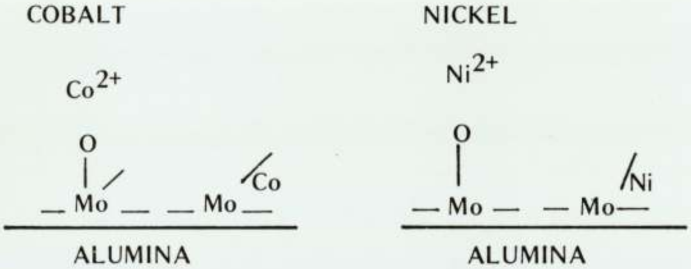

Figure 3.4. Molybdenum and promoter (Co or Ni) bilayer on alumina surface.

model the active phase consists of small, well-dispersed particles of $MoS_2$ and $Co_9S_8$ closely associated and giving rise to the phenomenon of 'contact synergy' (86). In the intercalation model, the promoter (Co or Ni) ions are considered to be intercalated at the edges of layers of $MoS_2$, giving rise to sites consisting of exposed $Mo^{+3}$ ions (84). The various models have been discussed extensively in several reviews (67, 77, 73, 74, 79, 87). There is controversy as to whether $MoS_2$ in sulphided $Co-Mo/Al_2O_3$ catalysts is in the form of discrete particles or is present as a monolayer (88, 89). In the absence of in-situ structural information on the working catalysts, it is difficult to assess the validity of the different models.

Mossbauer emission spectroscopy (MES) studies by Topsoe et al. (90, 91) have recently revealed that a portion of the cobalt promoter atoms in sulphided $Co-Mo/Al_2O_3$ catalysts may be present as a mixed Co-Mo-sulphided phase. A schematic diagram is shown in Figure 3.5. It has been observed that the formation of the Co-Mo-S phase is very sensitive to preparation parameters and the type of support (92). It has been found that the promotion of HDS activity in sulphided Co-Mo system is specifically linked to the presence of Co-Mo-S structure (90, 91). It is proposed that the Co-Mo-S structure can be regarded as a $MoS_2$-like phase with the Co atoms located at the edges (91, 93).

In addition to the research on the structural features and activity, summarised above, considerable research has also been devoted to understanding the deactivation of the hydrotreating catalysts. This is discussed in the next section.

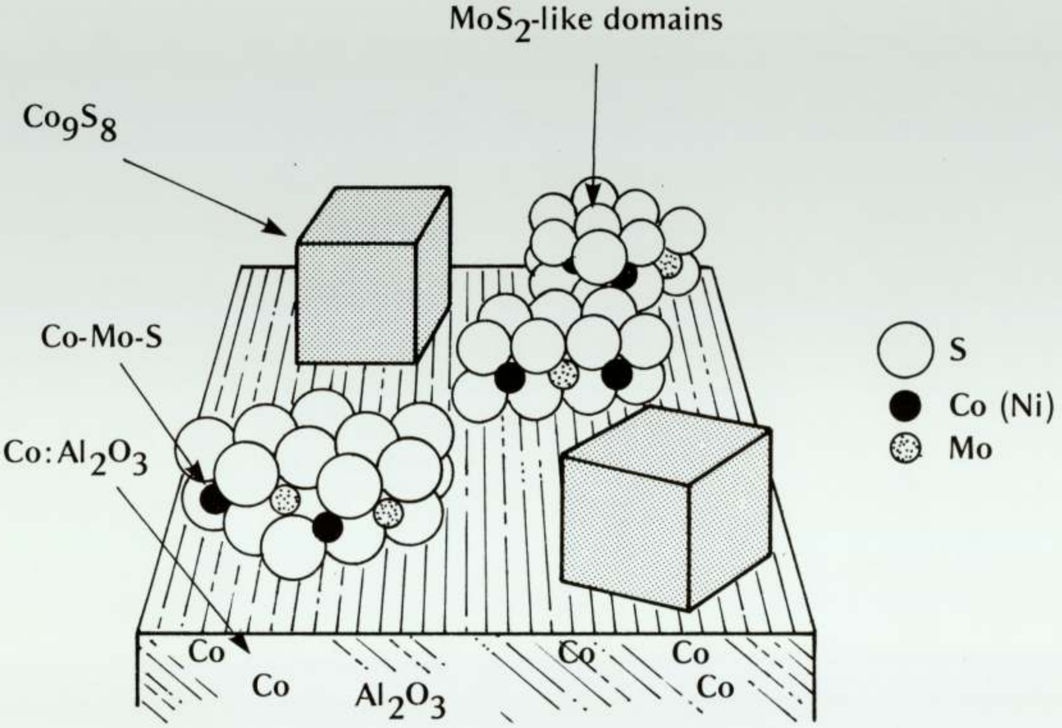

Figure 3.5. Schematic representation of the different phases present in a typical alumina-supported catalyst.

## 4.0 DEACTIVATION AND REGENERATION OF HYDROTREATING CATALYST

### 4.1 Introduction

Catalysts used in the hydroprocessing of residue deactivate rapidly and have a relatively short life ranging from 3 months to 6 months. The rate of deactivation, normally, depends on the process reactions, operating conditions and specific form of catalyst (94). Table 4.1 summarises typical catalyst lives, and factors determining these lives, for some industrial catalysts.

Deactivation is primarily caused by metal and coke deposits. Most investigators (95, 96, 97) have found that catalysts deactivation occurs in two steps: a rapid decline in activity early in the run due to coke deposition, followed by a relatively long period of constant deactivation rate caused by metals deposition. In fixed bed operation the average temperature of the reactor is normally raised to compensate for the deactivation and to hold a particular product specification constant. Eventually a pre-set end-of-run temperature is reached (usually in the range 410-450°C), when the catalyst must be regenerated or replaced. A typical temperature-time curve is shown in Figure 4.1. The plot is "S" shaped and it is almost common for deactivation of hydrotreating catalysts.

Three characteristic zones can be identified in such a plot:

- An initial period of very rapid, but continuously declining, rate of deactivation (I) attributed to coke deposition.
- An intermediate period of slower and almost constant deactivation rate (II).
- A final period of rapidly increasing deactivation rate (III), due to constriction of the catalyst pore mouths by metal deposits.

Even though the extent of the three zones may differ widely depending on the process conditions, feedstock characteristics and catalyst properties, it is generally accepted that the deactivation is caused by coke and metal deposits.

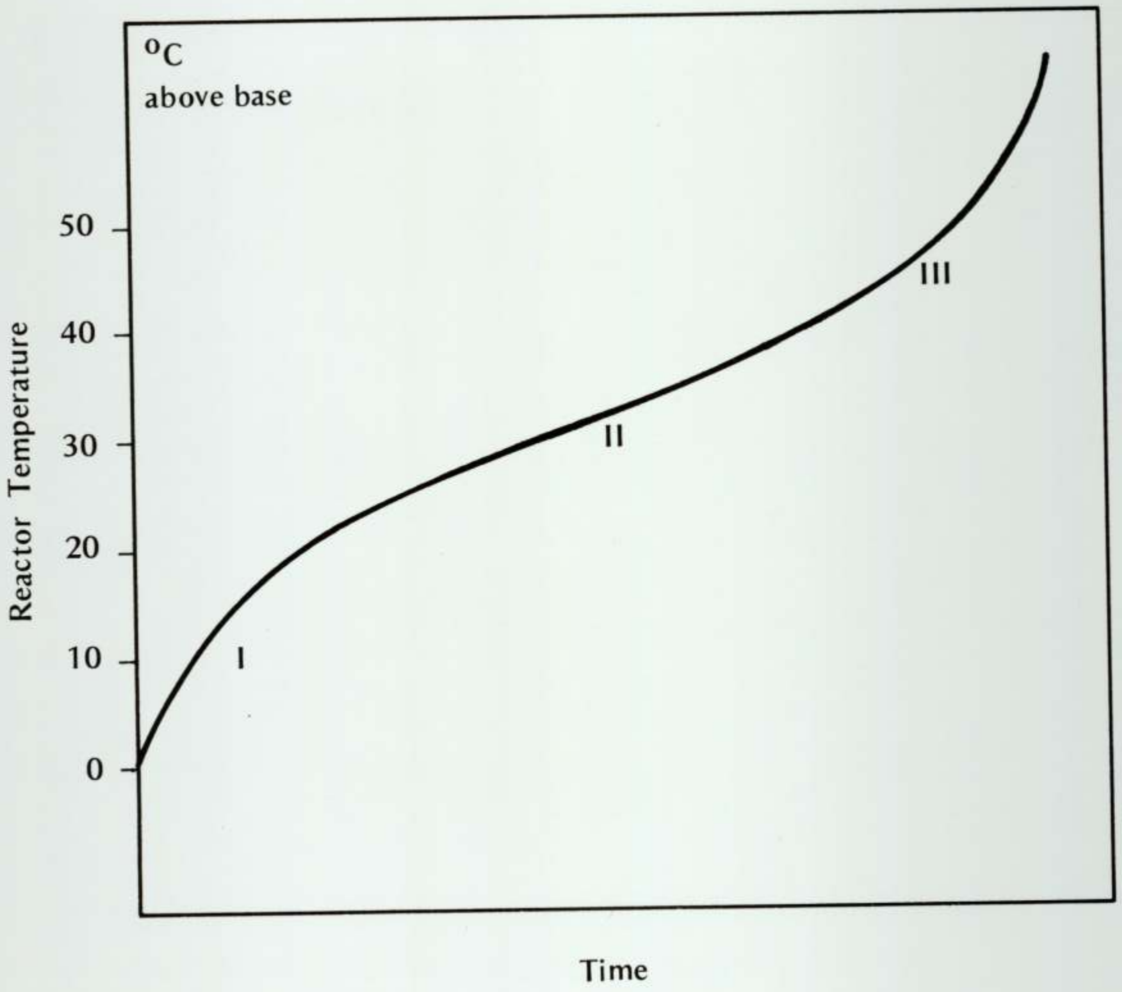

Figure 4.1. Residual oil hydrotreating, typical reactor temperature vs. time behaviour.

Table 4.1. Typical Lives and Factors Determining the Life of Some Important Industrial Catalysts

| Reaction | Operating Conditions | Catalyst | Typical Life (Years) | Process Affecting Life of Catalyst Charge | Catalyst Property Affected |
|---|---|---|---|---|---|
| Ammonia synthesis<br>$N_2 + 3H_2$ --> $2NH_3$ | 450-550°C<br>200-500 ats | Fe with promotors ($K_2O$) & stabiliser ($Al_2O_3$) | 5-10 | Slow sintering | Activity |
| Methanation (ammonia & hydrogen plants) $CO/CO_2 + H_2$ --> $CH_4 + H_2O$ | 250-350°C<br>30 ats | Supported nickel | 5-10 | Slow poisening (eg. S & As from plant upsets) | Activity |
| Acetylene hydrogenation ("front end") $C_2H_2 + H_2$ --> $C_2H_4$ | 30-100°C<br>50 ats | Supported palladium | 5-10 | Slow sintering, increased bed temperature | Activity |
| Sulphuric acid<br>$2SO_2 + O_2$ ---> $2SO_3$ | 420-600°C<br>1 ats | Vanadium & potassium sulphates on silica | 5-10 | Slow physical deterioration (formation of dust) | Pressure drop & mass transfer<br>Activity |
| Mathanol synthesis (low temperature)<br>$CO + 2H_2$ --> $CH_3OH$ | 200-300°C<br>50-100 ats | Copper on zinc & aluminium oxides | 2-8 | Slow sintering | |
| Low temperature carbon monoxide shift $Co + H_2O$ --> $CO_x + H_2$ | 200-250°C<br>30 ats | Copper on zinc and aluminium oxides | 2-6 | Slow poisoning & accelerated sintering by poisons | Activity |
| Hydrocarbon hydrodesulphurisation (including natural gas)<br>$R_2S + 2H_2$ ---> $2RH + H_2S$ | 300-400°C<br>30 ats | Cobalt and molybdenum sulphides on aluminium oxide | 2-8 | Slow coking, metal deposits in some cases (feed-stock important) | Mass transfer pressure drop |
| High temperature carbon monoxide shift<br>$CO + H_2O$ --> $H_2 + CO_2$ | 350-500°C<br>30 ats | $Fe_3O_4$ on chromia | 2-4 | Slow sintering, pellet breakage due to water condensation | Activity & pressure drop |
| Steam reforming, natural gas<br>$CH_4 + H_2O$ --> $CO + 3H_2$ | 500-850°C<br>30 ats | Nickel on calcium aluminate or alumina | 2-4 | Sintering, occasionally carbon formation and pellet breakage due to plant upsets | Activity pressure drop |

Table 4.1. (Continued)

| Reaction | Operating Conditions | Catalyst | Typical Life (Years) | Process Affecting Life of Catalyst Charge | Catalyst Property Affected |
|---|---|---|---|---|---|
| Ethylene partial oxidation<br>$2C_2H_4 + O_2$ ---> $2C_2H_4O$ | 200-270°C<br>10-20 ats | Silver on α-alumina with promoters | 1-4 | Slow sintering increasing bed temperature | Activity & selectivity |
| Benzene oxidation to maleic anhydride<br>$C_6H_6 + O_2$ ---> $C_4H_2O_3$ | 350°C<br>1 ats | Vanadium & molybdenum oxides with promoters on α-alumina | 1-2 | Irreversible formation of inactive vanadium phase | Activity & selectivity |
| Reduction of aldehydes to alcohols<br>$RCHO + H_2$ --> $RCH_2OH$ | 220-270°C<br>100-300 ats | Copper on zinc oxide | 0.5-1 | Slow sintering, pellet breakage (depends on feed-stock) | Activity or pressure drop |
| Partial oxidation of methanol to formaldehyde<br>$CH_3OH$ ---> $CH_2O + H_2$<br>$CH_3OH + 1/2\ O_2$-->$CH_2O$<br>$H_2O$ | 600-700°C<br>1 ats | Silver granules | 0.3-1 | Poisoning, eg iron, some coking (due to poisons) | Selectivity |
| Ammonia oxidation<br>$2NH_3 + 5/2\ O_2$ --->$2NO + 3H_2O$ | 800-900°C<br>1-10 ats | Platinum alloy gauze | 0.1-0.5 | Surface roughness, loss of platinum poisons in some cases | Selectivity |
| Acetylene hydrogenation ("tail end") $C_2H_2 + H_2$ --> $C_2H_4$ | 30-100°C<br>50 ats | Supported palladium | 0.1-0.5 | Coke & oil formation (regeneration possible) | Mass transfer |
| Oxychlorination of ethylene to ethylene dichloride<br>$2C_2H_4 + 4HCl + O_2$ ---><br>$2C_2H_4Cl_2 + 2H_2O$ | 230-270°C<br>1-10 ats | Copper chlorides on alumina (fluidised bed) | 0.2-0.5 | Loss by attrition, and other causes resulting from plant upsets | Fluidised state, activity |
| Catalytic hydrocarbon reforming | 460-525°C<br>8-50 ats | Platinum alloys on treated alumina | 0.01-0.5 | Coking (depends on hydrogen pressure), frequent regeneration | Mass transfer |
| Catalytic cracking of oils | 500-560°C<br>2-3 ats<br>(fluidized bed) | Synthetic zeolites | 0.000002 | Very rapid coking (continuous regeneration) | Mass transfer |

## 4.2 Metal Deposition

Unlike coke deposition, metals deposition rate is nearly constant with time. Oxenreiter et al (98) reported the amount of deposited vanadium to be as high as 56% and nickel to be up to 17% wt. Several investigators (98-101) studied the metals deposition on the catalyst with a scanning electron x-ray microprobe analyser. All these investigators found that vanadium deposits in the thin outer shell of the catalyst, whereas nickel tends to be more uniformly distributed across the diameter of the catalyst. From a study applying microprobe analysis in combination with pore diffusion theory, Sato et al (101) concluded that the effective diffusivity for vanadium is less than 10% of that for nickel. However, Todo et al (102) reported that the maximum deposition of both vanadium and nickel occurred near the outer edge and the concentration profiles were U-shaped for both metals. The maximum deposition of the metals occurred near the inlet of the reactor for fixed bed reactors and decreased toward the reactor outlet while, in the case of ebulated bed reactors, the metal content does not depend on its location as shown in Figure 4.2 (98, 101, 103, 104). Several workers (105, 106, 107) observed that, at the entrance of the bed, the maximum in the metal deposition occurs inside the catalyst so that the metal deposition profiles resemble an M-shape (Shell maximum). Tamm et al (105) and Jacobson et al attributed this to the diffusion controlled reaction of metal species with hydrogen sulphide inside the catalyst extrudate. At the exit section of the bed, the maximum moved to the external surface and the metal deposition profiles were U-shape.

These findings suggest that hydro-demetallation (HDM) reactions are diffusion controlled and auto-catalytic. High metal concentration at the edge of the catalyst pellet slowly blocks the pores and makes the interior of the catalyst inaccessible to the reactants. It has been proposed that pore mouth plugging is the major cause in limiting the total catalyst life in residue hydroprocessing (95, 110, 111).

Although pore blockage by metal deposits is a major reason for discarding residue hydrotreating catalysts after use, Bogdanor and Rase (112) demonstrated that decline in activity can result from molybdenum and nickel migration and an apparent molybdenum agglomeration that occurs under operating and regeneration conditions.

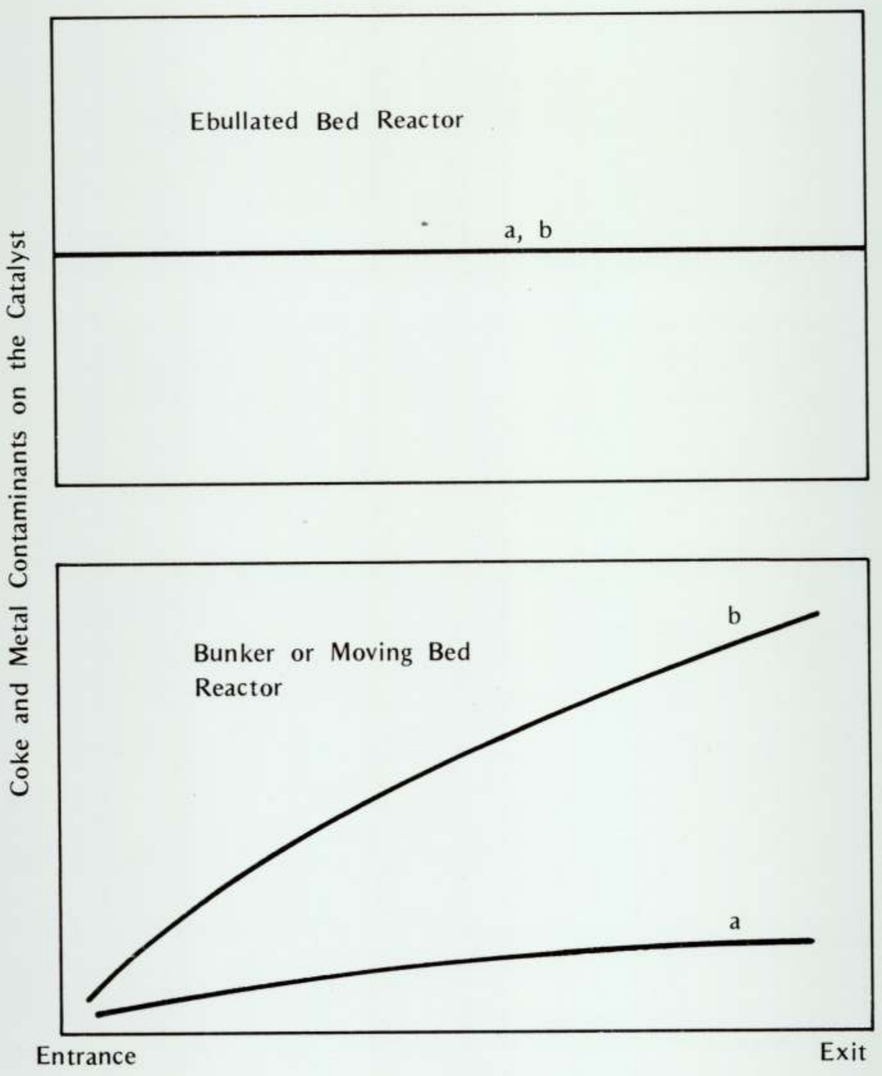

Figure 4.2. Representation of position-dependent foulant deposition profiles; (a) coke and (b) metals.

### 4.3 Coke Deposition

Coke is believed to be responsible for the rapid deactivation of catalyst which occurs in the early part of a process run (113, 105).

As early as 1963, Beuther and Schmid (113) observed that half of the total carbon deposited on the residues hydrotreating catalyst in 16 days of operation, was deposited in the first 12 hours. The nearly stable value of coke on the catalyst is explained by a dynamic equilibrium between the hydrocracking rate and the hydrogenation rate on the catalyst surface. The mechanism of coke formation has been investigated by several workers. Beuther et al (114) used hot-stage microscopy to observe the formation of coke in the presence of $CoMo/Al_2O_3$ catalysts using a vacuum tower residue. Actual coke formation is preceded by an ordering and stacking of aromatic molecules. In fixed bed processing of heavy feed, coke was invariably found to be concentrated on the external surface of the catalyst. In an expanded bed reactor it is found to be uniformly distributed throughout the catalyst pellets.

Coke deposition was generally found to increase from the entrance to the exit of a fixed bed hydrotreater (65, 105). Because hydrotreating catalysts retain a significant level of activity even when heavily coked, and because the coke may have a large surface area (and often contains high levels of catalytic metals), it is reasonable to suggest that the coke deposits have some catalytic properties (115, 116) or may not stop access of reactants to the catalyst.

### 4.4 Effect of Various Parameters on Catalyst Deactivation

Since the rate and extent of deposition of coke and metals on the hydroprocessing catalyst are governed to a large extent by factors such as feedstock characteristics, catalyst characteristics and operating conditions, it is important to understand the relation between these parameters and catalyst deactivation.

#### 4.4.1 Process parameters

Temperature. Increase in temperature usually leads to an increase in coke formation and metal deposition and thus the deactivation rate. Pazos et al (117) and Tamm et al (105) found higher metal build-up near the catalyst edge with increasing temperature. As mentioned earlier, the metal build-up at the catalyst edge or external surface is detrimental to catalyst life as it will progressively block the diffusion of the reactant molecules into the interior of the catalyst.

Hydrogen pressure. An increase in hydrogen pressure within the range 5-12 x $10^6 N/m^2$ has been found to decrease the coke content of the catalyst but to increase metal deposition at the exterior surface of the catalyst pellet (105, 109, 117). Thus, an increase in hydrogen partial pressure has a favourable effect if the catalyst deactivation is caused by coke formation, but results in shorter catalyst life if metal deposition is the primary cause of catalyst ageing.

Space velocity. The beneficial effects of a decrease in space velocity have been reported by several authors (118). A decrease in space velocity in the range (LHSV 1.5 - 1.0) results in an increase in catalyst efficiency in HDS and life.

The above review of the literature on residue hydroprocessing indicates that alumina based Co-Mo and Ni-Mo catalysts are extensively used in both the fixed and ebullated bed type reactors. The catalyst experiences deactivation because of contamination by coke and metals. The metal build-up at the exterior surface of the catalyst is detrimental to catalyst life as it blocks the passage of the reactant molecules into the interior surface of the catalyst. The deactivation rate is governed by the feedstock characteristics, catalyst properties and process conditions. The rapid rate of catalyst deactivation can be alleviated at least partially by minimising coke and metals deposition.

### 4.4.2 Feedstock characteristics

Residual oils contain a high proportion of sulphur, nitrogen, metals, asphaltenes and Conradson carbon residue. The amounts of S, N, asphaltenes and organometallic impurities vary widely in the residues from different sources, Table 4.2.

The asphaltenes present in the feed pose a major problem to the catalyst life. Asphaltenes are complicated compounds in which heteroatoms such as nickel, vanadium, sulfur, nitrogen and oxygen are built in a matrix of large aromatic structures that have low hydrogen content (119). The relatively high concentrations of asphaltenes, organo-metallic impurities (V and nickel porphyrins), and Conradson carbon in the residues have a significant effect on the life of hydroprocessing catalysts.

Table 4.2. Properties of Residuum Feedstocks from Different Sources

| Feedstock | 343°C Arabian Light | 343°C Alaskan North Slope | 548°C Arabian Light | 299°C Arabian Heavy | 343°C Iranian Heavy | 342°C Venezuelan (Morichal) |
|---|---|---|---|---|---|---|
| Gravity, °API | 17.6 | 15.3 | 7.6 | 14.0 | 16.9 | 8.6 |
| Sulfur, wt% | 3.0 | 1.7 | 4.1 | 4.3 | 2.5 | 3.5 |
| Nitrogen, ppm | 1250 | 3250 | 2900 | 1900 | 3300 | 5700 |
| Vanadium, ppm | 29 | 38 | 63 | 83 | 136 | 386 |
| Nickel, ppm | 8 | 17 | 16 | 25 | 48 | 114 |
| Iron, ppm | 3 | 3 | 6 | 15 | 6 | 11 |
| Molecular weight | 490 | 530 | 900 | 530 | 470 | 850 |
| Asphaltenes[(a)] wt% | 4.3 | 1.2 | 9.1 | 10.4 | 5.5 | 11.8 |
| Conradson Carbon, wt% | 9.3 | 9.4 | 19.7 | 12.5 | 11.7 | 17.7 |

(a) Hot heptane insolubles.

Henke (120) studied the effect of four types of residues (from Kuwait, Khafji, Agha Jari and Gach Saran) on the catalyst life. Among the four residues, the Kuwait residue with the lowest metal content and Conradson carbon residue (CCR) gave the longest cycle, while the Gach Saran with the highest metal content gave the shortest cycle. The degree and manner of distribution of the metals in the asphaltenes and resins has also been reported to have an effect on catalyst life. Studies conducted by Pazos et al (117) and Tamm et al (105) on the effect of feed source indicate that intraparticle distribution parameters and the position of maximum concentration in the catalyst extrudate depend upon the feedstock. The amount of coke deposition on the catalyst has been found to depend upon the feedstock (113). Beuther and Schmid (113) showed that coke formation can be alleviated to some extent by deasphalting the residues. Several others have reported remarkable improvements in catalyst life by feed pretreatment (65, 121).

Two techniques are commonly used for feed pretreatment. The first is based on an extraction technique to remove asphaltenes (deasphalting) whilst the second is a metal removal process in a guard chamber using a demetallization catalyst. Remarkable increase in HDS rate has been noted to accompany deasphalting treatment (121, 122). Silbernagel and Riley (123) performed deactivation tests on three feeds: a high metal content Venezuelan whole crude, its deasphalted oil and the HF treated, demetallized version of the same crude. The HDS activity was higher for deasphalted oil (DAO) than for the other two feeds, while the deactivation rate was slower for the demetallized HF treated feed.

The benefits of feed pretreatment by hydrodemetallization in guard bed reactors have been demonstrated by several researchers (65, 121, 124). Hastings et al (125) found that a high degree of desulphurization can be achieved by demetallization of the feed separately in a catalyst bed upstream from the main reactor. Composite catalyst beds and reactor staging have been strongly advocated for residue processing in recent years (124, 126, 127).

### 4.4.3 Effect of catalyst properties

Pore Size Distribution. Catalysts play a very important role in heavy residue hydroprocessing. In addition to promoting the rate of hydrodesulphurization, hydrodenitrogenation and hydrodemetallization, the catalyst is important in the hydrocracking and hydrogenation reactions of asphaltenes and their fragments. Several factors limit the effectiveness of the catalysts in residue hydroprocessing. These can be divided into two types: mass transfer and activity factors. For heavy feedstocks, which contain high proportions of high molecular weight asphaltenes, consideration has to be given to the mass transfer or the diffusion of the large asphaltenic molecules into the catalyst pore structure. As mentioned previously, the main cause of catalyst deactivation is metal deposition in pore mouths which restricts the access of further reactant molecules to the active catalyst surface within the pores. This suggests that the deactivation rate would be slower, and the life of the catalyst longer, if the large pores in the catalyst are increased to allow for more even deposition of metals within the pores. Several researchers have studied the effects of catalyst pore size on its activity and stability and have reported the beneficial effects of increasing pore diameter.

Tamm et al (105) have shown that concentrations of vanadium near the external surface are significantly higher for small pore diameter catalyst than for the large pore catalyst, indicating a poor metal distribution and increased diffusional limitations for the former, (Figure 4.3). Improved metal distribution through the pellet and longer catalyst life have been observed for large pore diameter catalysts by Jacobson et al (110) and Plumail et al (128). Catalysts with bimodal pore size distribution have been found to retain activity for a longer period of time than those with small micro pores. Large pore catalysts have also been found to be desirable for hydroprocessing of solvent refined coal (129). Bimodal catalysts were found to accommodate more metals than unimodal catalysts and, for microporous catalysts (10-20 nm diameter range), vanadium was deposited only at the periphery of the particle. Its penetration into the particle did not exceed 10% of the particle diameter. In macroporous catalyst pellets of 100-1000 nm diameter range, vanadium was deposited homogeneously while in bimodal catalyst particles, vanadium deposition was through the pellet, but mainly at the periphery, (Figure 4.4).

Particle Size. It is recognized that the effectiveness of a catalyst can be improved by decreasing the particle size and by maximizing the exposure of its surface. Literature data indicate the use of 0.8 to 1.6 mm diameter extrudates for long duration operation. Nielsen et al (124) have shown that, at lower pressure, the larger particle had a longer life than the smaller diameter catalyst while, at higher pressures, the latter had a longer life. However, the initial deactivation rate of the smaller catalyst was significantly higher than that of the large size catalyst at both pressures (Figure 4.5). Similar results were also obtained by Tamm et al (105) and Shah and Paraskos (130). Since a decrease in particle size maximizes the exposure of its surface, external cracking and metal removal reactions are enhanced leading to high concentrations of coke and metal deposits on the catalyst particles. This would mean that the small size catalyst would lose its activity at a faster rate than the large size catalyst, as observed by several workers (105, 110, 130, 131).

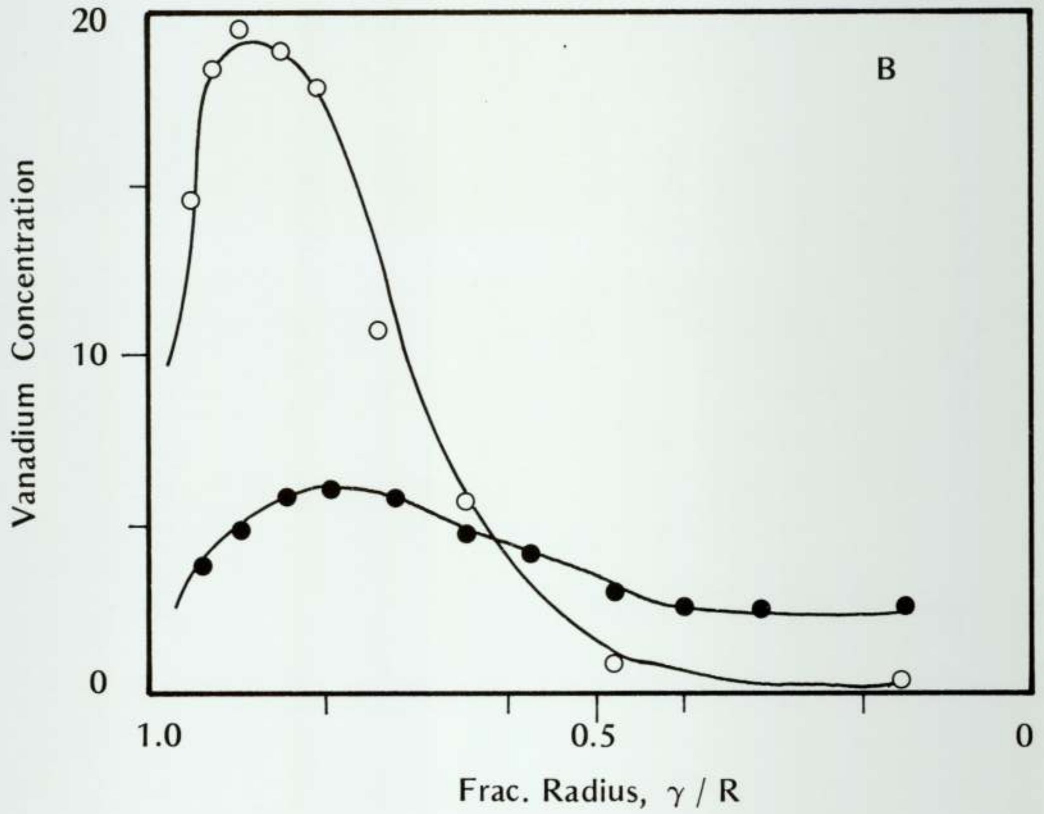

Figure 4.3. Effect of pore diameter on vanadium deposition.
○ Small pores, $\theta_V = 0.15$
● Large pores, $\theta_V = 0.20$

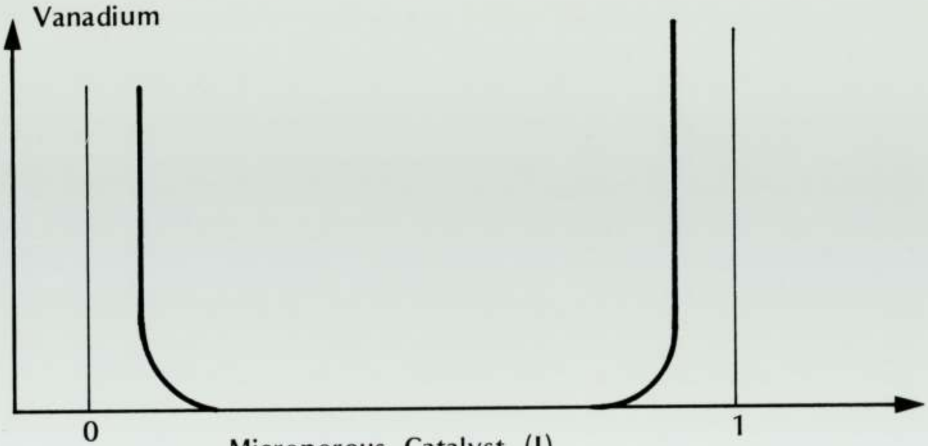

Microporous Catalyst (I)

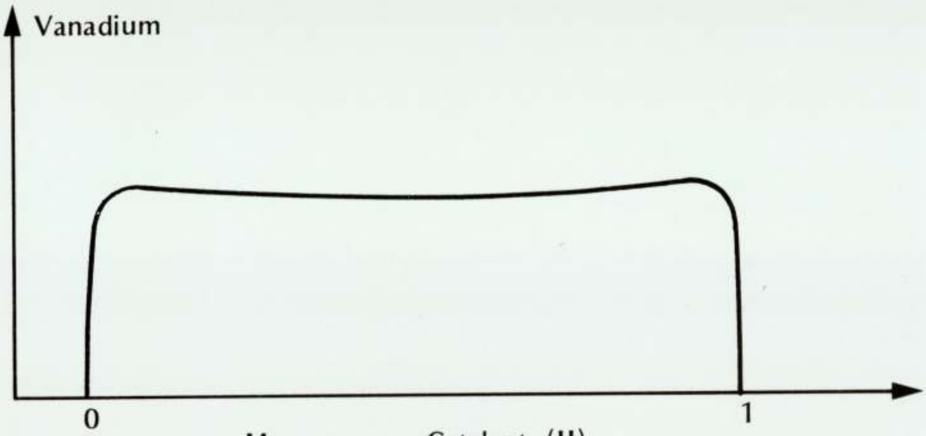

Macroporous Catalyst (II)

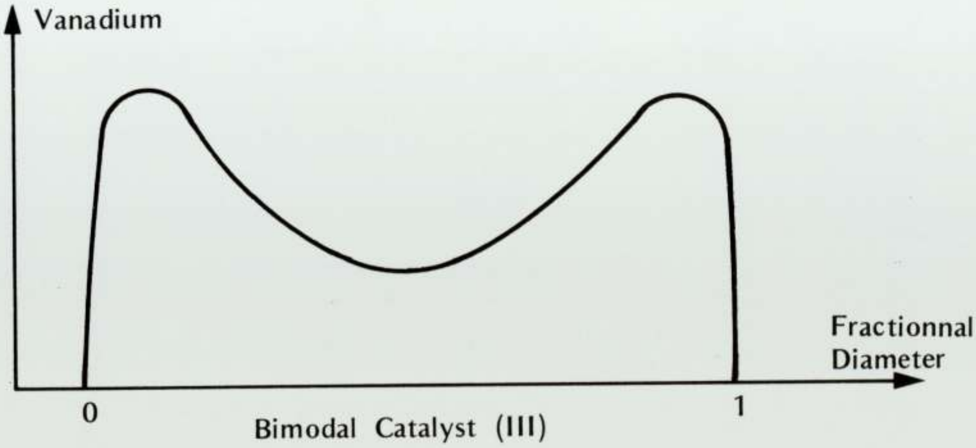

Bimodal Catalyst (III)

Figure 4.4. Effect of pore size on vanadium deposition.

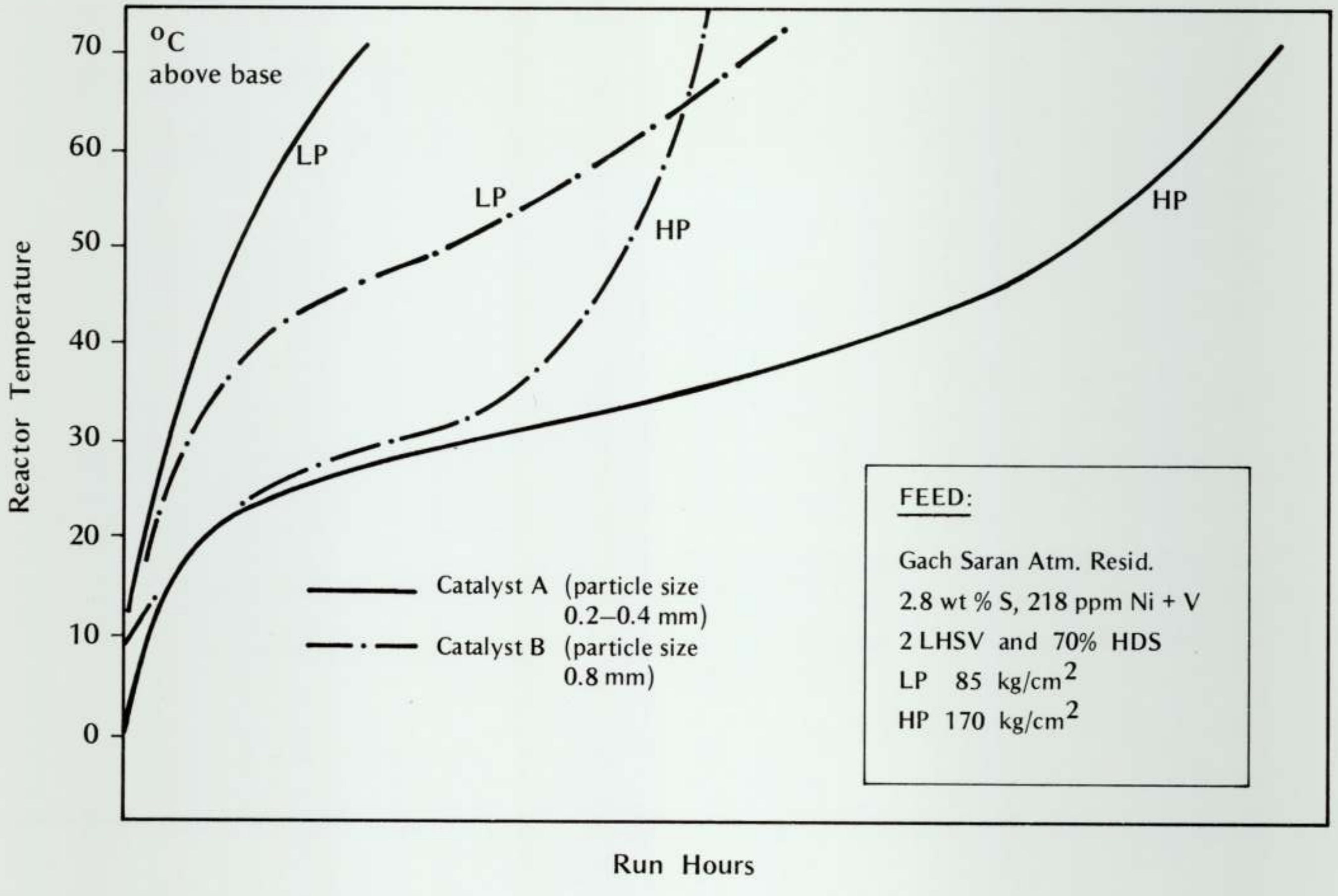

Figure 4.5. Influence of pressure on deactivation of two different catalysts.

## 4.5 Regeneration of Hydrotreating Catalyst

### 4.5.1 Introduction

One of the main technological challenges in the field of residue hydroprocessing is the regeneration of the deactivated catalysts. Regeneration by conventional regeneration procedures, using nitrogen-air or steam-air under controlled conditions, does not result in complete reactivation of the catalyst. Carbon is removed completely, but the metallic impurities remain on the catalyst and act as a diffusion barrier for the reactants. No commercial process is currently available for regeneration of the spent catalysts which are discharged as solid wastes. Safe disposal of the spent catalysts also creates a major problem since they contain toxic metals and can cause environmental pollution. Regeneration and reuse of the spent catalysts from the residue hydroprocessing operations would therefore, have potential advantages from both economical and environmental points of view.

### 4.5.2 Metal Removal

Several workers have attempted to regenerate/rejuvenate metals fouled, spent residue hydroprocessing catalysts by selective removal of vanadium deposits by chemical treatment.

Mitchel et al. (132) used an aqueous solution of oxalic acid as reagent for removing vanadium sulphide from spent residue hydroprocessing catalyst prior to burning off the coke. They claimed at least 30% removal of vanadium from the catalyst without affecting the active catalytic constituents. A process developed at IFP by Le Page et al. (133) involves treating the used catalyst with aqueous oxalic acid solution at 80°C after burning coke from the catalyst. Removal of at least 50% of the metallic impurities, (but less than 25% of catalytic constituents) with 80% recovery of initial activity has been reported in the process.

Another process developed by Farrell et al. (134) involves treating the deactivated catalyst prior to coke burn-off with an aqueous solution containing a mixture of oxalic acid and aluminium nitrate or nitric acid. They achieved removal of at least 50% of the vanadium plus nickel contaminants and restoration of at least 70% of the original HDS activity. It is claimed that the deactivated catalyst should not be de-coked prior to treatment with the regenerant solution, because the formation of $SO_2$ and/ or $SO_3$ plus $O_2$ attacks most hydrodesulphurization catalyst supports and also removes the active components of the catalyst. Beuther et al. (135) on the other hand stated that the chemical extraction of the metals from the coked catalyst would be quite difficult because the over-all metallo-organics are embedded in a coke matrix.

Recent studies by Hernandez (136) showed that oxalic and citric acid treatments of used catalyst after coke burning improved the equilibrium HDS activity of the catalyst (16.63%) compared with that of the fresh catalyst (8.93%). However, the initial HDS activity of the treated catalysts was lower (14.26%), than the initial HDS activity (22.51%) for fresh catalyst. However, in industrial catalysts, it is more important to maintain activity at a high level than to have a high initial activity and a steep decrease in activity. Another interesting observation reported by this author was that the hydrodemetallization HDM activity is enhanced by simple coke burning treatment. Silbernagel et al. (137) have reported that contacting metal contaminated hydro-desulphurization catalyst with a heteropoly acid, such as molybdophosphoric acid to which dilute hydrogen peroxide is added, results in a significant enhancement in the rate and extent of carbon and metals removal. This is due to the fact that $H_2O_2$ helps maintain the heteropoly acid in the highest oxidation state which will effect the extraction of vanadium, and to the fact that $H_2O_2$ assists in oxidizing $V^{4+}$ to $V^{5+}$, $VO^{2+}$ to $V_2O_5$ and $V_2S_2$ to $VOSO_4$: in general, higher oxidation state species are more soluble. A somewhat similar process involving two steps has been reported by the same authors (138). The process involves first contacting the catalyst with a sulphiding reagent ($H_2S/H_2$) and then treating the sulphided spent catalyst with a heteropoly acid such as molybdophosphoric acid.

In a process described by Coons et al. (139), catalysts used in residual oil hydroprocessing have their activity restored by contacting with a distillate oil such as naphtha, kerosene, diesel fuels, light intermediate or heavy straight run at about 315 to 427°C and 0 to 200 atm. pressure optionally in the presence of hydrogen. This is followed by purging with hydrogen to remove any excess of distillate oil or any contaminant or carbonaceous matter and then with nitrogen, to remove $H_2$; and by steaming at about 200 to 427°C and burning with an air steam mixture at a temperature below about 427°C. To remove the catalyst contaminants, air burn is initiated at 315.5°C at the inlet of bed, with a maximum burn front at below

399°C. The oxygen concentration also controls the burn front; it is maintained below Ca. 1% mole - 0.5% mole.

Anderson (140) discloses a method for removing vanadium by contacting a regenerated catalyst with a gas containing molecular oxygen at a temperature of 538°C, sulphiding at 400-870°C and washing with an aqueous mineral acid to remove the contaminated metal sulphide. An aqueous phase oxidation method for removing metal contaminants such as Ni, V, Fe, etc., from FCC has also been reported by Burke et al. (141). The process involves contacting the sulphided metals-contaminated catalyst with an aqueous solution containing soluble metal nitrate and nitrite ions. The oxidized catalyst is further treated with an aqueous oxidative wash in an aqueous peroxide solution and a reductive wash in an aqueous solution of $SO_2$.

Recently removal of 70-80% of the vanadium and 55-70% of the nickel without affecting the catalyst metals has been claimed by Hydrocarbon Research Inc. (142, 143). The process comprises

a. removing process oil by solvent washing,
b. treatment at 15-120°C with an aqueous solution of sulphuric acid and ammonium peroxydisulphate,
c. washing away the reagent, and
d. burning the carbonaceous deposit at 430-480°C.

Deposited metals are removed, but the catalyst metals remain and initial activity is restored.

In another patented process developed by Ioka et al. (144) the spent catalyst is treated with $Cl_2$ or NaClO in the presence of water at 50-100°C. Chlorinated V, Ni and Co are leached while Mo is not leached out during the chlorination process. It is reported that 83% V, 76% Ni and 81% Co and $<$ 5% Mo are extracted in the process. The treated catalyst can be reused after calcination at 550°C for 2 hr. Poezd et al. (145) disclosed a patent of a simple method involving grinding of the spent catalyst into a powder, adding calculated amounts of Co or Ni nitrate solution to the powder, treating the mixture with a 10-20% $HNO_3$ solution and then adding ammonium molybdate solution to the mixture. The material is subsequently moulded into pellets, dried at 120-160°C and calcined at 500-550°C. This method should be described as re-impregnation rather than regeneration.

Marcantonio (146) introduced a process for recovery of metals (Ni, Co, Mo, V) from spent hydroprocessing catalysts by first roasting at 400-600°C and then contacting twice with aqueous solutions of ammonia and ammonium salts which improves the metal recoveries (especially for Cobalt) from ca 50% to ca 90%.

Recently, Arteaga et al. (147, 148) investigated the changes brought about in catalyst characteristics and performance during regeneration of a Co-Mo-$Al_2O_3$ hydrotreating catalyst deactivated by coke deposition. An increase in HDS activity (about 130%) of the catalyst after regeneration was observed. Redistribution of Co and Mo phases occurred during regeneration, with an increase in the amount of Co and Mo ions present on the catalyst surface. The enhanced surface exposure of the Co and Mo containing species during regeneration was found to be responsible for the increased activity.

Recently, regeneration of coked HDS catalyst by air in a thin layer was studied experimentally by Klusacek et al (149). A simple model was developed to simulate the reactivation reactions. By using kinetic data for deposited coke oxidation, the catalyst pellet temperature versus time was predicted and the conditions under which coke ignites spontaneously were determined. Under spontaneous ignition conditions, the catalyst bed temperature cannot be controlled and this could result in irreversible deactivation. Sintering, phase transformation, loss of active Mo phase by sublimation, and formation of catalytically inactive complexes such as cobalt aluminate, nickel aluminate and aluminium molybdate result from excessive temperatures during regeneration. Appreciable loss of catalyst crush strength can also occur.

It is clear that industrial interest in catalyst deactivation and regeneration is high, but that little data have been determined unambiguously particularly for catalyst regeneration by metals removal.

## 5.0 LEACHING: KINETICS

One of the main methods for removing metal deposits from spent catalysts is leaching with a liquid reagent. Leaching is a general term which describes dissolution of a solid into a liquid which may, or may not, involve a chemical reaction. In general, the process in its most complicated form can be described in terms of the individual steps.

a. A solution of a leaching reagent in a solvent is prepared and brought into contact with the solid.

b. The leaching reagent diffuses to the solid-liquid interface.

c. A reaction occurs between solid and the reagent to produce a product.

d. The product dissolves in the solvent.

e. The dissolved product diffuses away from the interface.

Any combination of the steps b-e may control the kinetics of leaching and the amount of material leached. A chemical reaction which goes to completion will not lead to effective leaching unless the product dissolves in and diffuses away from the interface. As a result, in order to estimate the efficiency of leaching, it is necessary to consider rates of mass transfer, the nature and kinetics of the chemical reaction, the kinetics of dissolution and the amount of product that can be dissolved in the solvent.

The situation is complicated by the nature of the solid to be leached. It is rare that such solids are chemically homogenous and non-porous. In the case of spent catalysts, for example, metal-containing impurities are deposited in the pores of the catalyst pellet and within a coke matrix also formed on the catalyst during reaction. Therefore, mass transfer may be expected to be important in the leaching process.

It is fortunate that kinetic treatments of different leaching systems have been developed (150). Of these, the progressive conversion model and the shrinking core model are pertinent to the different leaching processes of interest in the present studies.

## 5.1 The Unreacted Core Model

This model considers a solid which is of constant size but from which material is leached. This is a close approximation to the spent catalyst where constant size is maintained by the catalyst/coke matrix while metal sulphide deposits are leached from the solid.

### 5.1.1 Unreacted Core Model - Particles of Constant Size

The unreacted core model for particles of constant size was developed by Levenspiel (150). Five steps were assumed to occur in succession during reaction.

1. Liquid phase diffusion of liquid reactant to external surface of particle.
2. Diffusion of liquid reactant to the reaction interface (through reacted solid).
3. Reaction at the solid surface.
4. Diffusion of liquid products from the reaction interface to the external surface of particle.
5. Diffusion of liquid products from the external surface to the bulk fluid.

In this respect the following conversion equations were developed.

#### i. Diffusion Through Liquid Film Controlling

If the liquid reactant is not present at the surface, then for the reaction:-

$$A_{(l)} + bB_{(s)} \longrightarrow \text{Products} \qquad (1)$$

$$dN_B = b dN_A$$

and for a spherical particle of unchanged exterior surface $S_{ex}$

$$-\frac{1}{S_{ex}} \frac{dN_B}{dt} = \frac{-1}{4\pi R^2} \left[ \frac{dN_B}{dt} \right] = \frac{-b}{4\pi R^2} \left[ \frac{dN_A}{dt} \right] \tag{2}$$

$$= bk_1 \left( C_{Al} - C_{AS} \right) = bk_1 \, C_{Al} = \text{Constant}$$

If $\rho_B$ is the molar density of B in solid and V is the volume of solid particle,

$$N_B = \rho_B V = \left( \frac{\text{moles B}}{\text{cm}^3 \text{ solid}} \right) \left( \text{cm}^3 \text{solid} \right) \tag{3}$$

The decrease in volume, and hence radius, of the unreacted core corresponding to the disappearance of $dN_B$ moles of solid or $bdN_A$ moles of liquid reactant is then given by:

$$-dN_B = -bdN_A = -\rho_B \, dV = -\rho_B d \left( \frac{4\pi r_e^3}{3} \right) \tag{4}$$

$$= -4\pi \, \rho_B \cdot r_e^2 \cdot dr_e$$

$$\therefore \quad -\frac{1}{S_{ex}} \left[ \frac{dN_B}{dt} \right] = \frac{-1}{4\pi R^2} \left[ \frac{dN_B}{dt} \right] = -\rho_B \left( \frac{r_e}{R} \right)^2 \frac{dr_e}{dt} \tag{5}$$

$$= bk_1 \, C_{Al}$$

Where $k_1$ is the mass transfer coefficient for bulk diffusion. Rearranging and integration gives,

$$\frac{-\rho_B}{R^2} \int_R^{r_e} . \; r_e^2 \; dr_e = bk_1 \, C_{Al} \int_o^t dt$$

where t = time of leaching

$$\therefore \quad t = \frac{-\rho_B}{R^2 \, bk_1 C_{Al}} \left[ \frac{r_e^3}{3} \right]_R^{r_e} = \frac{\rho_B}{3R^3 bC_{Al} k_1} \left[ R^3 - r_e^3 \right] \quad (6)$$

$$\therefore \quad t = \frac{\rho_B \, R}{3bk_1 \, C_{Al}} \left[ 1 - \left( \frac{r_e}{R} \right)^3 \right] \quad (7)$$

The time required for complete reaction is:

$$\tau = \frac{\rho_B R}{3b \, k_1 C_{Al}} \quad (\text{since } r_e = 0) \quad (8)$$

By combining equations 7 and 8, we obtain

$$\therefore \quad \frac{t}{\tau} = 1 - \left( \frac{r_e}{R} \right)^3 \quad (9)$$

This can be expressed in terms of fractional conversion:-

Fraction unconverted

$$= (1-X_B) = \left[ \frac{\text{Vol. of unreacted core}}{\text{Total vol. of particle}} \right] = \frac{\frac{4\pi r_e^3}{3}}{\frac{4}{3}\pi R^3} = \left( \frac{r_e}{R} \right)^3 \qquad (10)$$

$$\therefore \quad X_B = \frac{t}{\tau} = 1 - \left( \frac{r_e}{R} \right)^3 \qquad (11)$$

### ii. Diffusion Through Solid Product Layer Controlling

Both reactant A and the boundary of unreacted core move towards the centre of the particle. The diffusion of A is much faster than the shrinkage of the core and, as a result, the assumption of a stationary unreacted core is a reasonable one.

The reaction of A at any time t is given by

$$- \frac{dN_A}{dt} = 4\pi r^2 Q_A = 4\ \pi R^2 Q_{AS} = 4\pi r_e^2\ Q_{AC} \qquad (12)$$

$$= \text{constant}$$

Let the flux of A within the product layer be given by Fickian diffusion.

$$Q_A = D_e \frac{dC_A}{dr} \qquad (13)$$

where $D_e$ is diffusivity of A in reaction product layer.

Substituting for $Q_A$ gives

$$- \frac{dN_A}{dt} = 4\pi r^2\ D_e \left[ \frac{dC_A}{dr} \right] = \text{Constant}$$

Integrating from R to $r_e$ across the product layer

$$- \frac{dN_A}{dt} \int_R^{r_e} \frac{dr}{r^2} = 4\pi D_e \int_{C_{A1} = C_{AS}}^{C_A = 0} dC_A$$

$$-\frac{dN_A}{dt}\left(\frac{1}{r_e}-\frac{1}{R}\right) = 4\pi D_e C_{Al} \tag{15}$$

For the second part of the analysis, consider the change in size of the unreacted core with time.

For a given size of unreacted core, $dN_A/dt$ is a constant. However, as the reacted layer increases, the diffusion of A must increase. Integration of the above expression with respect to time should yield the required relationship. As this equation contains three variables, t, $N_A$ and $r_e$, one must be eliminated before integration.

As with film diffusion, $N_A$ may be eliminated by writing the equation in terms of $r_e$

$$-dN_A = -\frac{dN_B}{b} = (-4\pi\rho_B\ r_e^2\ dr_e/b)$$

$$\therefore\ -\rho_B \int_{r_e=R}^{r_e} \left(\frac{1}{r_e}-\frac{1}{R}\right) r_e^2\ dr_e = bD_e C_{Al} \int_o^t dt$$

$$\therefore\ t = \frac{\rho_B R^2}{6bD_e C_{Al}}\left[1-3\left(\frac{r_e}{R}\right)^2 + 2\left(\frac{r_e}{R}\right)^3\right] \tag{16}$$

For complete conversion $r_e = o$, and the time required is

$$\tau = \frac{\rho_B R^2}{6\ bD_e C_{Al}} \tag{17}$$

The progress of reaction in terms of functional conversion, as given in equation (10), becomes

$$\frac{t}{\tau} = 1 - 3\ (1-X_B)^{\frac{2}{3}} + 2\ (1-X_B) \tag{18}$$

### iii. Chemical Reaction Control

Since the concentration of A at the reaction interface is the same as in the bulk fluid, the quantity of material reacting is proportional to the surface area of unreacted core. Then the rate of reaction for the stoichiometry of equation (1) is

$$\therefore \frac{-1}{S_{ex}} \left[ \frac{dN_B}{dt} \right] = - \frac{1}{4\pi r_e^2} \left[ \frac{dN_B}{dt} \right] = \frac{-b}{4\pi r_e^2} \left[ \frac{dN_A}{dt} \right] \tag{19}$$

For 1st order reaction at the surface, with a rate constant, $k_S$:-

$$\frac{-1}{4\pi r_e^2} \left[ \frac{dN_B}{dt} \right] = bk_S\, C_{Al}$$

writing $-dN_B = -4\pi\rho_B\, r_e^2\, dr_e$ gives

$$- \frac{1}{4\pi r_e^2}\, \rho_B\, 4\pi r_e^2 \frac{dr_e}{dt} = - \rho_B \frac{dr_e}{dt} = bk_S\, C_{Al} \tag{20}$$

On integration,

$$-\rho_B \int_R^{r_e} dr_e = bk_s\, C_{Al} \int_o^t (dt) \tag{21}$$

$$t = \rho B$$

The time required for complete conversion is given when $r_e$=0 or

$$\tau = \frac{\rho_B R}{bk_s C_{Al}} \tag{22}$$

And, the degree of conversion is given by

$$\frac{t}{\tau} = 1 - (1-x_B)^{1/3} \tag{23}$$

## 5.2 Shrinking Particle Model

For a reaction producing a shrinking particle, any one of the following three steps which occur in succession may be rate controlling.

1. Diffusion of reactant A from the liquid bulk to the surface of the solid.
2. Reaction on the surface between reactant A and solid.
3. Diffusion of reaction products from the surface of the solid through the liquid film into the bulk fluid.

The rate equations in each case will be as follows.

### i. Chemical Reaction Controls

The behavior will be identical to that of particles of constant size, and the rate equation will be as in equations 21 or 23.

### ii. Liquid Film Diffusion Controls

Film resistance at the surface of a particle depends on a number of factors, including relative velocity between fluid and solid, particle size and fluid properties. During reaction, the particle diameter changes. For small particles, Stokes law may be applied.

$$K_1 \alpha \frac{1}{dp} \text{ when } \mu \text{ is small} \tag{25}$$

while, in large particles,

$$K_1 \alpha \left( \frac{\mu}{dp} \right)^t \text{ when velocity } \mu \text{ is large} \tag{26}$$

So for small particles, at the time when a particle of original size $R_o$ has shrunk to R,

$$dN_B = \rho_B dV = 4\pi\rho_B R^2 dR$$

Thus from equation (7),

$$\therefore \quad \frac{-1}{S_{ex}} \frac{dN_B}{dt} = -\frac{\rho_B\, 4\pi R^2}{4\pi R^2} \frac{dR}{dt} = -\rho_B \frac{dR}{dt} = bk_1\, C_{Al} \qquad (27)$$

Since, in the Stokes regime, equation (24) reduces to

$$k_1 = \frac{2\,D}{d_p y} = \frac{D}{R\,y} \qquad (28)$$

where D is diffusivity of reacting liquid and y is mole fraction of reacting liquid in the bulk fluid.

Combination of equations 27 and 28 and integration gives,

$$-\rho_B \frac{dR}{dt} = b\, k_1\, C_{Al} \qquad (27)$$

$$\text{Since } K_1 = \frac{2D}{d_p\, x} = \frac{D}{Ry} \qquad (28)$$

$$-\rho_B \frac{dR}{dt} = \frac{b}{Ry} D\, C_{Al}$$

$$\therefore \quad \int_{R_o}^{R} R\, dR = \frac{bC_{Al}D}{\rho_B\, Ry} \int_o^t dt$$

$$\therefore \quad t = \frac{\rho_B\, yR_o^2}{2bC_{Al}\, D} \left[ 1-\left(\frac{R}{R_o}\right)^2 \right] \qquad (29)$$

For complete conversion, R = 0

$$\therefore \quad \tau = \frac{\rho_B\, yR_o^2}{2bC_{Al}\, D} \qquad (30)$$

On combining, equations 29 and 30,

$$\frac{t}{\tau} = 1 - \left( \frac{R}{R_o} \right)^2 = 1 - (1-X_B)^{2/3} \qquad (31)$$

## Summary

### For Particles of Constant Size (Spent Catalyst)

a) Liquid phase diffusion controls

$$\frac{t}{\tau} = X_B$$

b) Diffusion through reaction rim controls

$$\frac{t}{\tau} = 1 - 3(1-X_B)^{2/3} + 2(1 - X_B)$$

c) Surface chemical reaction controls

$$\frac{t}{\tau} = 1 - (1 - x_B)^{1/3}$$

### For Particles of Changing Size (Pure Metal Sulphides)

a) Chemical reaction controls

$$\frac{t}{\tau} = 1 - (1 - x_B)^{1/3}$$

b) Liquid phase diffusion through the pores controls

$$\frac{t}{\tau} = 1 - (1 - x_B)^{2/3}$$

The two kinetic processes that may be important in the context of leaching are the rate of the chemical reaction or the rate of mass transfer. For a chemical reaction, this rate may be expressed by

$$\text{rate} = k\,(A)^{\alpha}\,(B)^{B}\,\eta$$

where $\eta$ is the effectiveness factor that gives some measure of the importance of mass transfer.

The rate constant, k, depends on temperature according to the Arrhenius relationship.

$$k = A_e{}^{-E/RT}$$

Therefore, the dependence of the rate of leaching on temperature will be exponential if the rate of the chemical reaction controls the overall process.

Mass transfer control, on the other hand is described by Fick's law of diffusion.

$$N_{AX} = -D \ \frac{dc}{dx}$$

where N, flux of A in the x-direction

D, diffusion coefficient $cm^2 s^{-1}$

The dependence of D with respect of temperature will follow the Arrhenius relationship (152)

$$D = D_o \ e^{-Q/RT}$$

where, Q is activation energy, and $D_o$ the frequency factor. Therefore, the dependence of the rate of leaching on temperature will also be exponential, but the apparent activation energy Q will be smaller (152).

## 5.3 Rate of Dissolution Controls

One alternative process may be rate-controlling. If the leaching reaction produces a solid product, then the rate of dissolution of that product may be rate controlling.

The equilibrium amount in solution is limited by the solubility of the solid in the solvent. However, the rate of dissolution is not controlled by solubility, but will depend more on surface area of the product, temperature and the degree of agitation.

Little general information was found in the literature that can be used to predict rates of dissolution. The possiblity of such processes being rate controlling must, however, be borne in mind.

In summary, the rate of leaching from particles may be controlled by mass transfer, by reaction or by the dissolution of products. In each case, a predictive model may be generated. Comparisons of the predictions with experimental results should allow resolution of the rate controlling process(es) in the different samples.

## 6.0 EXPERIMENTAL INVESTIGATION

A program was devised to study the regeneration of the deactivated hydrotreating catalysts by removal of contaminated metals such as vanadium and nickel deposited during the hydrodesulphurization reaction. The program comprised the following sections:

1. Study of physical, chemical and mechanical characterization of fresh, spent and decoked catalysts.
2. Investigation of metal leaching by organic complex forming reagents with and without promoter, and a comparison between their selectivities for vanadium and nickel removal. This included consideration of the leaching of pure sulphides to investigate the kinetics of the reactions.
3. Physical, chemical and mechanical characterization of decoked and leached catalyst.
4. Assessment of the activity for hydrodesulphurization catalyst after regeneration.

## 6.1 Materials, Sources and Preparation

### 6.1.1 Catalysts

Spent residue hydrotreating catalyst was obtained from the atmospheric residue hydrodesulphurizaton unit of Kuwait National Petroleum Company. The spent catalyst for all the experimentation was collected from one batch. The corresponding fresh catalyst was from the same lot prior to use. The catalysts were in the form of spheres. The fresh catalyst was of type UOP-RCD-5A, and contained CoO and $MoO_3$ supported on $\gamma$-alumina.

The spent catalyst contained residual oil, sulphur, carbon, vanadium and nickel deposits in addition to the catalyst metals (Co and Mo) originally present. The contaminated residual oil was cleaned by thoroughly washing with naphtha in a mechanical shaker. The cleaned catalyst was then dried in an oven at 120°C for 24 hours. The characteristics of fresh and spent catalyst are summarized in Chapter 7.

### 6.1.2 Reagents

BDH, Analytical reagent grade oxalic acid, malonic acid and acetic acid were used as extracting reagents. Aluminium nitrate, aluminium sulphate, ammonium nitrate and nitric acid which were used in the metal extraction experiments were all of analytical reagent grade obtained from Baker and BDH.

### 6.1.3 Pure Metal Sulphides

Sulphides of vanadium ($V_2S_3$) molybdenum ($MoS_2$), nickel (NiS) and cobalt sulphide (CoS) of 99.9% purity were obtained from Winlab Limited.

The nitrogen and air used for decoking were supplied by the Kuwait Oxygen Company.

## 6.2 Equipment and Procedures

### 6.2.1 Metal Leaching

A special apparatus shown in Figure 6.1 and Plate 1 was constructed for leaching of metals from the spent catalyst. It consisted of a double jacketed glass reactor (R) of length 45 cm and diameter 2 cm, a dosing pump (P), and a glass reagent vessel. The reagent was pumped continuously through the catalyst bed from the bottom of the reactor (up-flow). The liquid product which was collected in the reagent vessel was circulated continuously through the catalyst bed for the required period of time by the pump. For studies involving higher temperatures (50°C, 75°C), water heated to the required temperature (±1°C) was circulated continuously through the jacket around the reactor.

### 6.2.2 Decoking

A fixed bed reactor (volume 200 cc) length 70 cm and diameter 3 cm as shown in Plate 2 was used for decoking of the catalyst under controlled temperature conditions. 100 g spent catalyst was charged to the reactor. The reactor was loaded with 50 ml of glass beads below and above the catalyst bed so that the catalyst remained at the centre of the reactor. A thermocouple inserted into a thermowell at the center of the catalyst bed was used to monitor the reactor temperature during regeneration.

The following procedure was adopted. After loading the catalyst, nitrogen was passed at a rate of 100 l/h (2.7 $cm^3/s$) and the temperature was increased up to 370°C at a rate of 100 l/h. After maintaining the temperature at 370°C for 30 minutes, a mixture of 2% oxygen in nitrogen

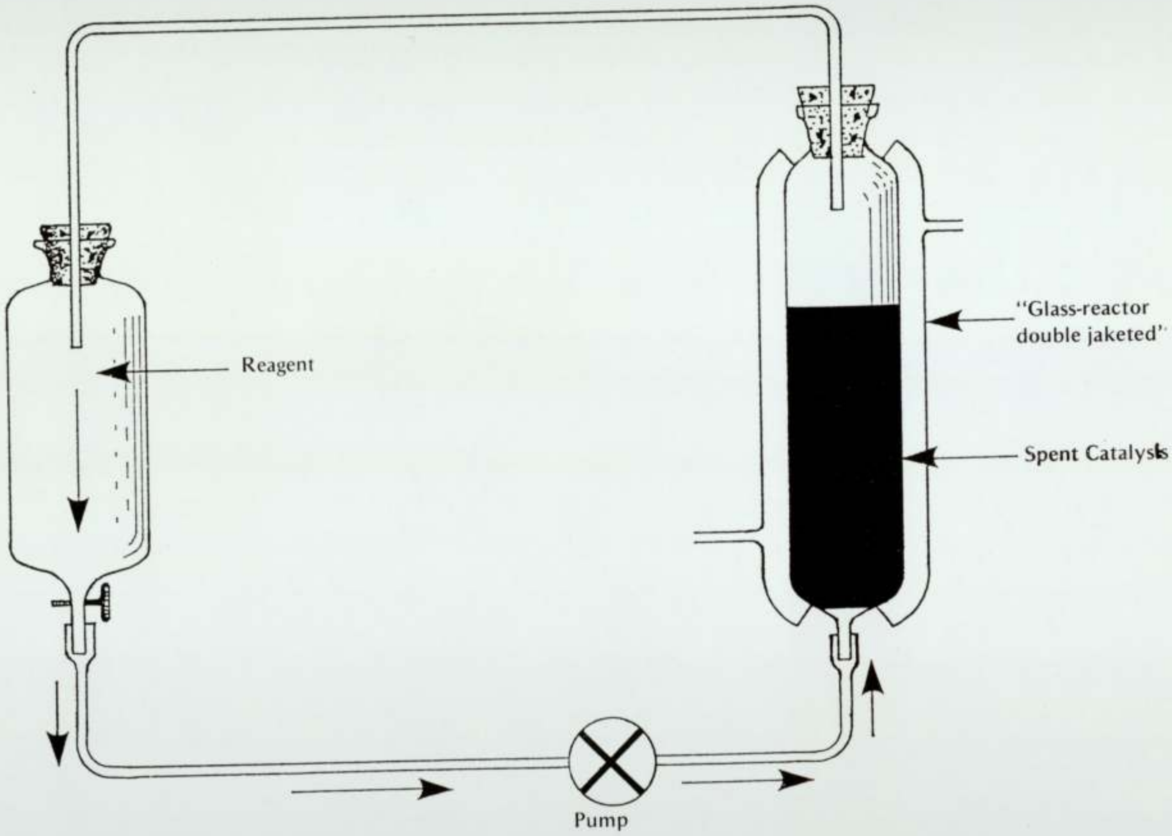

Figure 6.1. Schematic diagram of metal leaching apparatus

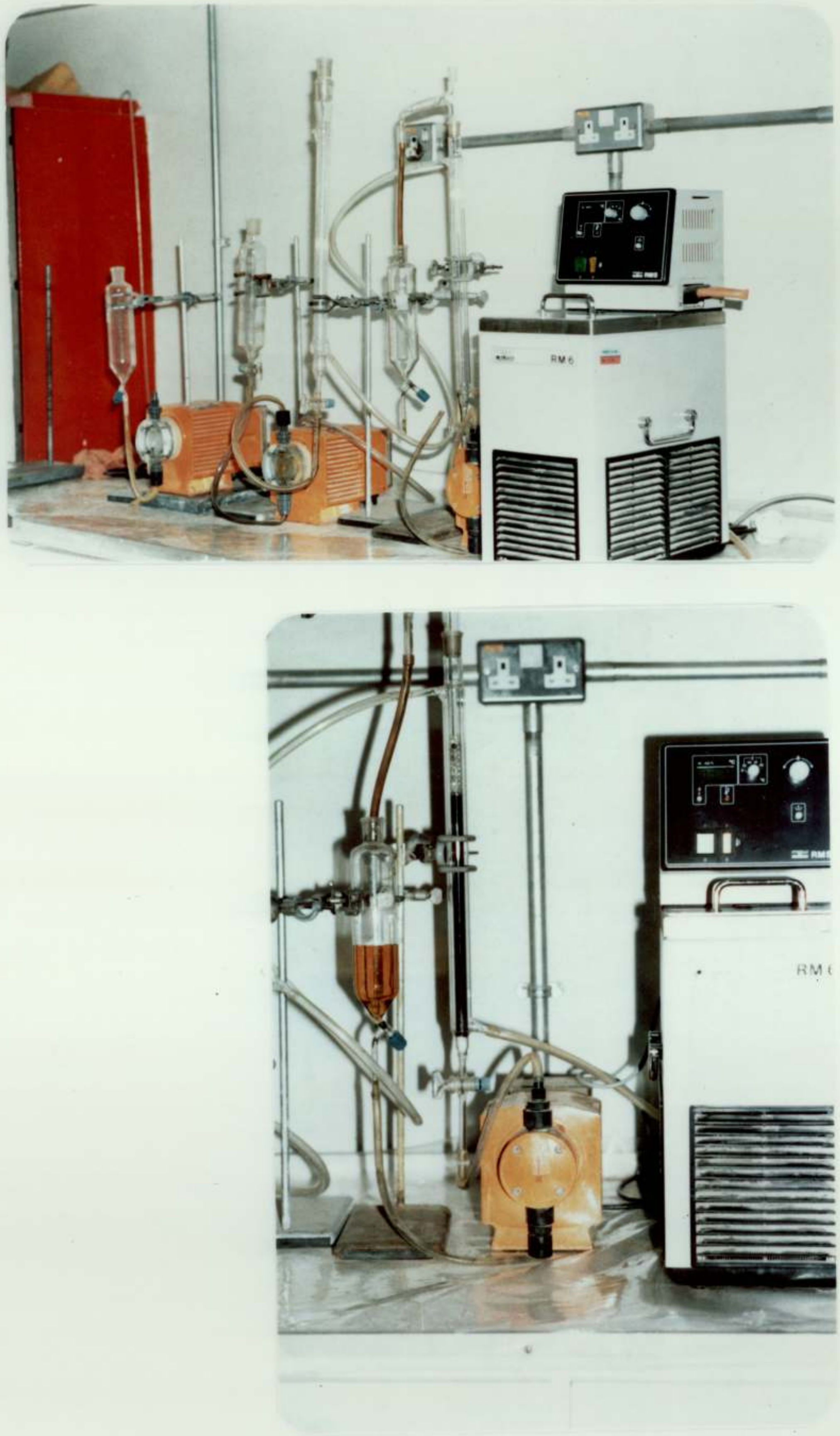

Plate 1. Arrangement of leaching apparatus and thermostatistically-controlled, circulating water bath.

was passed for a period of 8 h at the same flow rate. The gas was then changed to 5% oxygen in nitrogen, and temperature was increased to 400°C and maintained for a period of 4 h. The temperature was then increased up to 450°C and the regeneration gas was changed to air and maintained for a period of 2 h. Finally the reactor was cooled down to room temperature and the sample was characterized.

### 6.2.3 Leaching of Pure Metal Sulphides

A round-bottomed three necked flask was used for pure metal sulphide leaching experiments as shown in Plate 3. A known weight of the metal sulphide was agitated with the reactant in a thermostatically controlled round-bottom flask. A magnetic stirrer coated with inert plastic was used for agitation to avoid any possible metal contamination. Samples were taken at various time intervals and analysed by ICAP spectroscopy (Section 6.3.6).

### 6.2.4 Activity Testing

A fixed bed microreactor system (Figure 6.2 and Plate 4) was used for catalyst activity testing. Catalyst charges of 5 g were mixed with 5 g of carborundum and loaded in the reactor. Atmospheric gas oil containing 2% wt S was used as feed. The operating conditions were: Pressure: 40 bar, Temperature 350°C, $H_2$/oil ratio: 400 ml/ml/h, LHSV: 6 $h^{-1}$. The catalyst was presulphided in the reactor. The presulphiding procedure involved passing 3 wt% $CS_2$ in atmospheric gas oil over the catalyst maintained at 300°C and 40 bars pressure. LHSV was adjusted to 6 $h^{-1}$ and presulphiding was continued for three hours.

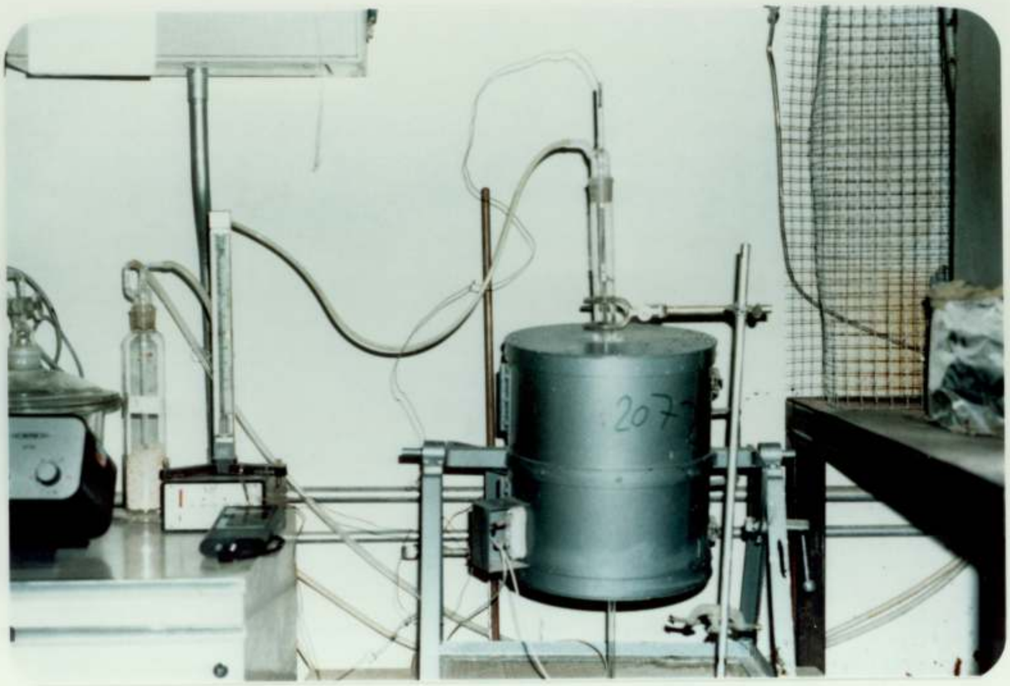

Plate 2. Decoking apparatus, general arrangement.
(Heater with internal column containing catalyst sample on the right.
Gas flow control and dehumidifier on the left.).

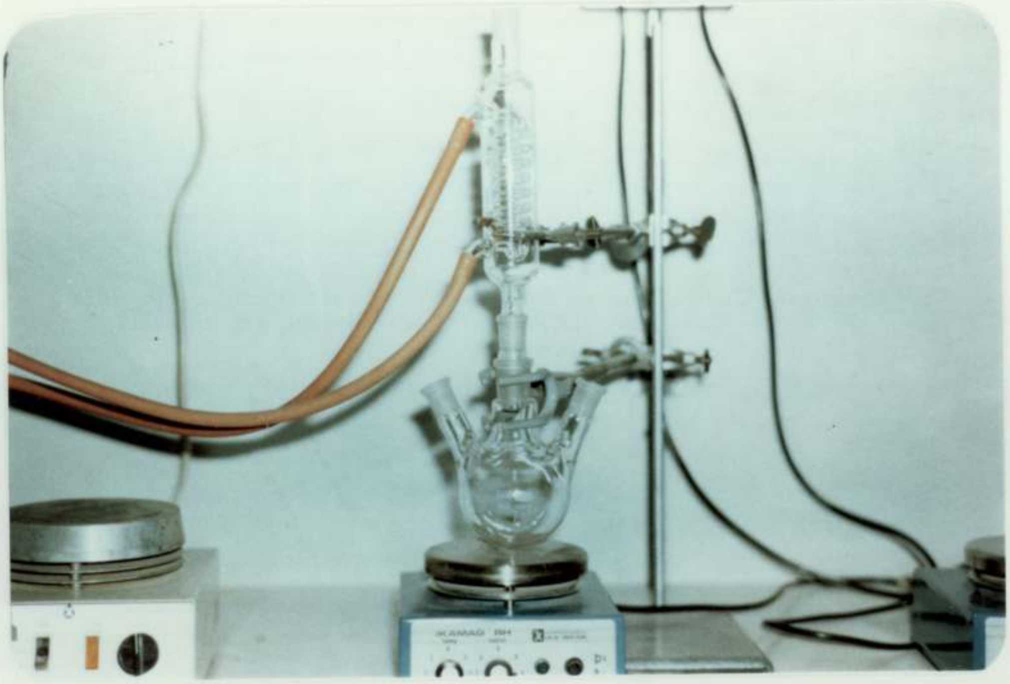

Plate 3. Pure metal sulphide leaching apparatus.
(one of 4).

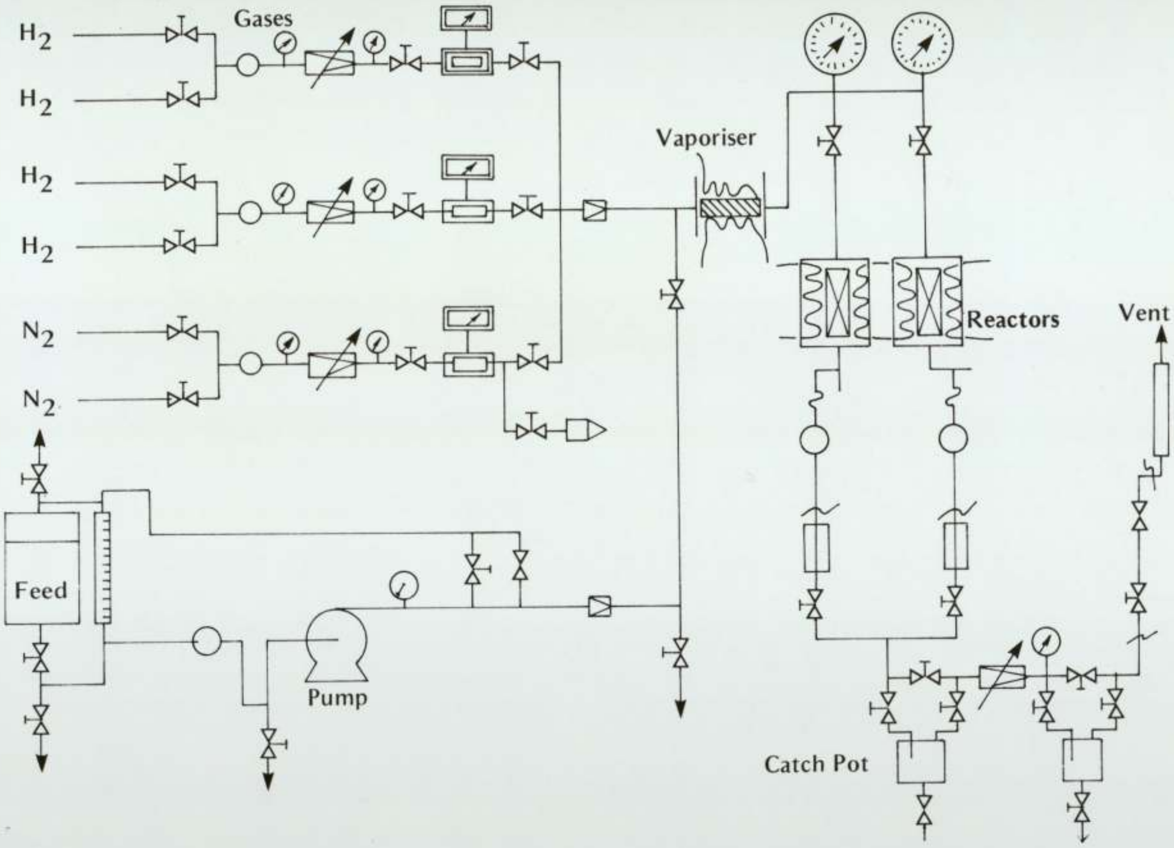

Figure 6.2. Schematic of the micro reactor assembly

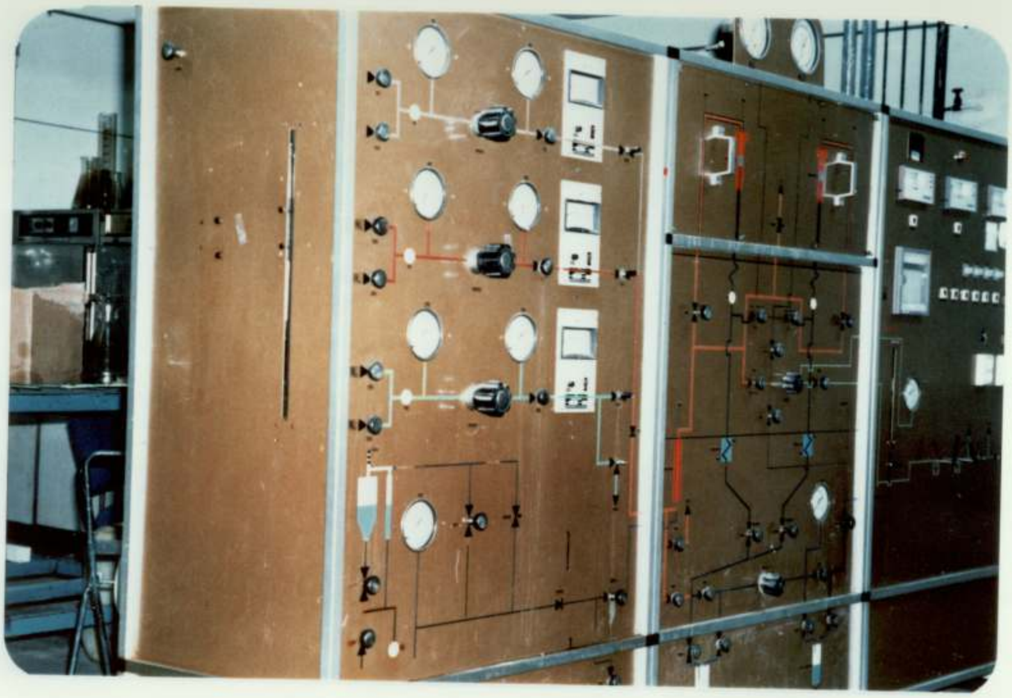

Plate 4. Front control panel of hydrodesulphurization microreactor.

## 6.3 Characterization and Analytical Techniques

### 6.3.1 Surface Area

The surface areas of the catalysts were determined by nitrogen adsorption (BET method). A Quantasorb adsorption unit manufactured by Quantachrome Corporation, U.S.A., was used for BET adsorption isotherm measurements. The experimental details are described fully in Appendix 1.3. The principle of the method is discussed below.

The usual form of the BET equation that describes the adsorption of a gas upon a solid surface is,

$$\frac{P/P_o}{V(1-P/P_o)} = \left(\frac{1}{V_m C}\right) + \left(\frac{C-1}{V_m C}\right) P/P_o$$

where V is the volume of gas adsorbed at pressure P; $P_o$ is the saturation pressure (the vapour pressure of liquified gas at the adsorbing temperature); $V_m$ is the volume of gas required to form an adsorbed mono-molecular layer; and C is a constant related to the energy of adsorption. When experimental data are plotted as $\{P/P_o\}/\{V(1-(P/P_o))\}$, the ordinate against $P/P_o$ as the abscissa, a straight line results for $P/P_o$ values between 0.05 and 0.35. The intercept and slope are $1/V_m C$ and $(C-1)/V_m C$, respectively.

$$\text{Slope + intercept} = \frac{C-1}{V_m C} + \frac{1}{V_m C} = \frac{1}{V_m}$$

The monolayer volume is thus expressed as the reciprocal of slope plus intercept. The total number of gas molecules (Nm) in the monolayer volume (in cc/stp) is given by:

$$Nm = \frac{V_m}{22400} \times \text{Avogadro's number}$$

Using 16.2 $A^2$ as the area covered by an adsorbed nitrogen molecule, the total surface area(s) is calculated.

$$S = \frac{V_m}{22400} \times 6.023 \times 10^{23} \times 16.2 \times 10^{-20}\ m^2 = 4.35 \times V_m m^2$$

### 6.3.2 Pore Volume

The pore volume of a catalyst sample was determined by measuring the volume of nitrogen adsorbed at a relative pressure of 0.98 at liquid nitrogen temperature. The same Quantasorb adsorption apparatus was used for this purpose. The pore volume was calculated using the following equation:

$$V_{pore} = \frac{P \times V_{ads}}{RT} \times V_m \qquad (1)$$

where

$P$ is the ambient pressure (1 atm);

$V_{ads}$ is the volume of nitrogen adsorbed per gram catalyst;

$T$ is the room temperature in degrees Kelvin;

$V_m$ is the molar volume of liquid adsorbate (34.7 $cm^3$ for $N_2$); and

$R$ is the gas constant (82.1 ml atm. $deg.^{-1}$ $mole^{-1}$).

Assuming that cylindrical pores constitute the nature of the entire surface, the average pore diameter can be calculated using the following equation:

$$d = \frac{4\ V_{pore}}{S} \times 10^4 \text{ Angstroms}$$

where

$V_{pore}$ is the pore volume per gram catalyst ($cm^3$) and

$S$ is the surface area ($m^2/g$)

### 6.3.3 Pore Size Distribution

The pore size distribution of the catalyst samples were obtained with a Micromeritics model 9305 mercury porosimeter. The method involves intrusion of mercury into the pores at various pressures (0-30,000 psi). Since the pressure exerted is related to the pore diameter by the following equation, the volume of mercury intruding the pores of varying diameters can be obtained.

$$D = \frac{-4\,\sigma\cos\theta}{P}$$

where

$D$ = Pore diameter

$\sigma$ = Surface tension of mercury (484 dynes/cm)

$\theta$ = Contact angle (generally varies between 130-142 degrees)

$P$ = The pressure exerted

### 6.3.4 Energy Dispersive X-ray Analysis

Energy dispersive X-ray analysis (EDAX) was used for detecting qualitatively, the presence of various contaminant elements (Ni, V, S, P) and catalytic metals (Mo, Co) in the catalysts.

### 6.3.5 Distribution Profiles of Metals

A scanning electron X-ray Microprobe Analyzer (Camebax) was used for measuring the distribution profiles of the various metals (V, Ni, Co and Mo).

Catalyst pellets were embedded in acrylic resin and ground by SIC paper without solvent. The polished samples were coated with a 30 µm thick layer of carbon in a vacuum of about $10^{-2}$ torr and were then scanned radially in the SEM to obtain concentration profiles for Mo, Co, Ni and V.

### 6.3.6 Chemical Analysis

Inductively coupled Argon plasma spectroscopy (Jarell-Ash Atom Comp. 750) was used to determine the concentration of various metals V, Ni, Co and Mo present in the catalyst samples and in leach liquids. The analytical procedure is described in detail in Appendix 1.7.

# 7.0 RESULTS

## 7.1 Solids Characterization

### 7.1.1 Characterization of Fresh, Spent, and Decoked Residue Hydrotreating Catalysts

As explained in 6.1.1 both the spent residue hydrotreating catalyst and the fresh catalyst were obtained from KNPC. The spent catalyst for all the experimentation was collected from one typical batch of used atmospheric residue hydrodesulphurization catalyst and the fresh catalyst was from the same batch prior to use.

The physical, chemical and mechanical properties of each sample were analyzed. Special tests were also performed using electron microprobe and X-ray diffraction techniques. The physico-chemical characterization of the spent catalyst was repeated after carbon combustion. The procedure for regeneration of spent catalyst by coke removal is discussed in Chapter 6. The characterization results are presented and discussed in the following section.

### 7.1.1a Physical and Mechanical Properties

The following techniques were used to characterize mechanical and physical properties. (Detailed procedures are described in Appendix 1.1 and 1.2).

#### Average diameter

The average diameter of the spherical catalyst particles was determined by measuring the diameter of 20 individual particles using a micrometer gauge. Results are summarised in Table 7.1.

#### Side Crushing Strength

A Pharma Test (Model PTB 300) was used to measure the side crushing strength of the catalyst particles. This method determines particle crushing strength by measuring the force in Newtons (N) required to crush the particle. Thirty particles were tested from each catalyst sample and the average value reported Table 7.1.

Bulk Density

A cylindrical P.V.C. container was used to determine the bulk density. The weight (in grams) of a known volume (100 ml) of the compacted catalyst was determined and the bulk density was calculated in g/ml (Table 7.1).

Table 7.1. Physical and Mechanical Properties of Fresh, Spent and Decoked Catalysts

| Catalyst | Shape | Average Diameter (mm) | Side Crushing (N/Pellet) | Bulk Density (g/ml) |
|---|---|---|---|---|
| Fresh | spherical | 1.44 | 39 | 0.716 |
| Spent | spherical | 1.522 | 34 | 1.306 |
| Decoked | spherical | 1.48 | 30 | 1.207 |

The catalysts were in the form of spheres. The fresh catalyst had an average diameter of 1.44 mm. The average diameters of the spent and decoked catalyst were 1.522 mm and 1.48 mm, respectively. The bulk density of the spent catalyst was significantly greater (by about 82%) than that of unused (fresh) catalyst, probably due to deposition of metals (V and Ni) during use. The crushing strength of the spent catalyst appeared to be slightly lower (12.8%) than that of the fresh catalyst.

### 7.1.1b Chemical Analyses

Inductively-coupled Argon Plasma Spectroscopy was used to determine the concentration of various metals (V, Ni, Co and Mo) present in the catalyst samples. The analytical procedures are described in detail in the Catalyst Characterization Handbook (156). The sample was atomized in a high temperature plasma, and the atomic spectra resolved into atomic lines of each element by an optical grating in an optical spectrometer.

The chemical compositions are presented in Table 7.2.

The spent catalyst had evidently accumulated considerable amounts of carbon (11.1 % wt), vanadium (15.1% wt), nickel (3.7% wt) and sulphur (8.34% wt) during the hydrotreating process. Small amounts of iron and sodium were also detected on the spent catalyst.

Table 7.2. Metal and Carbon Deposits in Fresh, Spent and Decoked Catalysts

| Element | Catalyst | | |
|---|---|---|---|
| | Fresh | Spent | Decoked |
| Carbon (wt %) | 0 | 11.1 | 1.4 |
| Sulphur (wt %) | 0 | 8.34 | 3.86 |
| Vanadium (wt %) | 0 | 15.1 | 16.5 |
| Nickel (wt %) | 0.2 | 3.7 | 4.1 |
| Cobalt (wt %) | 3.27 | 1.07 | 1.07 |
| Molybdenum (wt %) | 11.72 | 3.99 | 4.2 |
| Iron (wt %) | Nil | 0.18 | 0.13 |
| Sodium (wt %) | Nil | 0.10 | 0.23 |

Combustion of carbon under controlled conditions (decoking) resulted in the elimination of the majority of carbon and sulphur deposits, but left the metals in the catalyst. These results are generally in agreement with those reported in the literature (113, 105, 98, 101) and confirm that deposition of carbon and metals are the main causes of deactivation.

The presence of the contaminant metals such as vanadium and nickel along with the catalytic metals, Mo and Co, in the spent and decoked catalysts was further confirmed by Energy Dispersive X-ray Analysis (EDAX), Figures 7.1, 7.2 and 7.3. These contaminant metals were not present in the fresh catalyst (Figure 7.1).

The influence of the coke and metal deposits on catalyst deactivation was also assessed by measurement of the surface area and porosity of fresh, spent and decoked catalyst samples. The results of these tests are presented and discussed in the following sections.

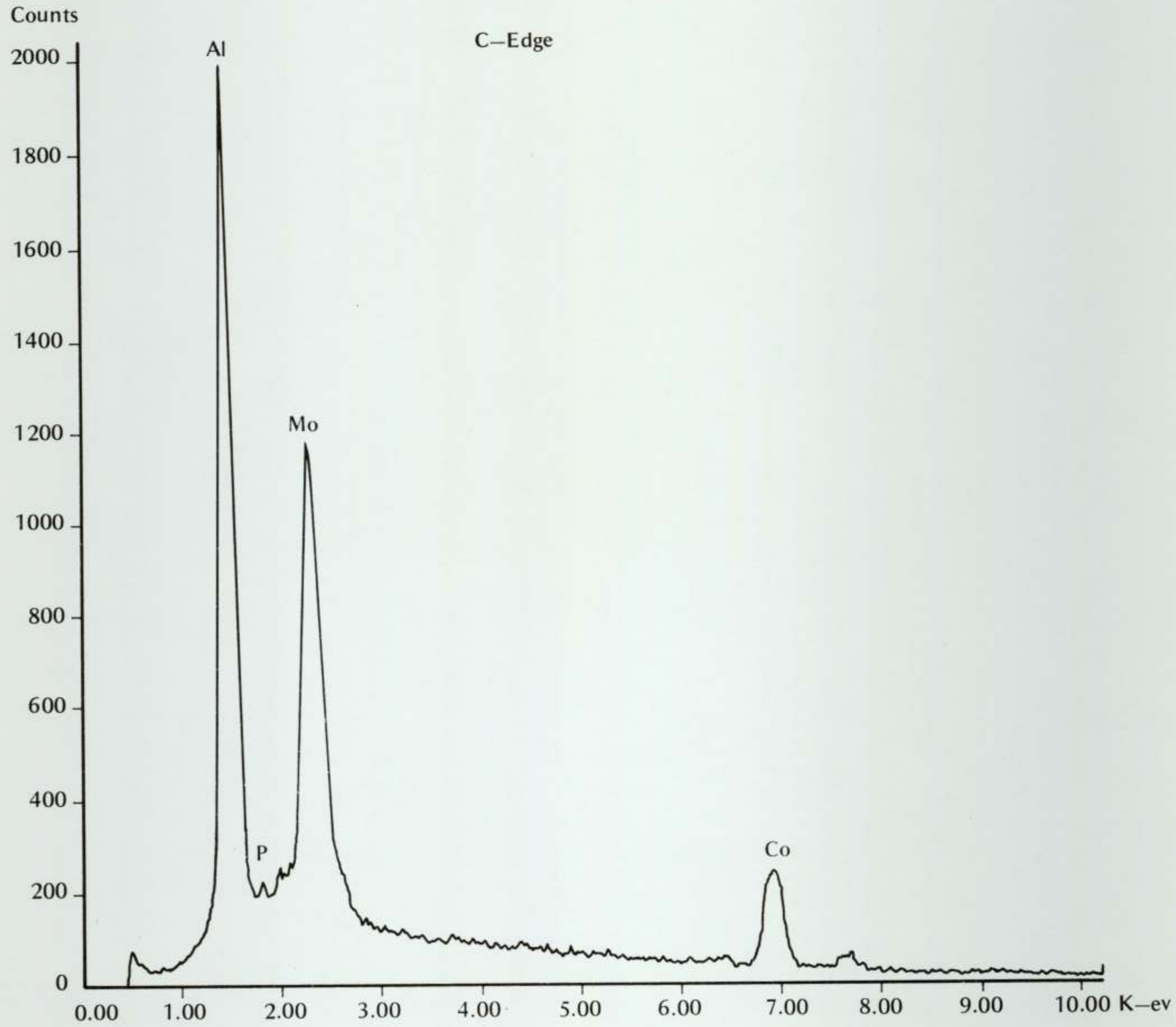

Figure 7.1. Energy dispersive X-ray analysis (EDAX) of fresh ARDS catalyst.

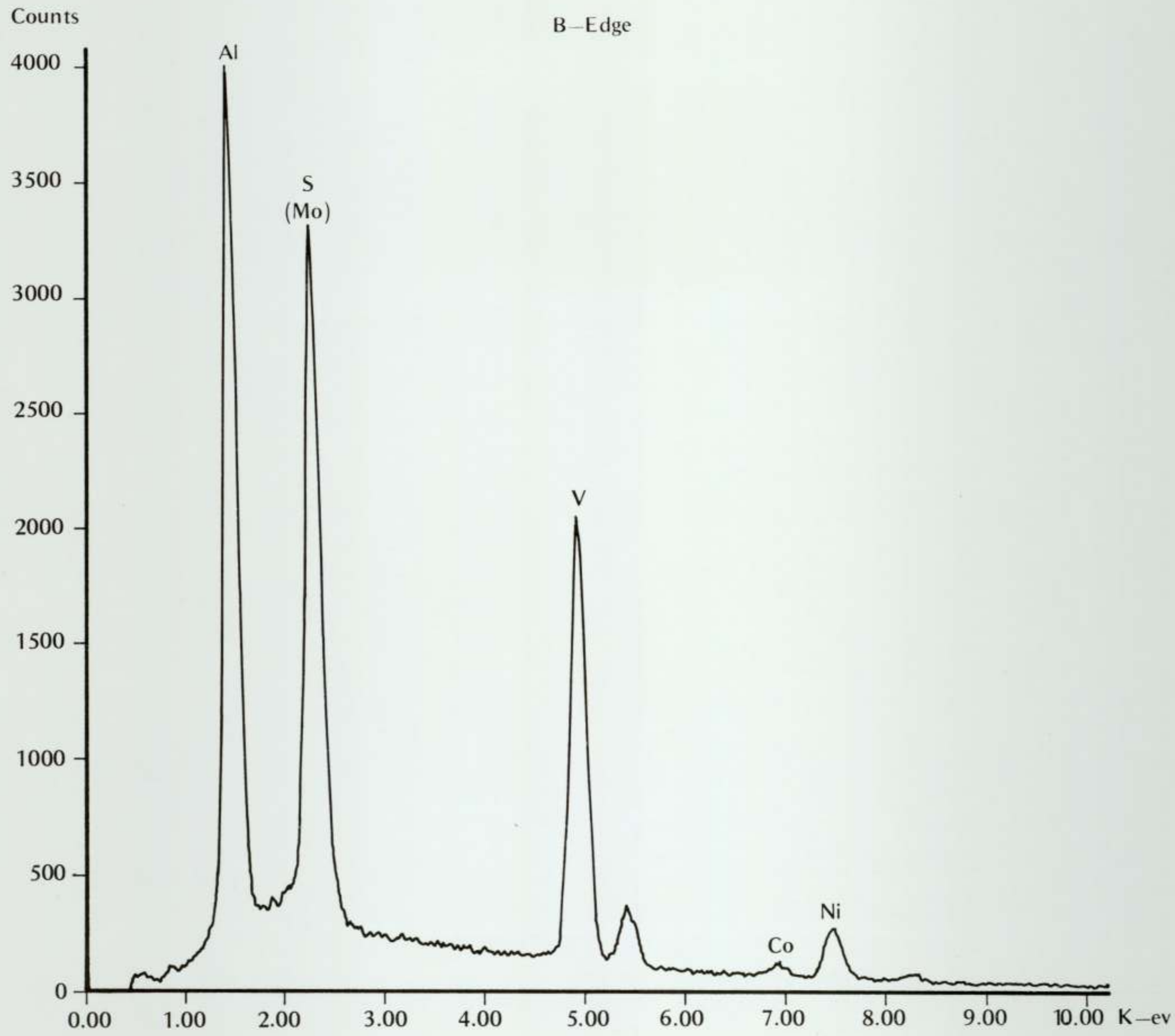

Figure 7.2. Energy dispersive X-ray analysis (EDAX) of spent ARDS catalyst.

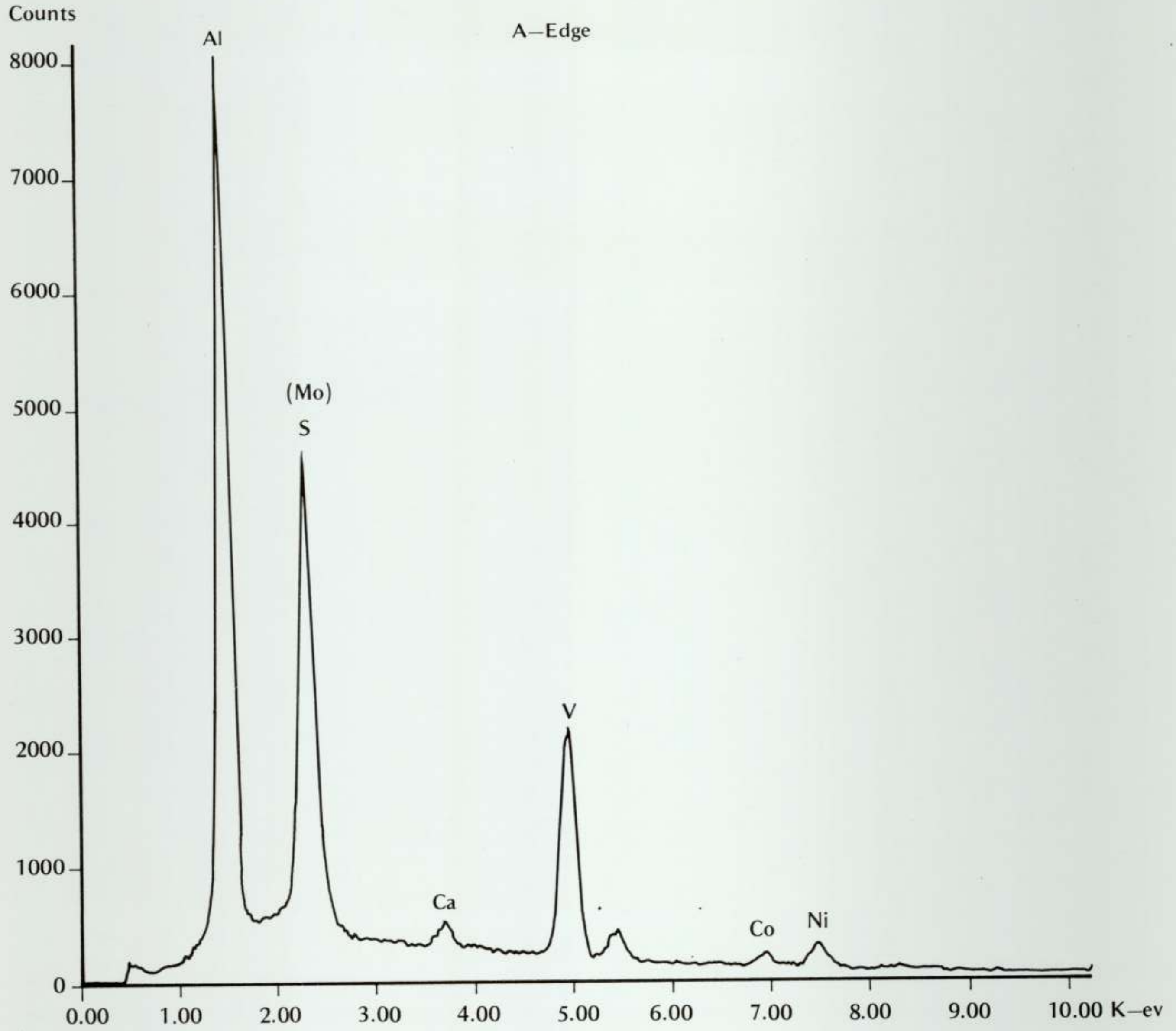

Figure 7.3. Energy dispersive X-ray analysis (EDAX) of decoked ARDS catalyst.

### 7.1.1c Surface Area and Pore Volume

Surface areas and pore volumes of catalyst samples were determined by the BET method using a Quantasorb adsorption unit manufactured by Quantachrome Corporation, USA. The experimental details are described fully in Appendices 1.3, and 1.4.

Table 7.3 shows the surface area and pore volume data for fresh, aged and decoked catalysts.

Table 7.3. Surface Area and Pore Volume of Fresh, Spent and Decoked Catalysts

| Catalyst | Surface area $m^2/g$ | Pore Volume (ml/g) |
|---|---|---|
| Fresh | 202.7 | 0.71 |
| Spent | 43.8 | 0.14 |
| Decoked | 60.4 | 0.22 |

The data indicate that the surface area and pore volume of the spent catalyst were, respectively, 78% and 80% lower than those of the fresh catalyst. While decoking of the spent catalyst under conditions of controlled combustion increased the surface area and pore volume to some extent, the values were still considerably lower than for the fresh catalyst. Thus, the surface area and pore volume of the decoked catalyst were, respectively, 70% and 69% less than the unused catalyst.

### 7.1.1d Pore Size Distribution

The pore size distribution in the various catalyst samples were measured by the mercury porosimetry technique. A Micromeritics mercury porosimeter model 9305 was used for this purpose.

Pore size distributions in fresh, spent and decoked catalysts are shown in Table 7.4. The fresh catalyst had a large portion of the pore volume distributed mainly in two ranges of pore diameter, 60-150 A° and > 10000 A°. About 16% of the pores were present in pore diameters less than 60 A°.

Most of the pores in the spent catalyst appeared to be closed or plugged by the deposits. The pores had been narrowed by the deposits, as indicated by the fact that approximately 66% of the available pores had diameters < 60 A°. A similar situation was observed for the decoked catalyst except that a small number of pores in the diameter range 60-150 A° were opened by coke removal.

These results clearly indicate that the metal deposits predominently contribute to the narrowing of the pores and pore mouth plugging.

Table 7.4. Pore Size Distribution Data

| Pore Diameter (A°) | Pore Volume ml $g^{-1}$ | | |
|---|---|---|---|
| | Fresh | Spent | Decoked |
| < 60 | 0.114 | 0.092 | 0.0877 |
| 60 - 100 | 0.10 | 0.00 | 0.0163 |
| 100 - 150 | 0.123 | 0.00 | 0.0735 |
| 150 - 250 | 0.005 | 0.00 | 0.00 |
| 250 - 500 | 0.012 | 0.00 | 0.0066 |
| 500 - 1000 | 0.006 | 0.0065 | 0.0081 |
| 1000 - 5000 | 0.009 | 0.0040 | 0.0115 |
| 5000 - 10000 | 0.003 | 0.0066 | 0.00 |
| > 10000 | 0.342 | 0.0311 | 0.0163 |

### 7.1.1e Electron Microprobe Analysis

The distribution profile of the metals within a catalyst particle was measured by electron microprobe analysis using a scanning electron X-ray microscope fitted with a dispervise X-ray analyzer (EDAX).

Figure 7.4 illustrates the concentration profiles of vanadium, nickel, molybdenum and cobalt across the diameter of a spent catalyst pellet. This demonstrates that the concentration of vanadium deposits was highest near the exterior surface and decreased to a minimum at the center. Nickel penetrated further into the interior of the catalyst pellet. The active catalyst metals (Co and Mo), originally present in the catalyst, were uniformly distributed within the pellet. The large amount of vanadium (approximately 15% by wt) deposited on the catalyst was probably responsible for plugging the pores, causing catalyst deactivation as observed by other authors (98, 101, 102).

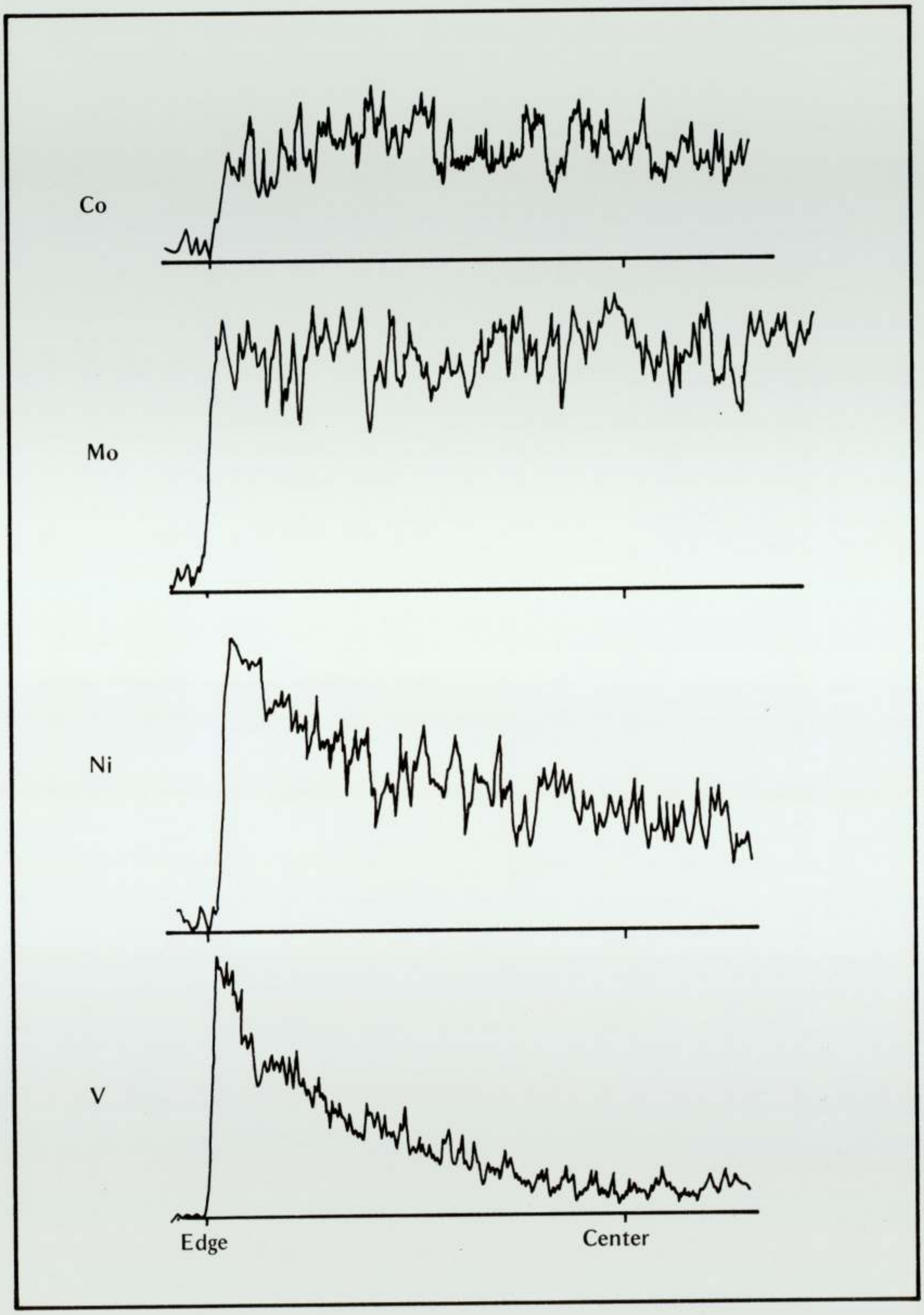

Figure 7.4. Concentration distribution profiles of V, Ni, Mo and Co in the spent catalyst.

### 7.1.1f X-ray Diffraction

X-ray diffraction patterns of fresh, spent and decoked catalysts were examined using a Philips PW 1410 X-ray spectrometer operated at 30 KV and 20 MA with Cu K α radiation to gain information on the nature of metal compounds, or phases, present in the catalyst before and after decoking. The results (Figure 7.5) indicate that vanadium was deposited on the spent catalyst mainly as sulphide ($V_2S_3$ and $V_7S_8$). No peaks corresponding to nickel sulphide or other nickel salts were detected. It is likely that nickel compounds are present in the spent catalyst either as small crystallites or in an amorphous form. The γ-alumina phase structure appears to be retained in the spent and decoked catalysts.

### 7.1.2 Characterization of Pure Metal Sulphides

Pure metal sulphides were obtained from Winlab Limited at a purity of 99.9%.

Surface areas, porosities and pore volumes of these solids were measured as described above. Results are summarized in Table 7.5.

Table 7.5. Surface Area, Pore Volume and Average Pore Size of Pure Metal Sulphides

| Compounds | Surface Area $m^2\ g^{-1}$ | Pore Volume ml/gm | Average Pore Size A° |
|---|---|---|---|
| $V_2S_3$ | 7.15 | $112 \times 10^{-3}$ | 31.4 |
| $MoS_2$ | 4.3 | $6.1 \times 10^{-3}$ | 28.4 |
| CoS | 1.53 | $3.45 \times 10^{-3}$ | 45.00 |
| NIS | 1.23 | $1.68 \times 10^{-3}$ | 27.4 |

These results indicate that $V_2S_3$ had the highest surface area (7.15 $m^2g^{-1}$) with respect to the rest ($MoS_2$ 4.3 $m^2g^{-1}$, CoS 1.53 $m^2g^{-1}$ and NIS 1.23 $m^2g$). Pore volume followed the same trend.

The low pore volumes indicate that the pure metal sulphides are essentially nonporous particles.

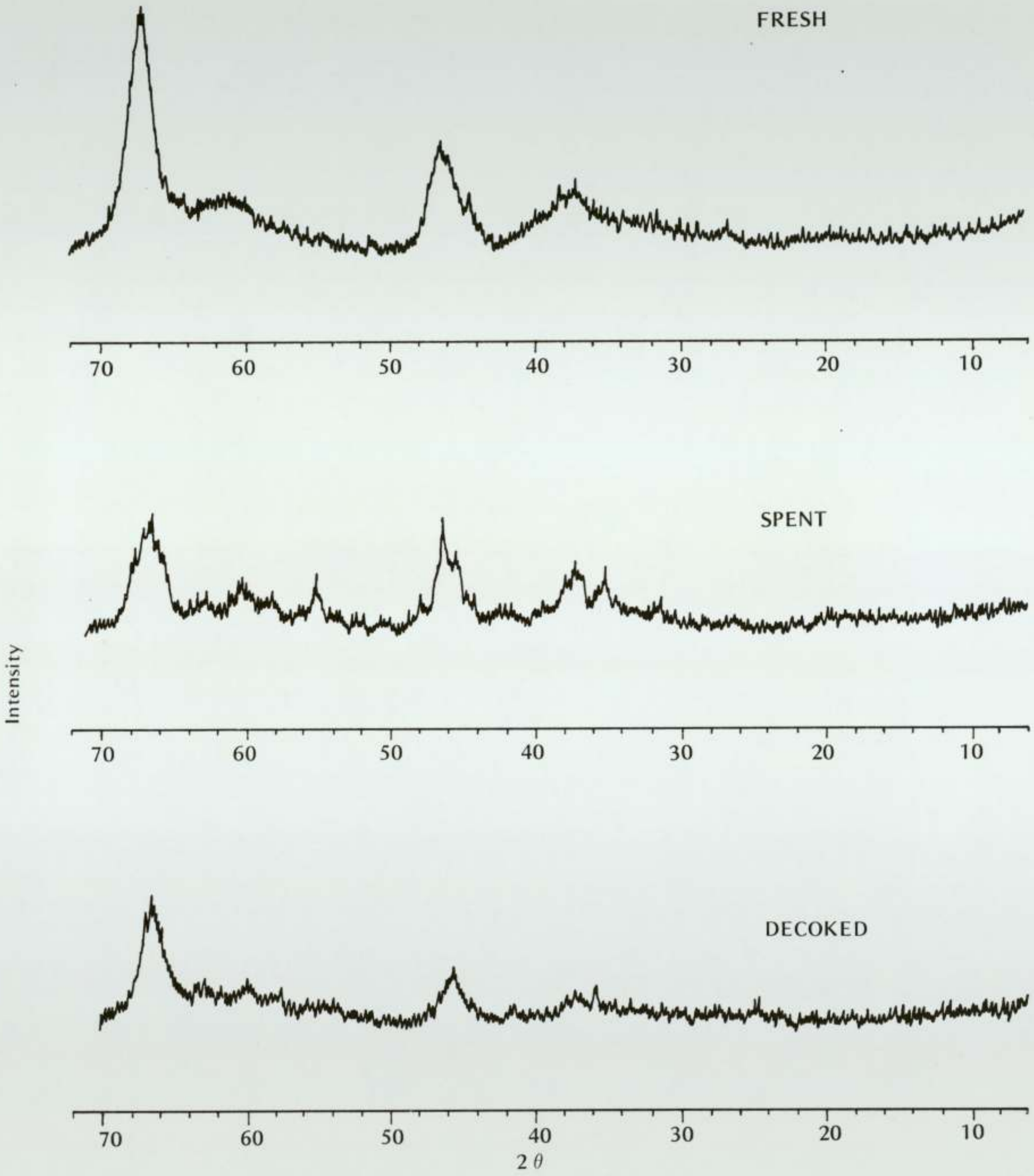

Figure 7.5. X-ray diffraction patterns of fresh, spent and decoked catalyst.

### 7.2 Regeneration of Spent Catalyst

Regeneration of hydrotreating catalyst by conventional methods to remove carbonaceous material was ineffective for restoring the catalyst activity due to the deposition of metals within the catalyst. Therefore regeneration of such hydrotreating catalyst should also aim to remove metal deposits.

#### 7.2.1 Leaching of Contaminated Metal Sulphides from Spent Catalyst

It is clear from the literature review and the characterization of catalyst that deactivation of catalyst is caused primarily by:

a. coke deposition.

b. metal deposition, mainly vanadium and to a lesser extent nickel.

c. decrease in porosity, and hence surface area, associated with (a) and (b) above.

The experimental program was designed to remove the contaminated metals mainly (V and Ni), by leaching of used catalyst after deoiling. The catalysts still contained carbon and were mainly in the sulphide form. Leaching was carried out using selective solvents of organic reagents capable of forming water-soluble metal complexes. The effect of different parameters such as reagent concentration, temperature, and extraction time were studied. The results of these studies are presented and discussed below.

##### 7.2.1.1 Effect of Different Acids

Three different acids (oxalic acid, malonic acid and acetic acid) were used as reagents for metal leaching from spent catalyst. The leaching experiments were conducted in a fixed bed laboratory glass reactor as described earlier. The influence of each acid at a fixed concentration of 0.33 M on the removal of vanadium is compared in Figure 7.6 as a function of extraction time. The efficiency of the acids for vanadium extraction was in the order.

oxalic acid › malonic acid › acetic acid

For example after a fixed time of 12 hours the amounts of vanadium removed by oxalic acid, malonic acid, and acetic acid were 12.3%, 8.4%, and 5% respectively. A similar behaviour is demonstrated in Figures 7.6 to 7.7 at higher acid concentration (1 Molar).

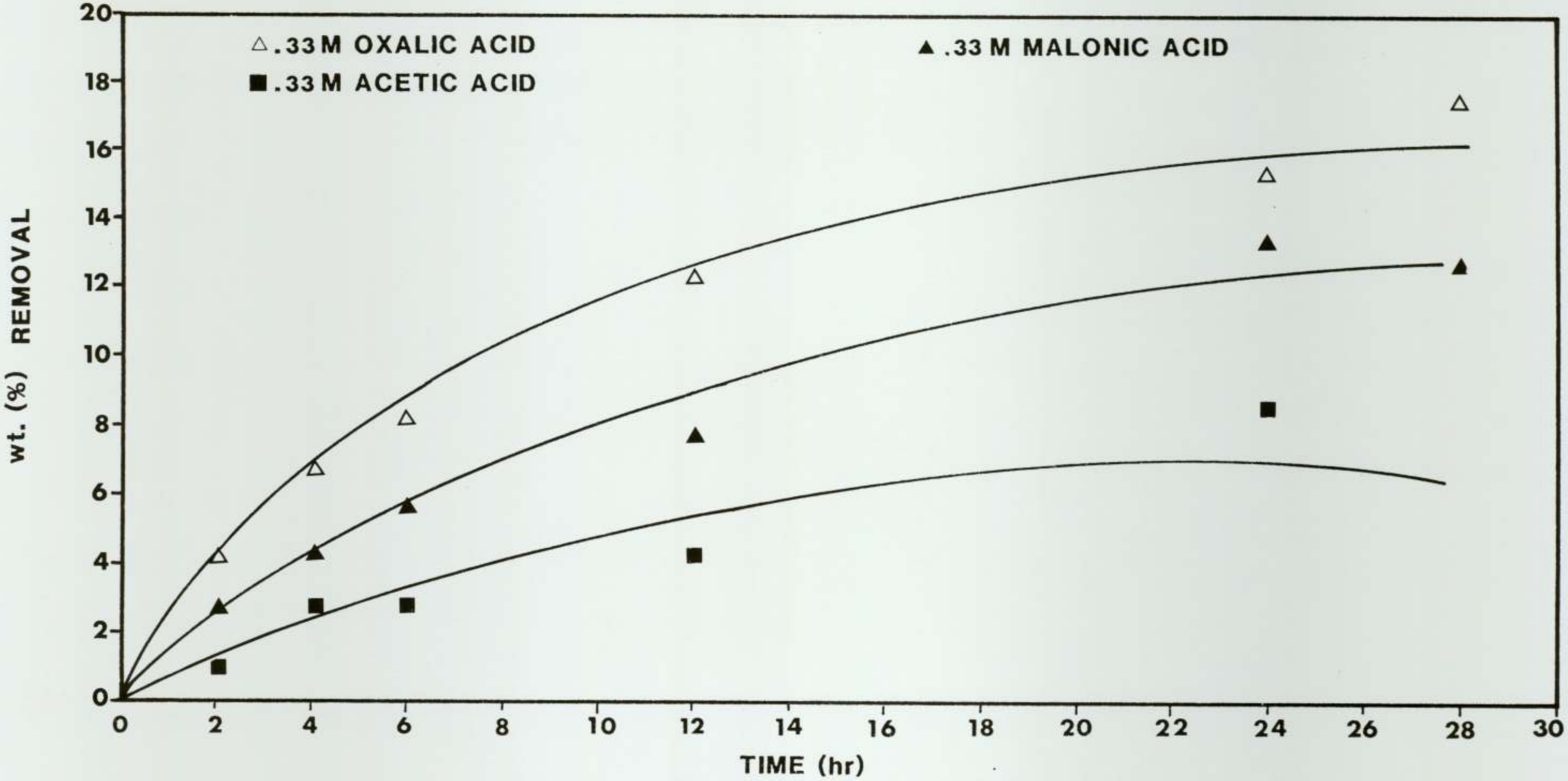

Figure 7.6. Effect of different reagents on V Removal. T = 25°C.

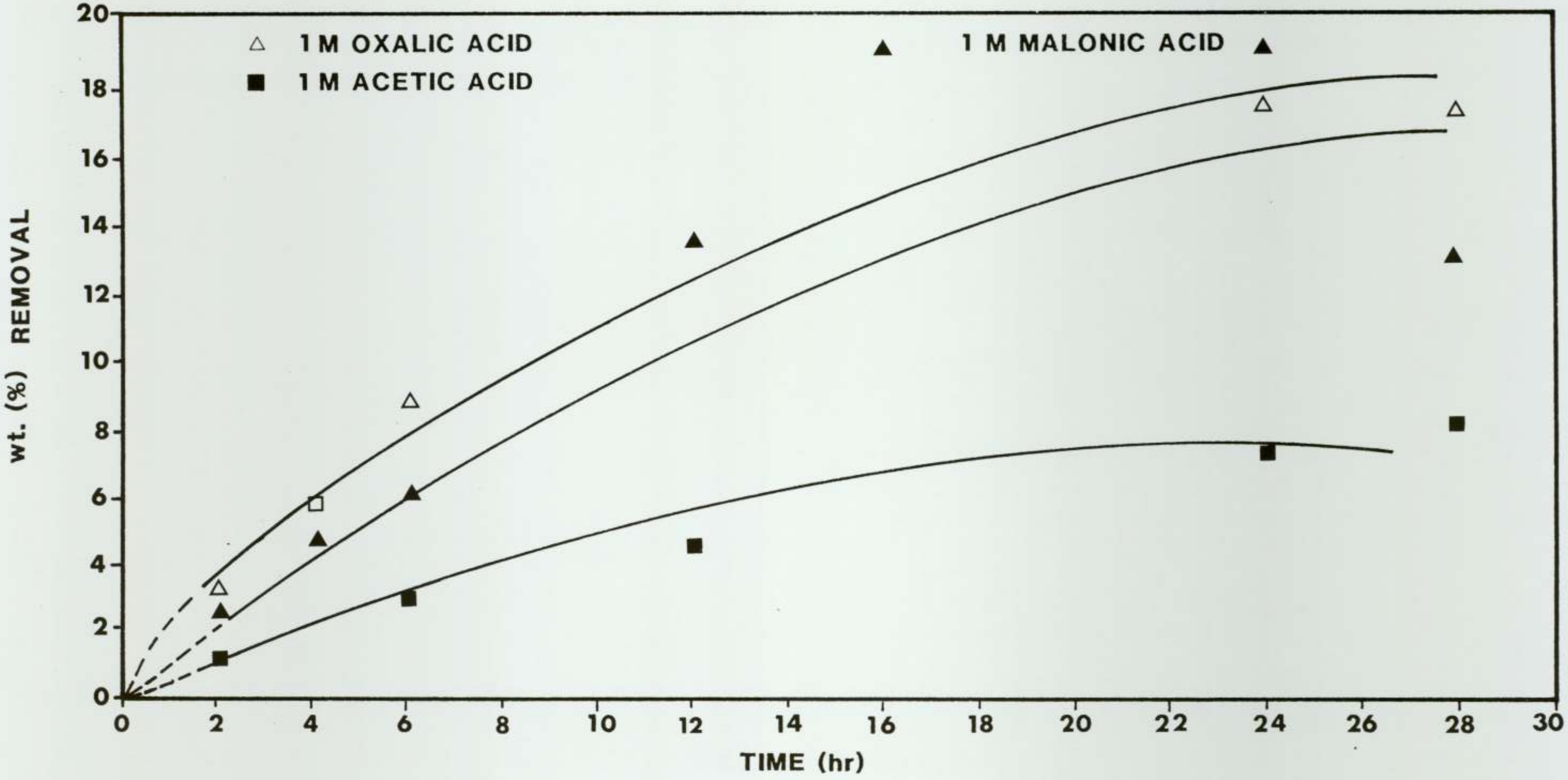

Figure 7.7. Effect of different reagents on V Removal. T = 25°C.

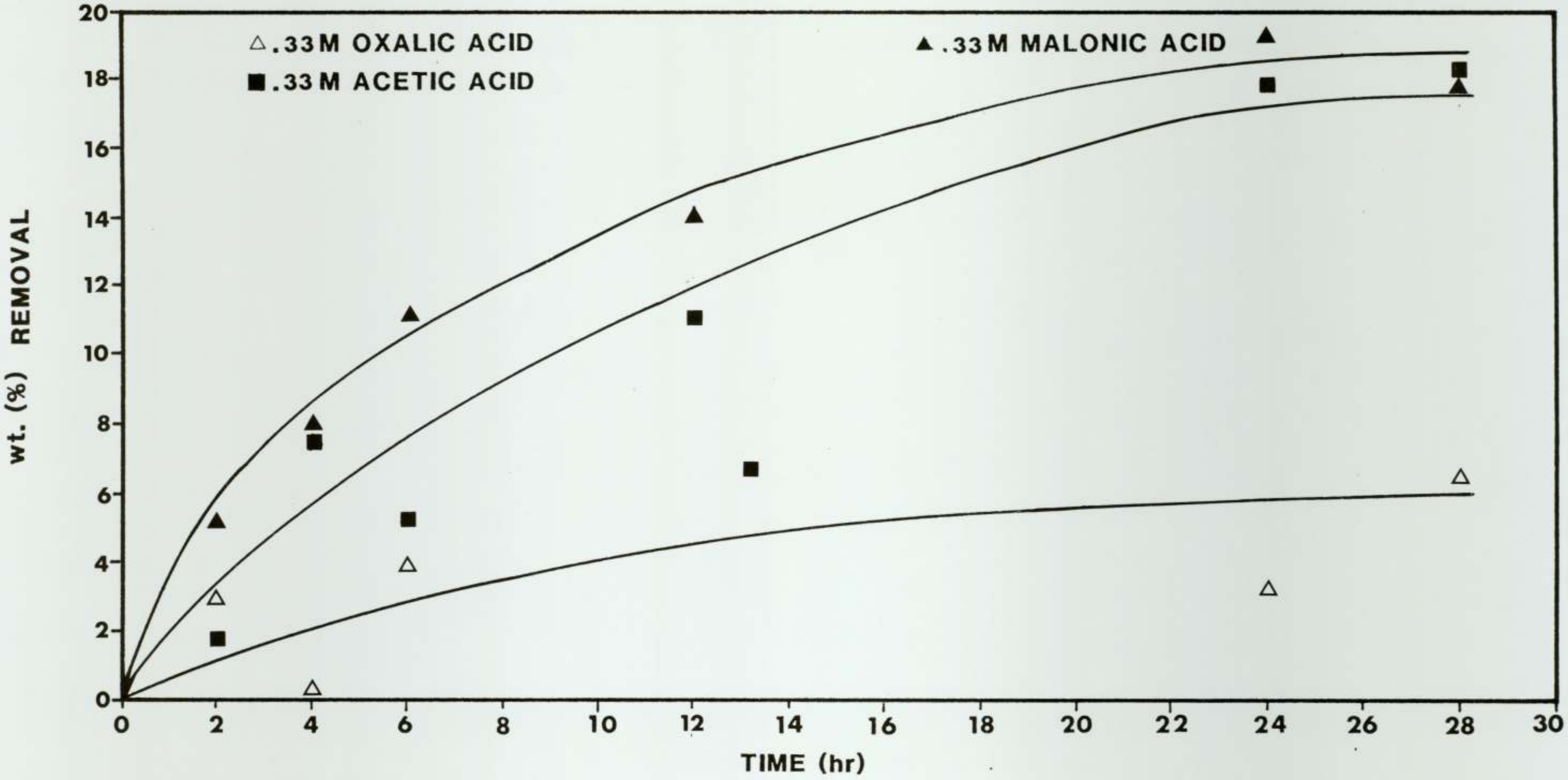

Figure 7.8. Effect of different reagents on Ni removal. T = 25°C.

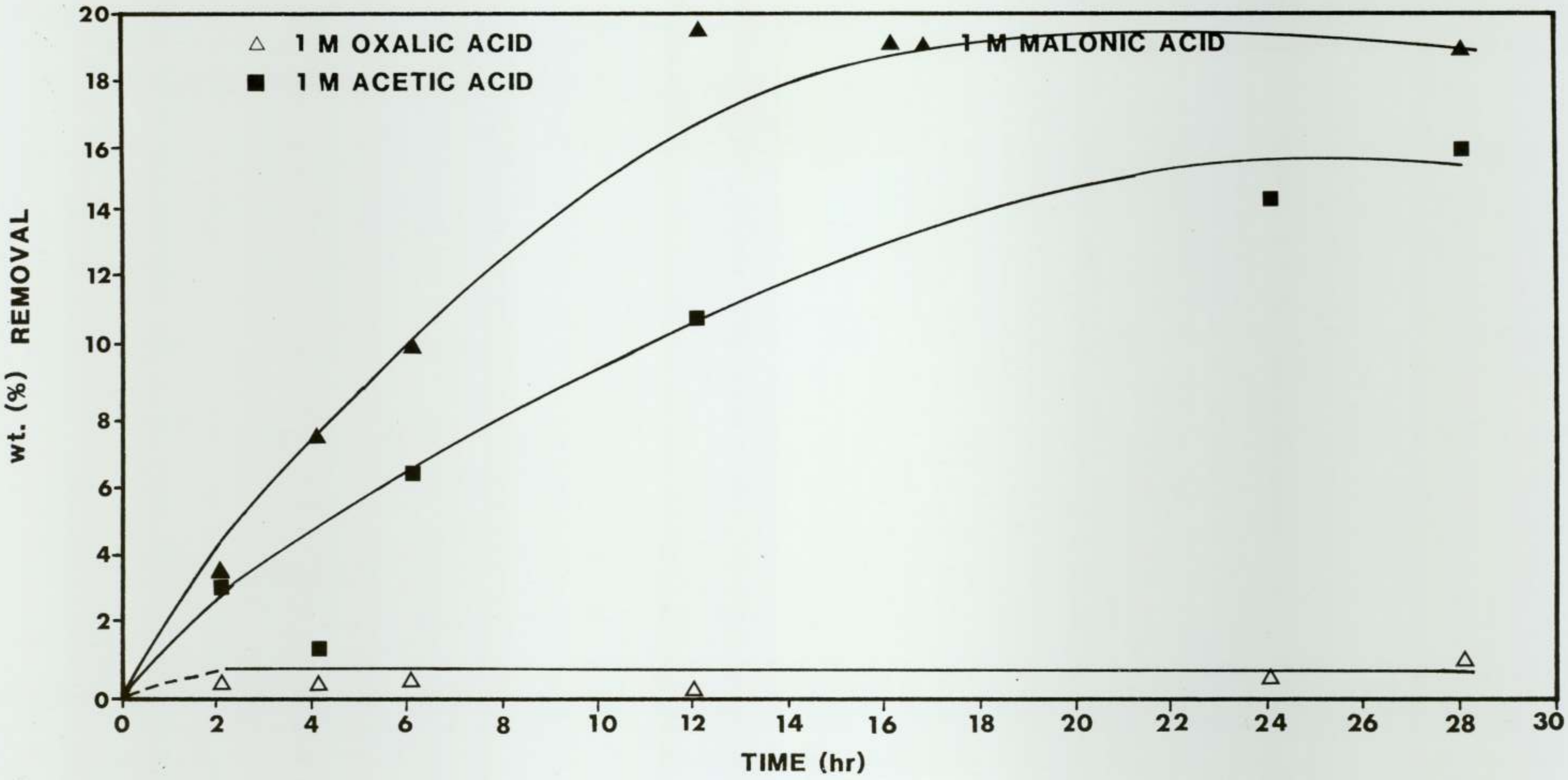

Figure 7.9. Effect of different reagents on Ni Removal. T = 25°C.

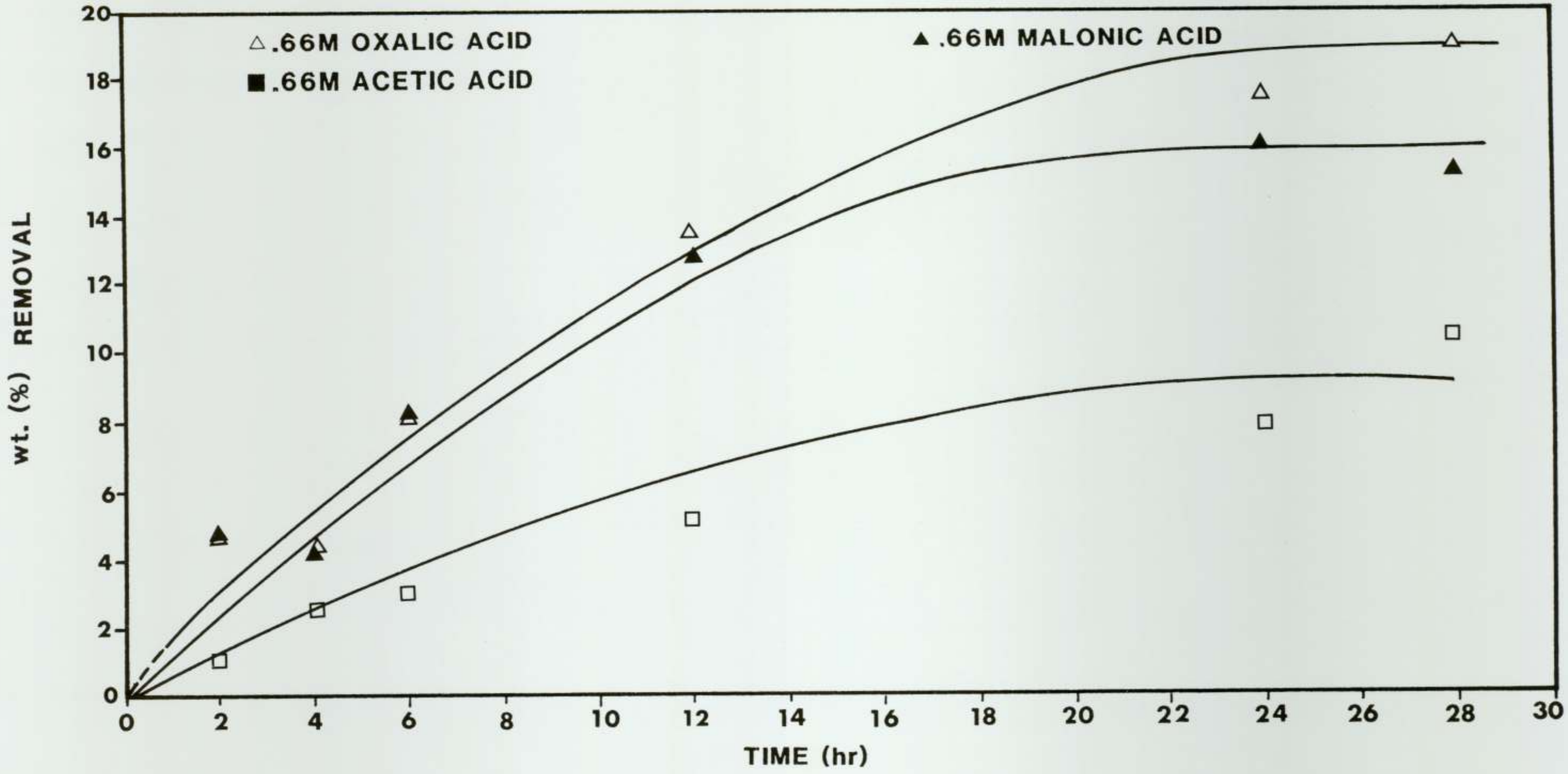

Figure 7.10. Effect of different reagents on V removal. T = 25°C.

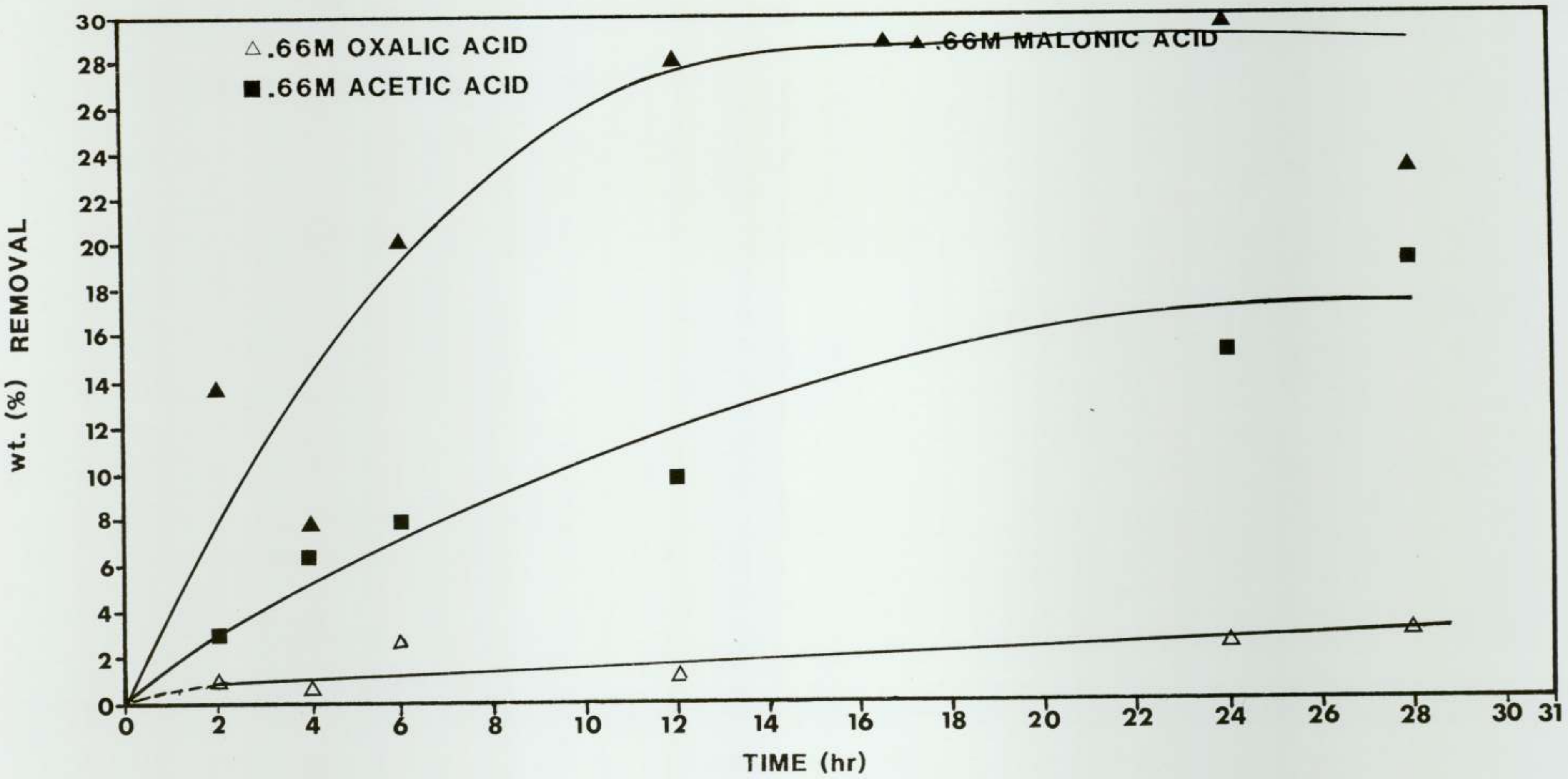

Figure 7.11. Effect of different reagents on Ni removal. T = 25°C.

In the case of nickel extraction, malonic acid appears to possess the highest activity. From data presented in Figures 7.8 and 7.9, it is evident that the activities of the acids for nickel extraction are in the order:

malonic acid > acetic acid > oxalic acid

### 7.2.1.2 Effect of Acid Concentration

The effect of acid concentration on metal leaching was studied at a constant temperature using three different concentrations (0.33 M, 0.66 M and 1 M) of the selected acids. A similar extraction procedure was used. The results presented in Figures 7.6 to 7.11 indicate that the reagent concentration had no significant effect on metals removal. For example, in the case of oxalic acid, vanadium levels after 24 hours were for the different concentrations, (0.33 M, 0.66 M and 1 M) 16%, 18% and 18% respectively. This conclusion is in agreement with previous studies conducted by Beuther (135), on the leaching of catalytic cracking catalyst.

### 7.2.1.3 Effect of Temperatures

The effect of temperature on the leaching behaviour of metals was investigated at constant concentration (0.66 molar) for all three acids and at different periods of time. The temperatures used in the study were 25°C, 50°C and 75°C. Results are shown in Figures 7.12 - 7.18. In some cases temperature had little effect on metal leaching, for example in the case of V leaching by malonic acid (Figure 7.12), and also in the case of V with acetic acid (Figure 7.14). In others, temperature increased the degree of leaching significantly, for example V and Ni with oxalic acid (Figures 7.15 and 7.16), Mo with malonic acid (Figure 7.17) and Ni with acetic acid (Figure 7.18).

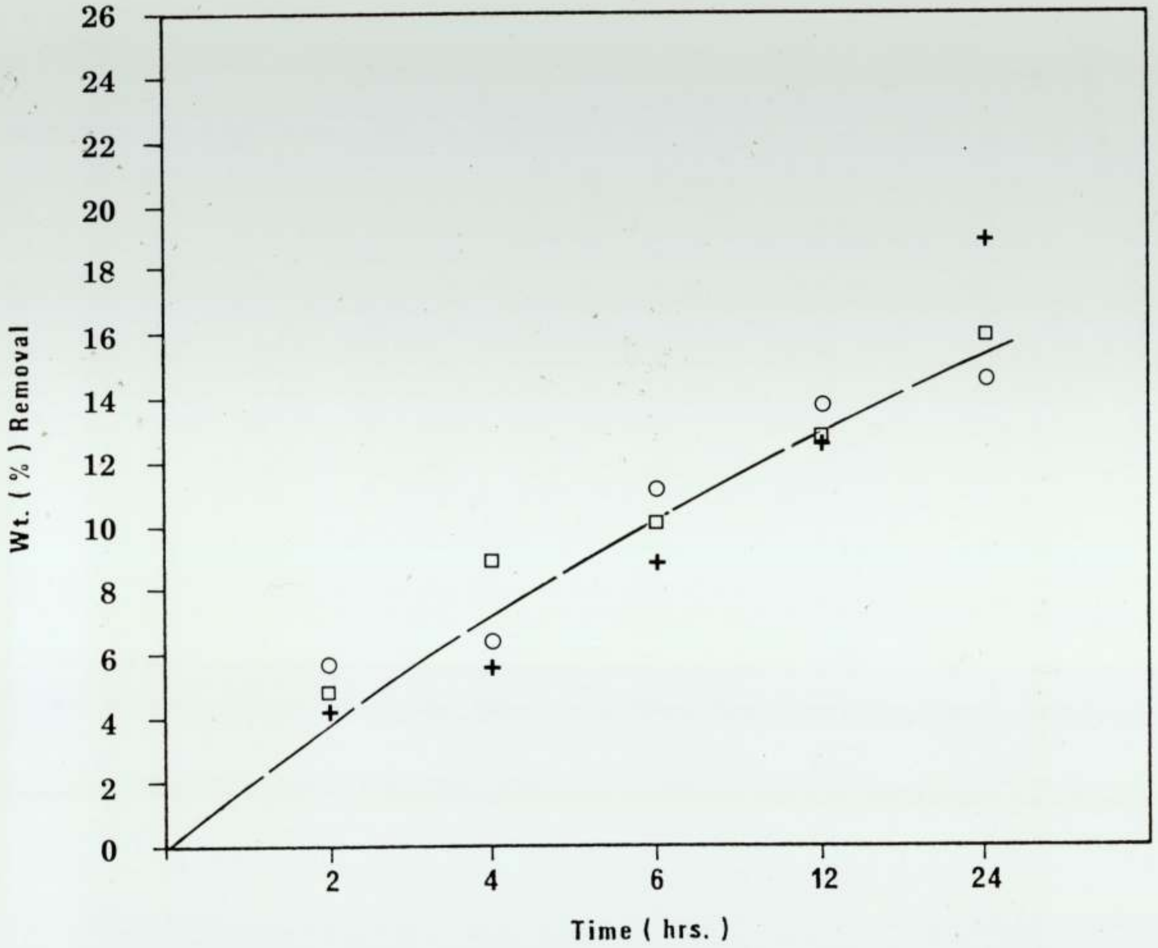

Figure 7.12. Effect of temperature on V removal using malonic acid without promoter at □ 25°C, + 50°C, ○ 75°C.
Acid concentration = 0.66 M.

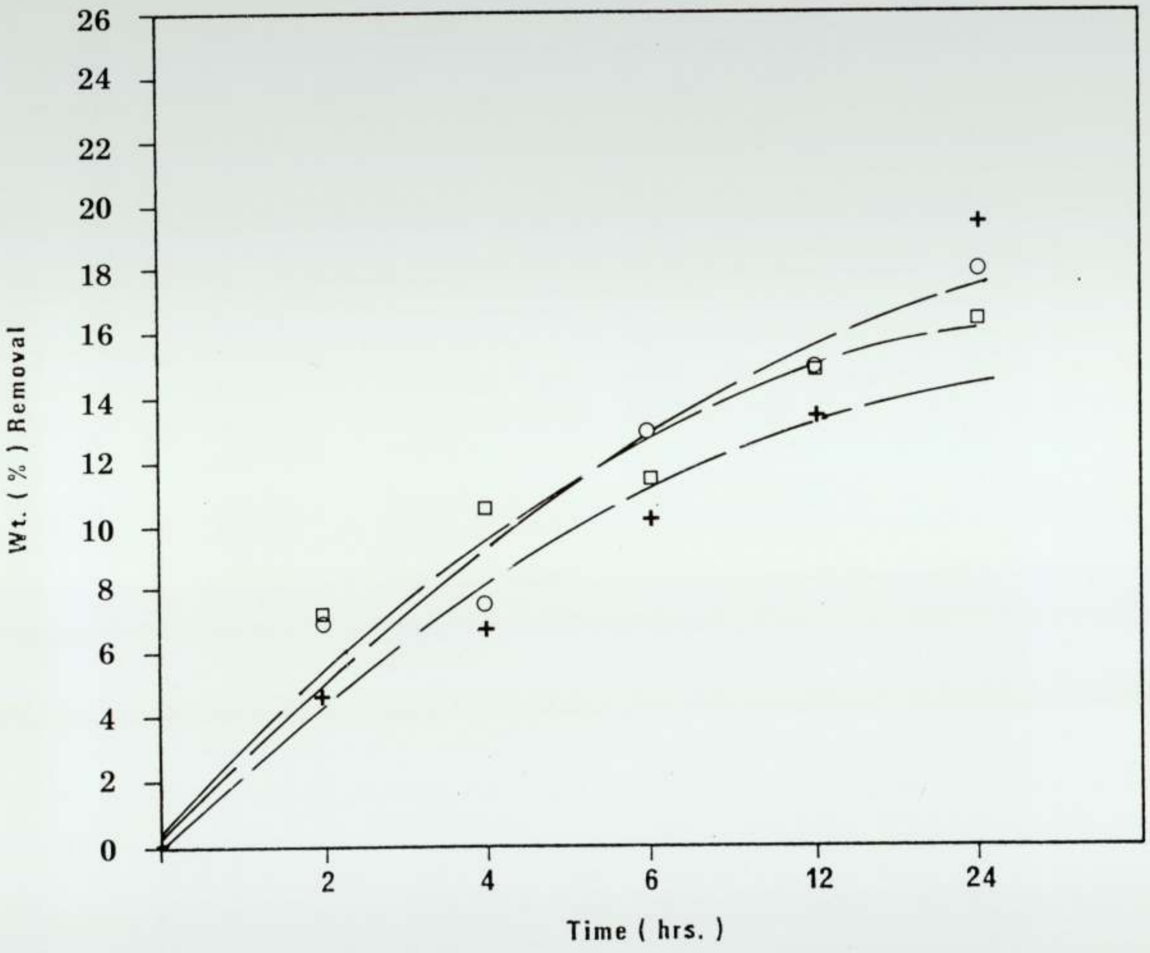

Figure 7.13. Effect of temperature on Co removal using malonic acid without promoter at □ 25°C, + 50°C, ○ 75°C.

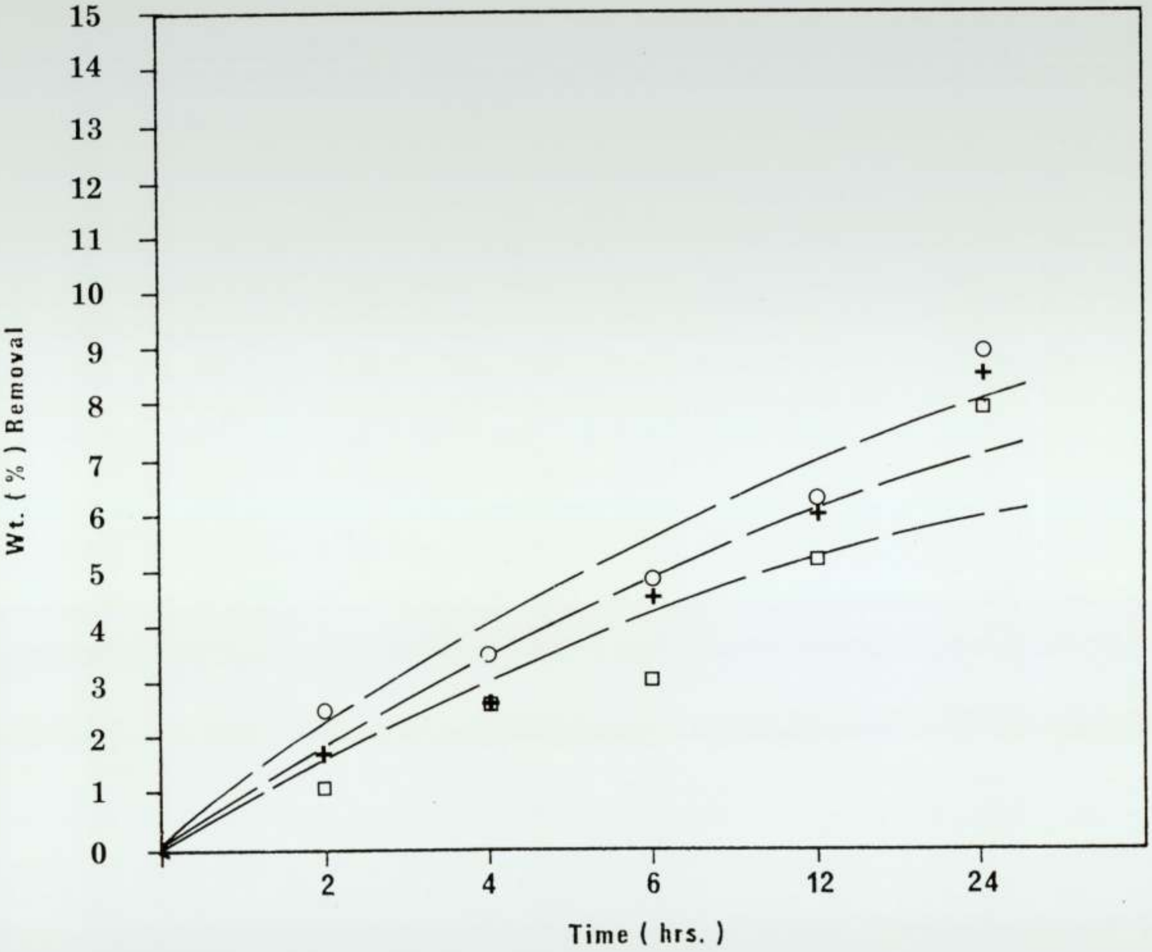

Figure 7.14. Effect of temperature on V removal using acetic acid without promoter at □ 25°C, + 50°C, ○ 75°C.
Acid concentration = 0.66 M.

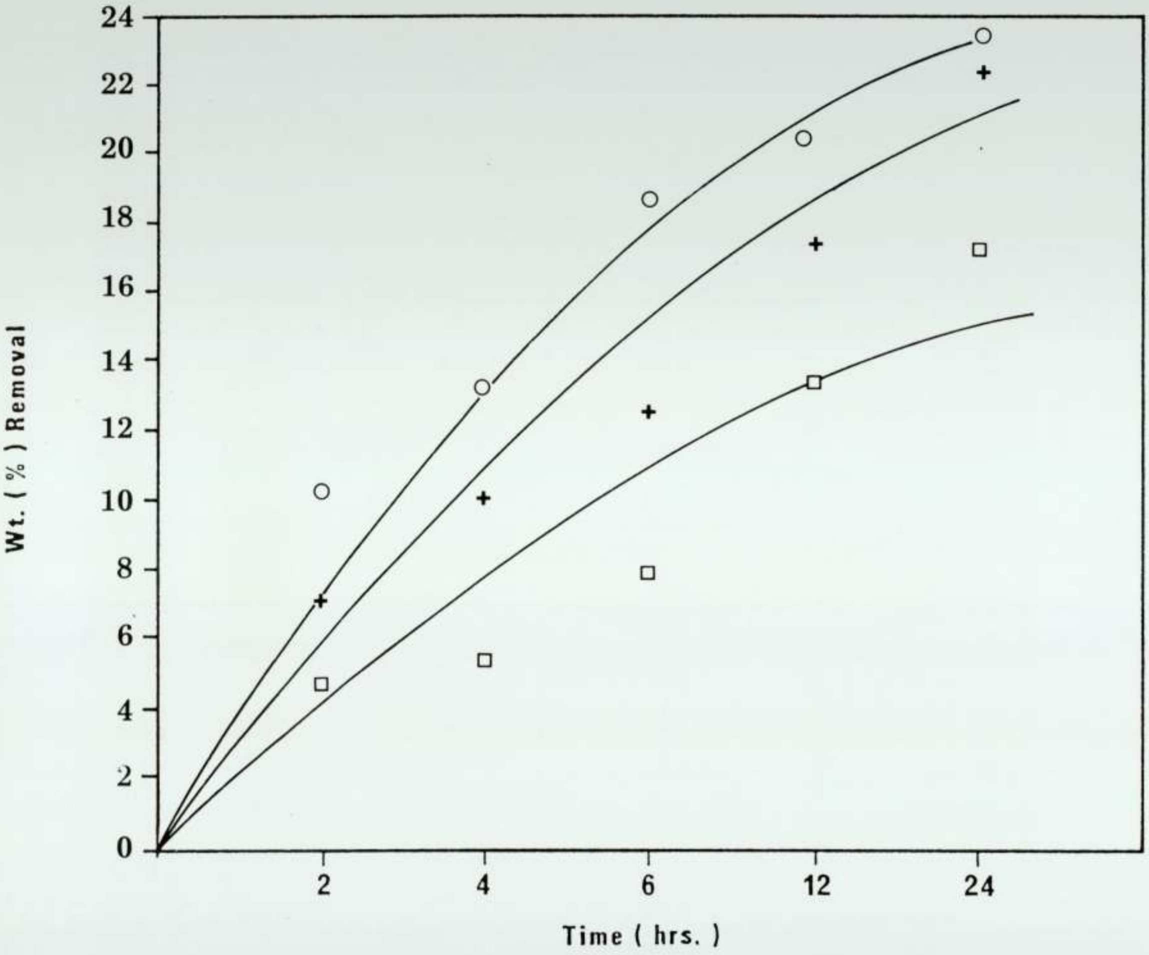

Figure 7.15. Effect of temperature on V removal using oxalic acid without promoter at □ 25°C, + 50°C, ○ 75°C.
Acid concentration = 0.66 M.

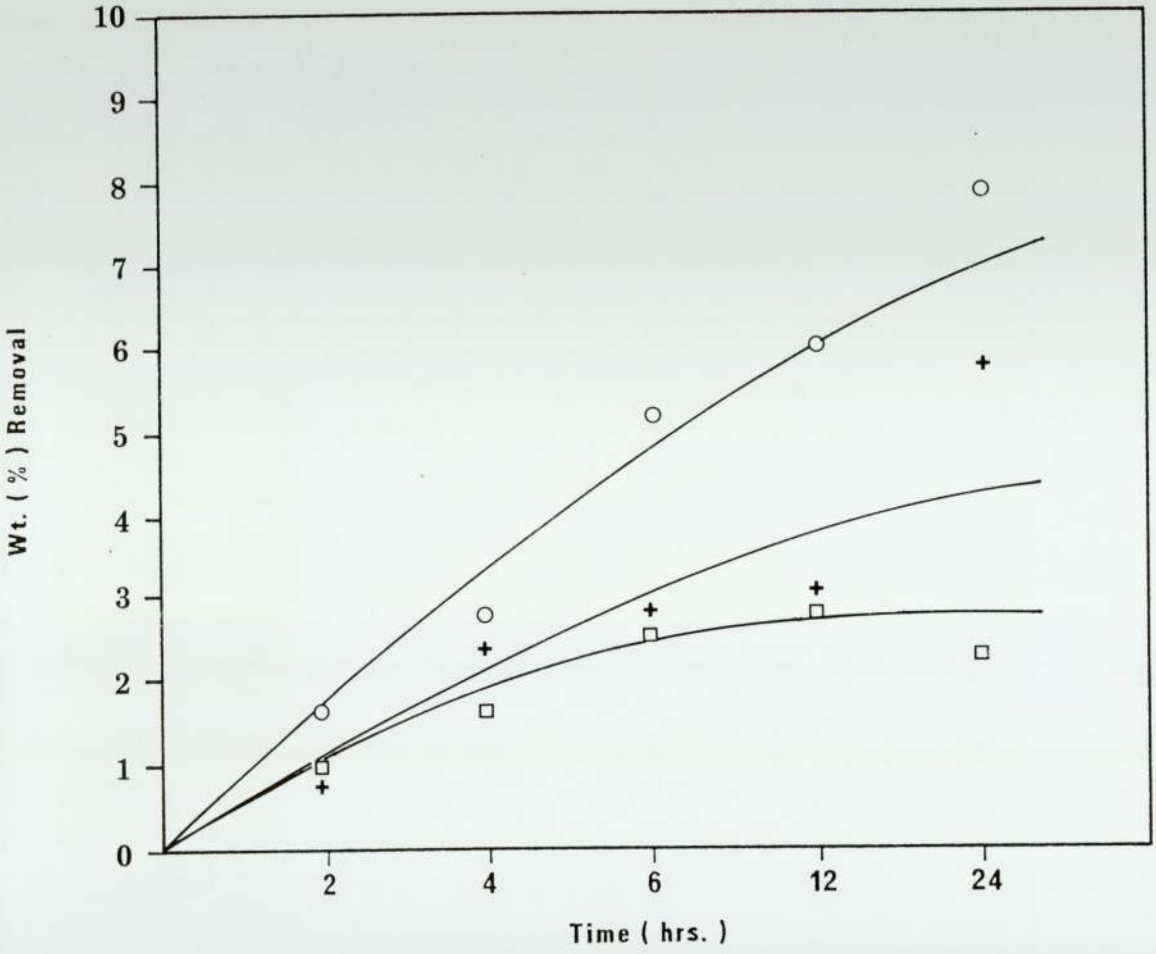

Figure 7.16. Effect of temperature on Ni removal using oxalic acid without promoter at □ 25°C, + 50°C, ○ 75°C.
Acid concentration = 0.66 M.

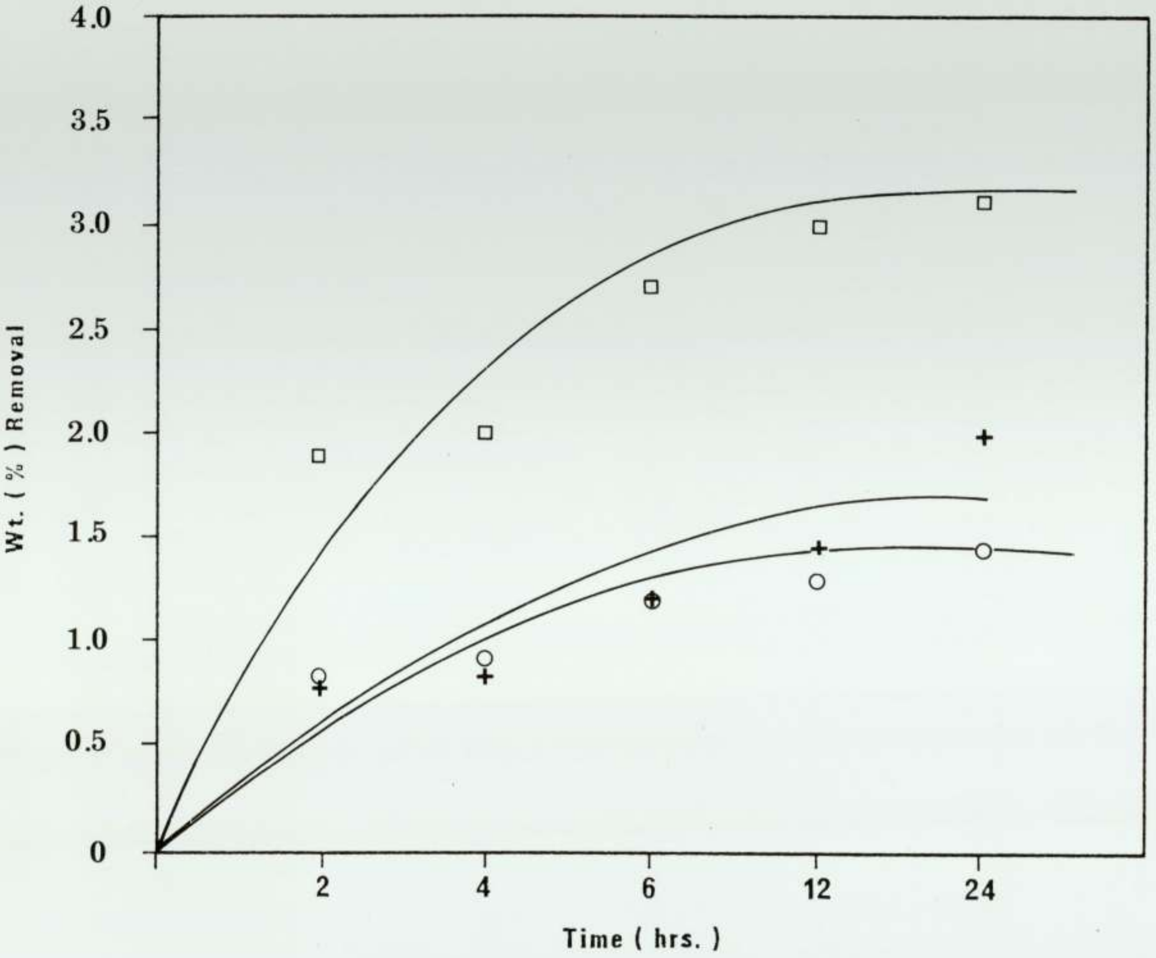

Figure 7.17. Effect of temperature on Mo removal using malonic acid without promoter at □ 25°C, + 50°C, ○ 75°C.
Acid concentration = 0.66 M.

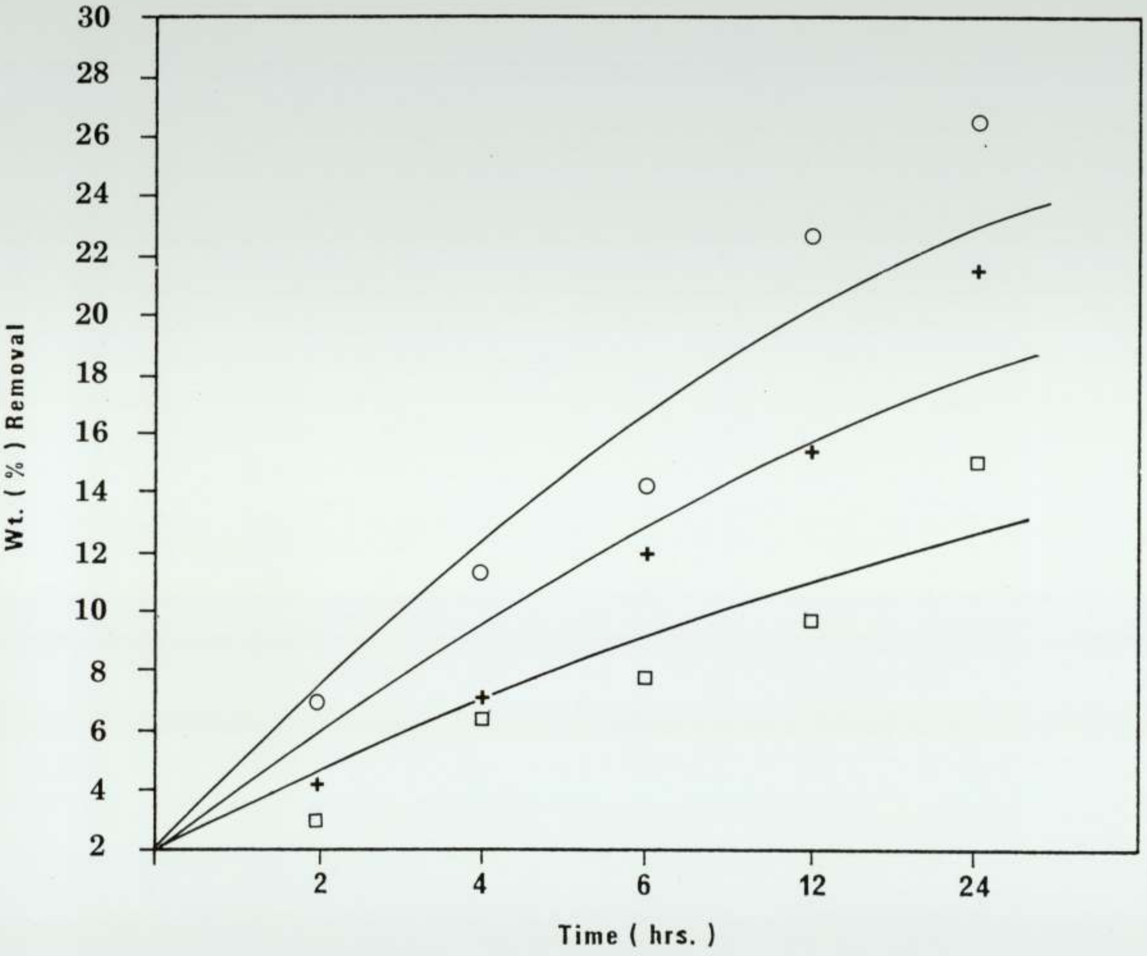

Figure 7.18. Effect of temperature on Ni removal using acetic acid without promoter at □ 25°C, + 50°C, ○ 75°C. Acid concentration = 0.66 M.

### 7.2.1.4 Effect of Time

Contact time was found to have a significant effect on the degree of metals removal. Thus, at 2 hours, the amount of vanadium removed was 4.7%; this increased to 13.5 wt % on increasing the contact time to 12 hours. The percent weight removal of metals in general levelled-off after 24 hours.

### 7.2.1.5 Effect of Promoter

Studies were conducted using each of the three acids mixed with aluminium nitrate, in order to investigate the promoting influence of the added salt on the metal extraction behaviour. The concentrations of aluminium nitrate and the acid in the mixed reagent were 1 M and 0.66 M respectively. The experiments were conducted at three different temperatures (25, 50 and 75°C) and the extent of leaching of the various metals was monitored as a function of time up to 28 hours.

The results presented in Figures 7.19 - 7.22 demonstrate the effect of oxalic acid with, and without, aluminium nitrate on removal of V, Ni, Mo and Co at one temperature (25°C). A remarkable increase in the percentage extraction of metals is evident when aluminium nitrate was present. For example, the extent of vanadium removal was 13.5% for oxalic acid at 12 hours whereas when oxalic acid and aluminium nitrate was used, the amount of vanadium extracted increased to 48.5 wt %. Similarly, for nickel, the extracted amount increased from 2.8 to 52.5 wt %. For other reagents the improvement was marginal (Figures 7.23 to 7.24).

Experiments were also carried out with aluminium nitrate mixed with each acid at different temperatures. Table 7.6 summarizes the results of the study.

The effect upon the leaching efficiency of selected promoters was also investigated, for oxalic acid only. As shown in Table 7.7, when nitric acid was added to oxalic acid, not only vanadium was removed (79.1%) but also the main catalyst constituents (Co + Mo) (60.2%, 27% respectively).

The percent weight metal removal in the case of oxalic acid with promoter $Al(NO_3)_3$ is almost comparable to the nitric acid case. This indicates that, during the reaction of oxalic acid with aluminium nitrate, nitric acid was formed and that this was responsible for the effective removal of metal contaminants. Oxalic acid and aluminium nitrate resulted

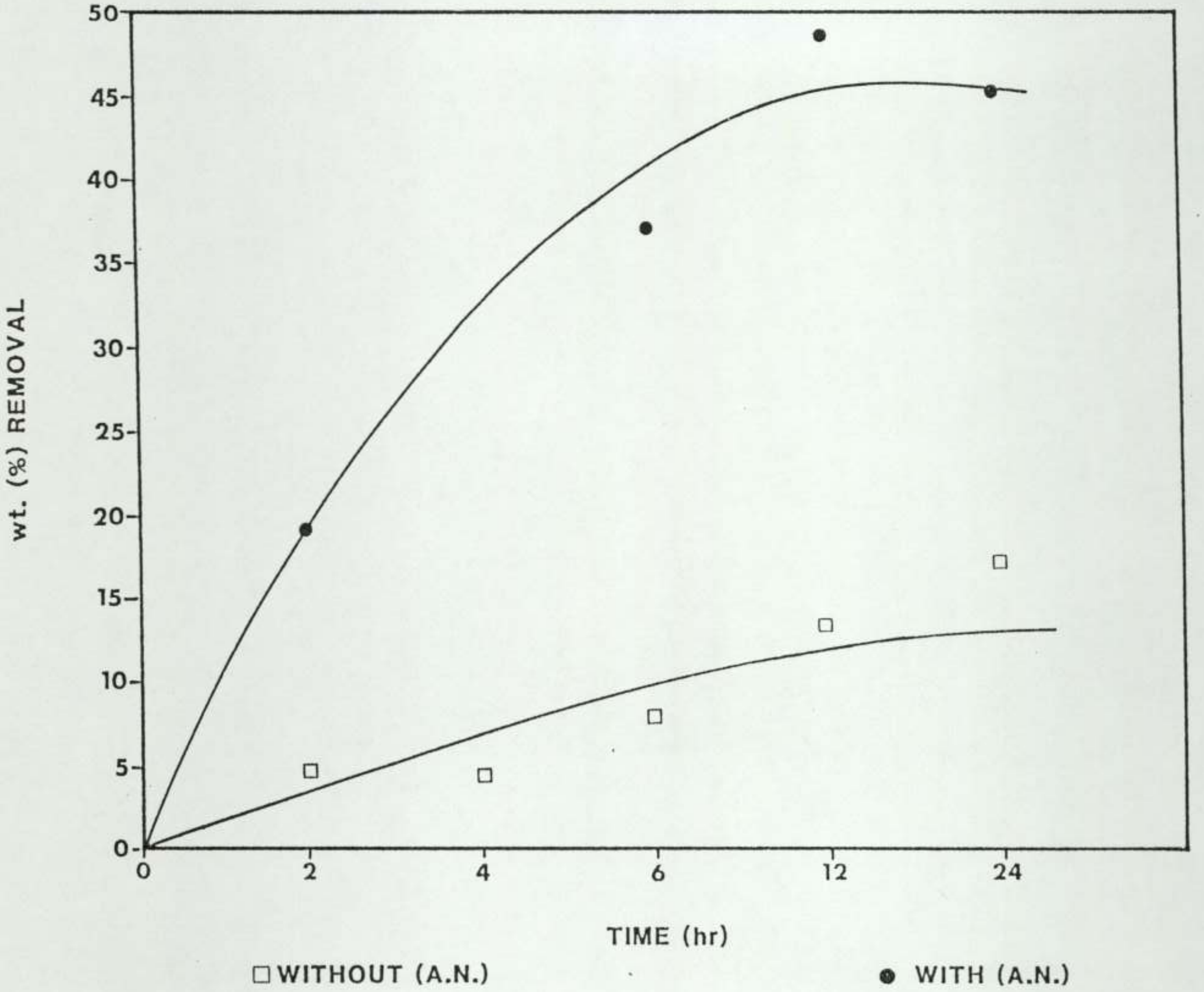

Figure 7.19. Effect of oxalic acid on V removal at 25°C. Acid concentration = 0.66 M. (A. N.), Aluminium nitrate = 1 M.

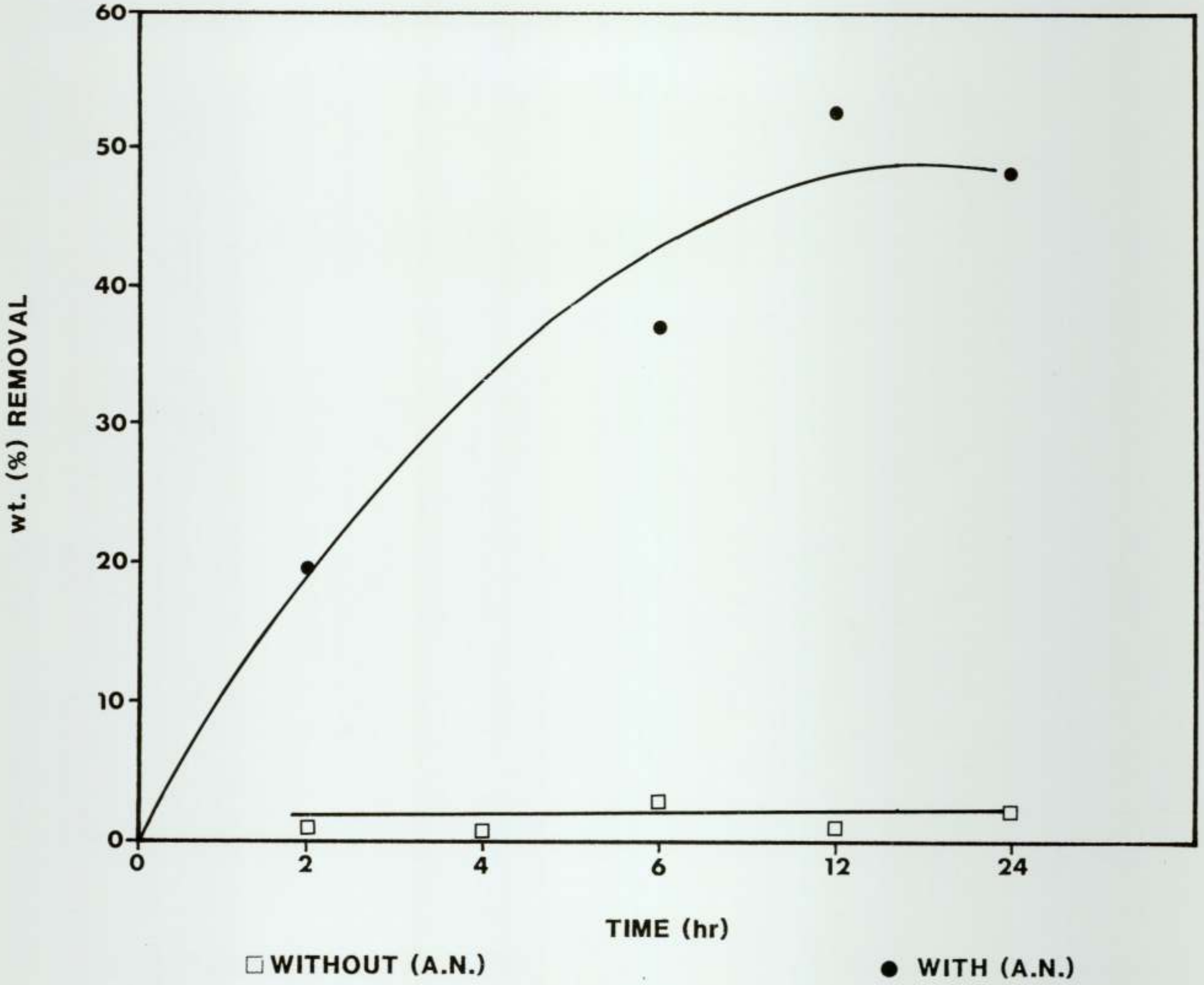

Figure 7.20. Effect of oxalic acid on Ni removal at 25°C. Acid concentration = 0.66 M. (A. N.). Aluminium nitrate = 1 M.

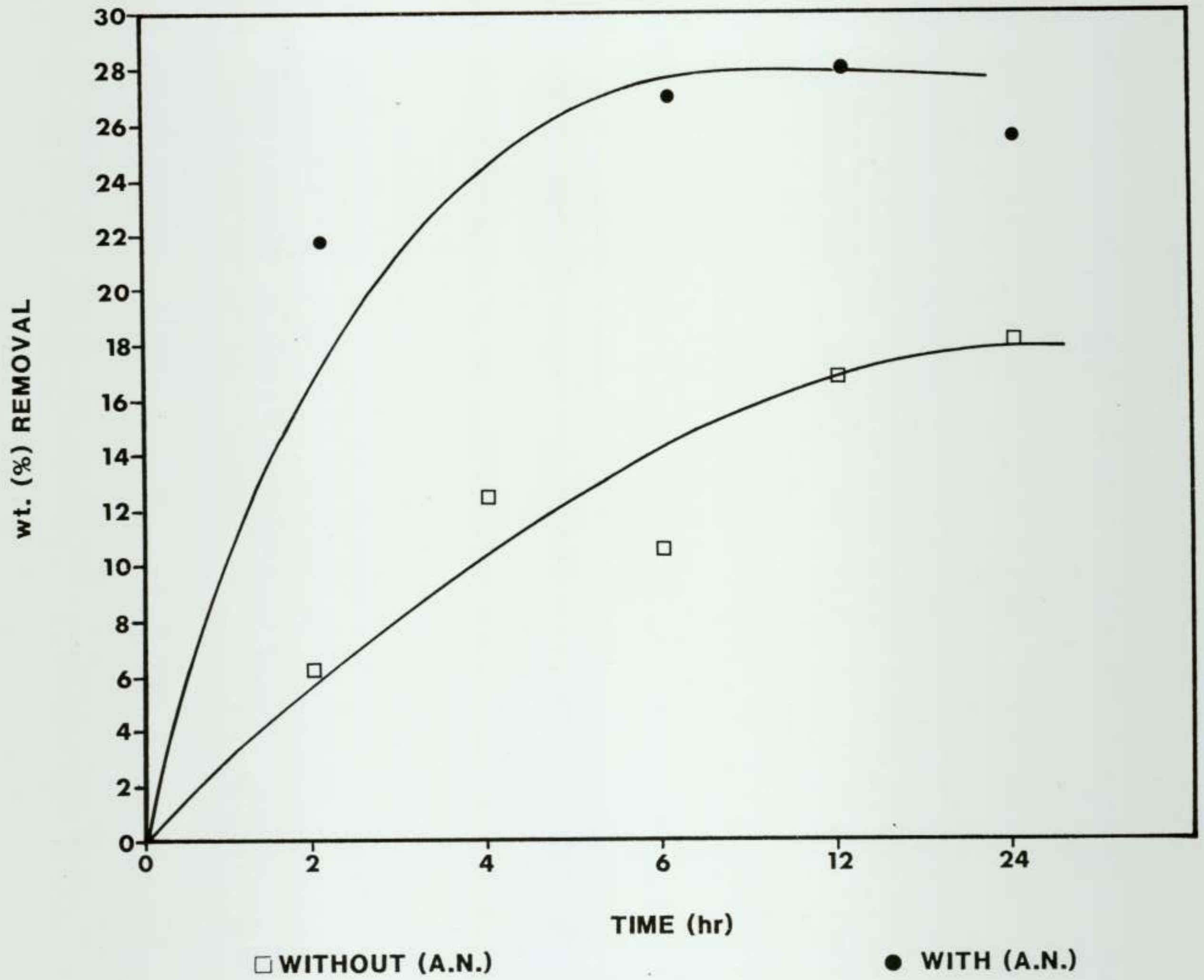

Figure 7.21. Effect of oxalic acid on Mo removal at 25°C. Acid concentration = 0.66 M. (A. N.), Aluminium nitrate = 1 M.

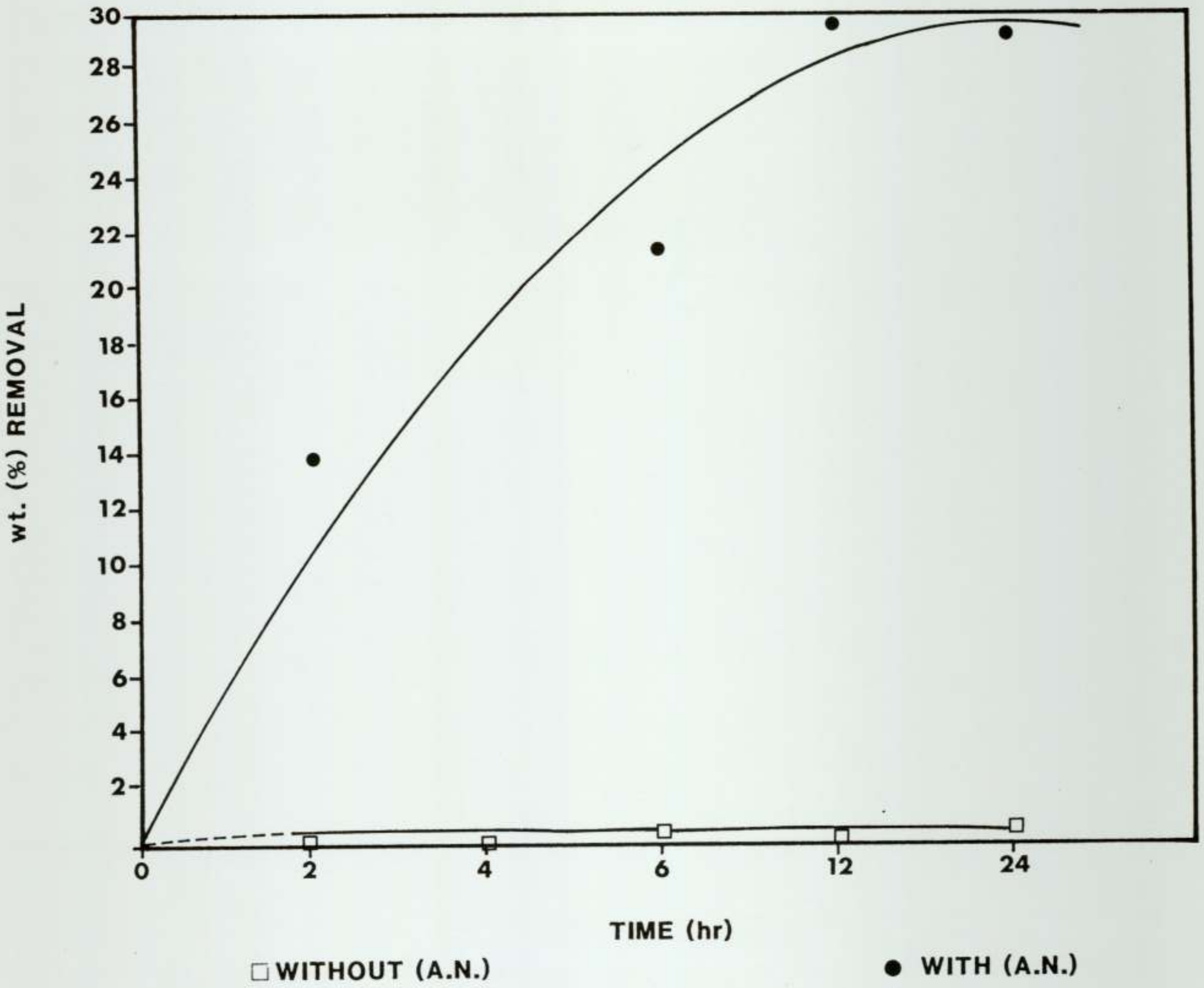

Figure 7.22. Effect of oxalic acid on Co removal at 25°C. Acid concentration = 0.66 M. (A. N.), Aluminium nitrate = 1 M.

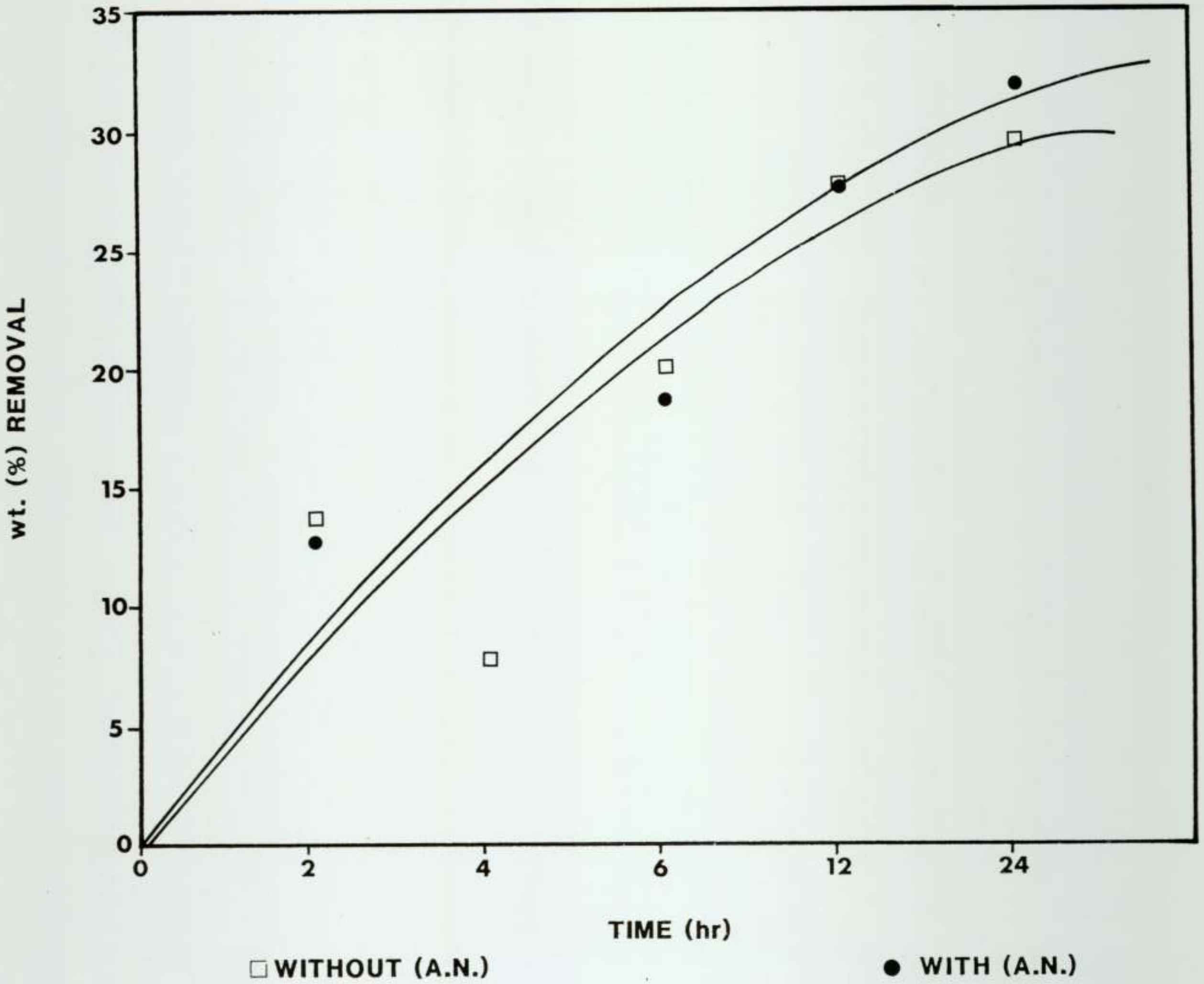

Figure 7.23. Effect of malonic acid on Ni removal at 25°C. Acid concentration = 0.66 M. (A. N.), Aluminium nitrate = 1 M.

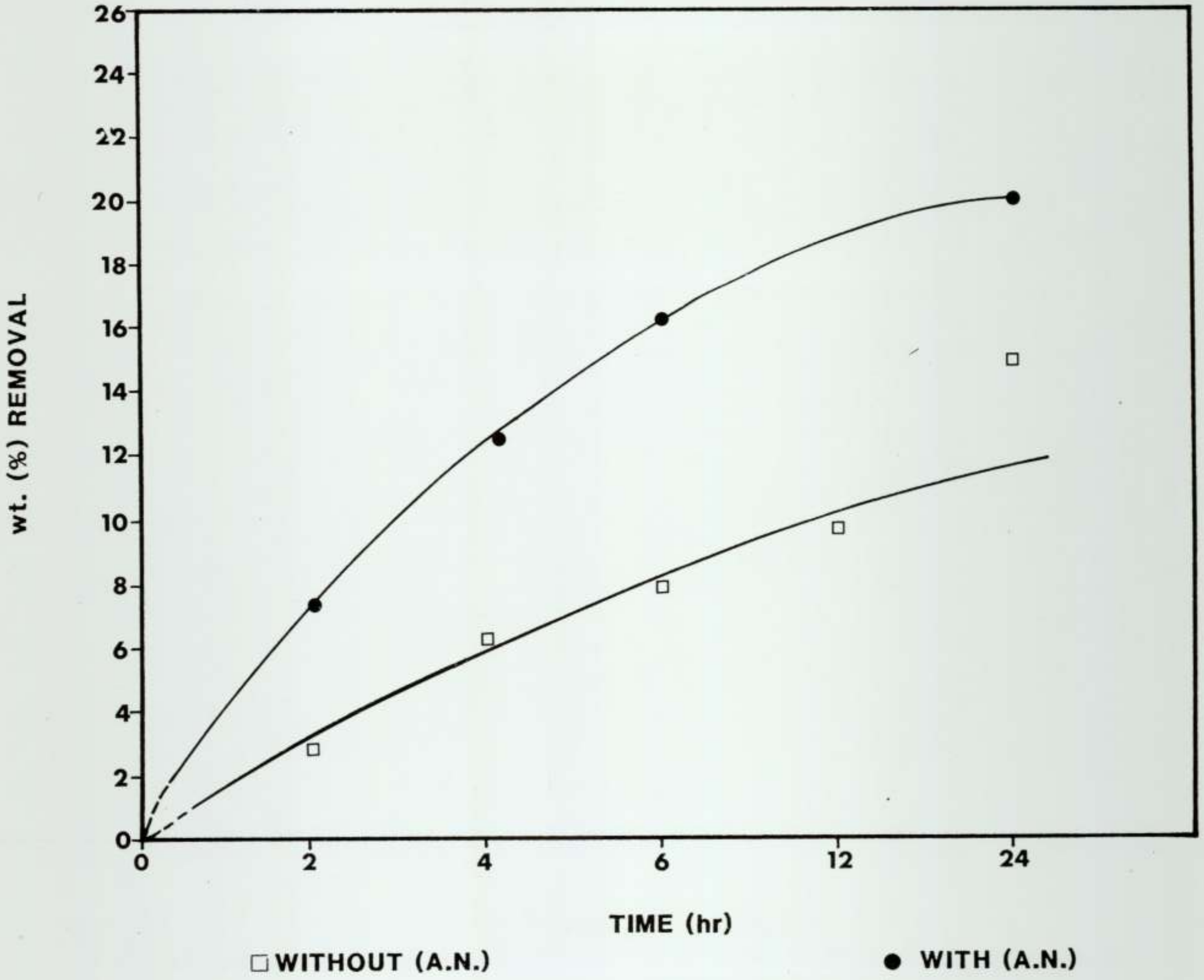

Figure 7.24. Effect of acetic acid on Ni removal at 25°C. Acid concentration = 0.66 M. (A. N.), Aluminium nitrate = 1 M.

Table 7.6. Wt % Removal of Metals After Leaching Spent Catalyst for 24 hrs Using Different Reagent, With & Without Promoter, at Different Temperatures

| Temp. | Oxalic Acid Wt % Removal | | | | Malonic Acid Wt % Removal | | | | Acetic Acid Wt % Removal | | | |
|---|---|---|---|---|---|---|---|---|---|---|---|---|
| °C | Mo | V | Co | Ni | Mo | V | Co | Ni | Mo | V | Co | Ni |
| 25 | 18.2 | 17.4 | 0.7 | 2.3 | 3.1 | 15.9 | 16.4 | 29.5 | 8.7 | 7.9 | 14.2 | 15.1 |
| 50 | 13.0 | 22.4 | 2.7 | 5.8 | 2.0 | 19.0 | 20.0 | 34.0 | 3.9 | 8.5 | 12.2 | 21.5 |
| 75 | 5.4 | 23.5 | 4.6 | 7.9 | 1.5 | 14.5 | 18.0 | 33.0 | 4.2 | 8.9 | 15.0 | 26.6 |
| With Promoter | | | | | | | | | | | | |
| 25 | 26.0 | 46.0 | 29.3 | 48.4 | 3.4 | 18.4 | 17.5 | 31.8 | 23.6 | 11.0 | 13.3 | 20.1 |
| 50 | 11.7 | 27.5 | 47.0 | 79.0 | 3.0 | 28.5 | 18.5 | 35.2 | 2.8 | 4.7 | 14.3 | 26.4 |
| 75 | 4.3 | 22.1 | 47.8 | 79.0 | 8.6 | 38.2 | 31.5 | 60.0 | 12.6 | 31.6 | 35.0 | 64.6 |

Note:

Concentration of acid in all cases = 0.66 molar.

Concentration of promoter $Al(NO_3)_3$ = 1 molar.

in the removal of 37 wt % of vanadium and nickel, while, when aluminum nitrate was used alone, the amount of metal removed was far lower, (vanadium 3.1%, nickel 19.2%).

Experiments were also conducted to find the optimum concentration of promoter, and it was observed that, after leaching for about 12 hours at ambient temperature (25°C), the removal of V was affected by the concentration of aluminium nitrate to a different extent. At 0.1 M concentration of $Al(NO_3)_3$, little increase in leaching was observed (Table 7.8). At 0.5 and 1.0 M the amount of leaching was roughly similar.

Table 7.7. Wt % Removal of Metals from Spent Catalyst Using Oxalic Acid with, and Without, Selected Promoters after Leaching for 12 hrs at 25°C

| Reagent | V | Ni | Co | Mo |
|---|---|---|---|---|
| | | Wt % Removal | | |
| With Oxalic acid (1 molar) | | | | |
| Aluminium sulphate (1 molar) | 15.1 | 30 | 19.3 | 18.4 |
| Aluminium nitrate (1 molar) | 65 | 50 | 32.4 | 45 |
| Nitric acid (1 molar) | 79.1 | 86.5 | 60.2 | 71.3 |
| Ammonium nitrate (1 molar) | 5.6 | 24.3 | 13.4 | 4.9 |
| Oxalic acid only | 16.4 | 0.8 | 0.4 | 36.1 |
| Without oxalic acid | | | | |
| Ammonium nitrate (1 molar) | 3.6 | 24.3 | 13.4 | 5 |
| Aluminium nitrate (1 molar) | 3.1 | 19.2 | 11.1 | 4 |
| Nitric acid (1 molar) | 45.2 | 44 | 27.7 | 15 |
| Nitric acid (pH 0.64) | 10.2 | 22 | 15 | 4.1 |
| $H_2O_2$ (1 molar) | 25.4 | 47.3 | 27.8 | 25 |

Table 7.8. Leaching After 12 hrs Using Different Concentrations of Aluminium Nitrate With Oxalic Acid at 0.66 M, at 25°C

| Metal Leached wt % Removal | Concentration of Aluminium Nitrate in (Molar) | | | |
|---|---|---|---|---|
| | 0.1 | 0.5 | 1.0 | 1.5 |
| V | 15.7 | 44.0 | 49.0 | 49.0 |
| Ni | 4.4 | 43.7 | 52.5 | 55.3 |
| Mo | 21.0 | 27.0 | 48.5 | 31.5 |
| Co | 1.6 | 25.6 | 29.5 | 32.5 |

## 7.3 Characterization of Regenerated Catalysts

### 7.3.1 Surface Area and Pore Volume

The surface area and pore volume of the catalyst samples treated with each of the three acids; both with, and without, promoter and at two different temperatures, e.g., 25 and 50°C were determined in order to examine the improvement in these properties as a result of the removal of the contaminant metals. The results are shown in Table 7.9.

Table 7.9. Surface Area and Pore Volume of Fresh, Spent and Treated Samples, After Leaching for 12 hrs. at 25°C With, and, Without Promoter

| Reference No. | Catalyst Samples/Experimental Conditions | Temp °C | Surface Area $m^2/g$ | Pore Volume ml/g |
|---|---|---|---|---|
| 1 | Fresh Catalyst | - | 202.7 | 0.710 |
| 2 | Spent Catalyst | - | 43.8 | 0.140 |
| 3 | Oxalic Acid | 25 | 100.2 | 0.116 |
| 4 | Oxalic Acid | 50 | 101.0 | 0.155 |
| 5 | Oxalic Acid + $Al(NO_3)_3$ | 25 | 125.0 | 0.307 |
| 6 | Oxalic Acid + $Al(NO_3)_3$ | 50 | 143.0 | 0.340 |
| 7 | Malonic Acid | 25 | 104.9 | 0.121 |
| 8 | Malonic Acid | 50 | 87.4 | 0.150 |
| 9 | Malonic Acid + $Al(NO_3)_3$ | 25 | 109.9 | 0.127 |
| 10 | Malonic Acid + $Al(NO_3)_3$ | 50 | 128.0 | 0.309 |
| 11 | Acetic Acid | 25 | 87.7 | 0.106 |
| 12 | Acetic Acid | 50 | 107.1 | 0.128 |
| 13 | Acetic Acid + $Al(NO_3)_3$ | 25 | 84.7 | 0.038 |
| 14 | Acetic Acid + $Al(NO_3)_3$ | 50 | 84.7 | 0.038 |

Note:

Promoter $Al(NO_3)_3$ = 1 molar
Acid Concentration = 0.66 molar

The surface area and pore volume for the spent catalyst decreased from 202.7 $m^2/g$ and 0.71 ml/g to 43.8 $m^2/g$. and 0.14 ml/g respectively, as a result of metal deposition on the pores of the catalyst. After oxalic acid treatment for about 12 hours the surface area, and pore volume of spent catalyst were increased to 100.2 $m^2/g$ and 0.116 ml/g. Significant improvement in these properties also occurred with malonic acid treatment. However, for acetic acid the increase was less pronounced.

An increase in leaching temperature with oxalic and acetic acids led to a remarkable increase in the surface area and pore volume whereas no improvement occurred in the case of malonic acid (Table 7.9). These results concerning the effect of temperature are in line with the metal extraction data (Figure 7.12) discussed earlier. It was shown that the rate of extraction of major contaminant metal (vanadium) was significantly influenced by higher temperatures with oxalic acid and acetic acid, but with malonic acid, temperature had no noticeable effect. The removal of the deposited metals from pore mouths and pore surfaces of the spent catalyst by acid leaching was clearly responsible for the improvements in pore volume and surface area. Since, in the case of malonic acid, increase in temperature had no effect on the amount of vanadium (major contaminant) removal, no significant improvement of surface area or pore volume would be expected.

Table 7.9 summarizes the surface area and pore volume data for the spent catalyst samples treated with acids containing aluminium nitrate. A comparison of these results with those of the samples treated with oxalic acid alone at 25°C clearly indicates that the improvement in surface area and pore volume are considerably higher for the samples leached with aluminium nitrate containing reagents. This is in agreement with the enhancing effect of aluminium nitrate on metal removal reported earlier for each of the three acids.

## 7.4 Leaching of Pure Metal Sulphides

Since the deposits on the catalyst will be in the form of sulphide the process of rejuvenation will comprise diffusion of reactant to the deposit, dissolution and/or reaction dissolution and diffusion of product into the bulk. Therefore, it was considered worthwhile to study the leaching of pure metal sulphides themselves. The experimental procedure was explained in section 6.3 of Chapter 6. The same three acids (oxalic, malonic and acetic) were chosen for this study. The experimental parameters investigated and the results obtained are discussed in the following section.

### 7.4.1 Effect of Different Acids

The results are given in Figures 7.25 - 7.27 for oxalic acid and malonic acid for removal of vanadium. A similar general trend was observed with acetic acid but not with the same degree of consistency and a typical plot is shown in Figure 7.27. For the other metals (Ni, Co, Mo), with all acids; results were shown in Table 7.10. It is clear from the data that the initial rate of metal removal was rapid and tended to level-off after approximately 10 minutes.

All the acids showed a higher activity for vanadium removal than for nickel and molybdenum. The best reagent in terms of vanadium removal appears to be malonic acid; for nickel there was no significant difference between the reagents.

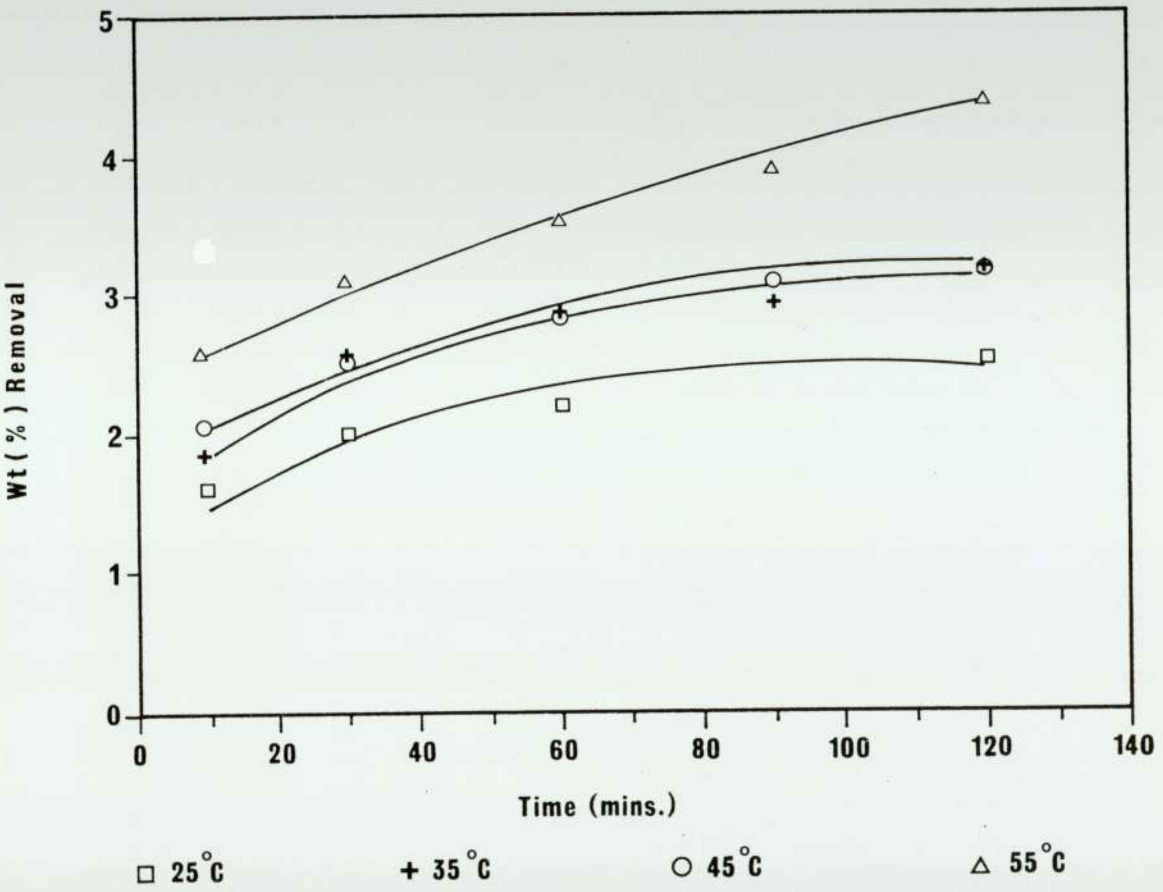

Figure 7.25. Effect of oxalic acid on $V_2S_3$.
Acid concentration = 0.66 M.

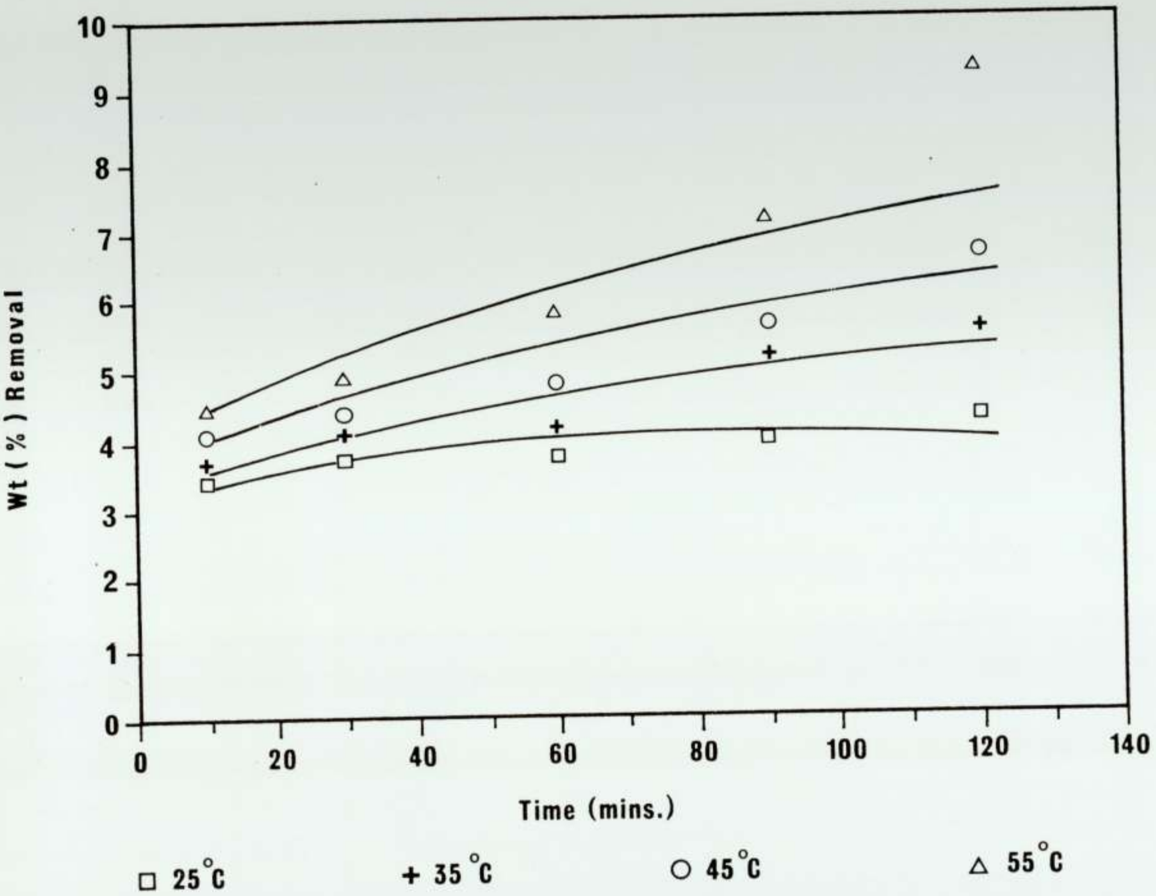

Figure 7.26. Effect of malonic acid on $V_2S_3$.
Acid concentration = 0.66 M.

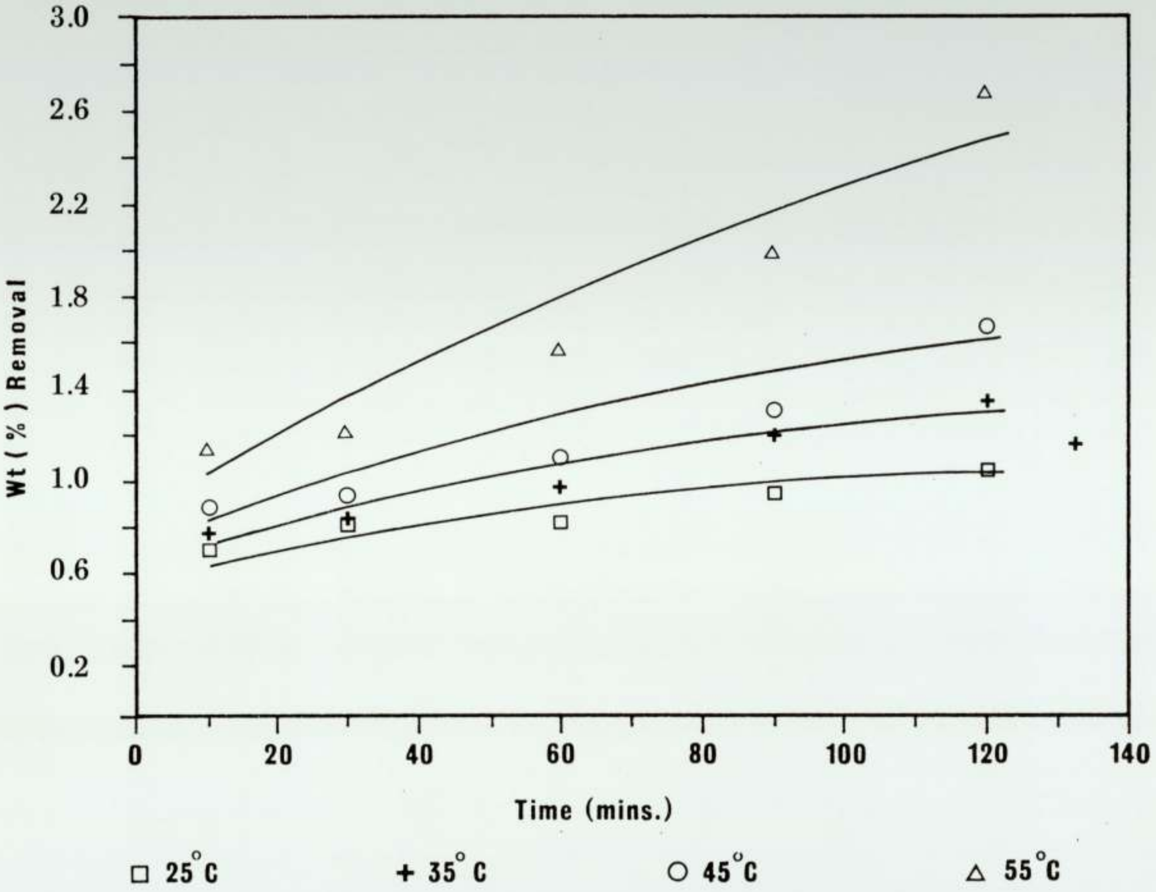

Figure 7.27. Effect of acetic acid on NiS.
Acid concentration = 0.66 M.

Table 7.10. Wt % Removal of Pure Metal Sulphides After Leaching With Different Acids at Different Temperatures

| Metal | Temp °C | Oxalic Wt % Removal | | Malonic Wt % Removal | | Acetic Wt % Removal | | Oxalic with Promoter Wt % Removal | |
|---|---|---|---|---|---|---|---|---|---|
| | | I | F | I | F | I | F | I | F |
| $V_2S_3$ | 25 | 1.60 | 5.70 | 1.60 | 5.00 | 3.40 | 14.90 | 5.40 | 26.00 |
| | 35 | 1.90 | 14.00 | 2.70 | 10.00 | 3.70 | 16.20 | 0.80 | 13.50 |
| | 45 | 2.30 | 11.00 | 2.10 | 10.10 | 4.00 | 85.00 | 0.80 | 39.00 |
| | 55 | 3.40 | 16.60 | 4.00 | 41.40 | 4.50 | 90.00 | 8.70 | 39.00 |
| NIS | 25 | 0.30 | 0.20 | 0.80 | 1.60 | 0.70 | 4.80 | 0.79 | 4.40 |
| | 35 | 0.37 | 0.24 | 0.91 | 2.50 | 0.80 | 4.20 | 0.86 | 6.50 |
| | 45 | 0.37 | 0.16 | 1.00 | 2.10 | 0.90 | 6.00 | 0.90 | 8.20 |
| | 55 | 0.44 | 0.16 | 1.20 | 4.50 | 1.10 | 4.00 | 1.10 | 4.20 |
| CoS | 25 | 2.00 | 1.20 | 2.00 | 9.50 | 3.10 | 8.70 | 1.60 | 10.90 |
| | 35 | 2.50 | 1.10 | 2.00 | 9.70 | 2.50 | 10.70 | 2.20 | 13.00 |
| | 45 | 2.70 | 1.20 | 2.00 | 11.20 | 2.40 | 12.30 | 3.00 | 10.40 |
| | 55 | 2.60 | 1.40 | 2.00 | 13.10 | 2.80 | 21.70 | 3.50 | 10.60 |
| $MoS_2$ | 25 | 0.10 | 0.52 | 0.08 | 0.56 | 0.10 | 0.52 | 0.13 | 28.50 |
| | 35 | 0.15 | 0.72 | 0.11 | 0.79 | 0.16 | 0.61 | 0.08 | 0.95 |
| | 45 | 0.19 | 1.10 | 0.13 | 0.93 | 0.12 | 0.64 | 0.15 | 0.86 |
| | 55 | 0.33 | 1.70 | 0.15 | 1.70 | 0.15 | 0.86 | 0.17 | 0.84 |

Note:
Acid concentration = 0.66 molar
Promoter $Al(NO_3)_3$ = 1 molar
I = Initial
F = Final

### 7.4.2 Effect of Temperature

The effect of temperature on dissolution of pure metal salts was similar to that on regenerated spent catalyst. As the temperature was increased, a slight increase in metal removal occurred (Table 7.10).

### 7.4.3 Effect of Promoter

A similar experimental program was applied as explained in Section 7.2.1.5. Only oxalic acid was used as it was considered the most promosing acid for vanadium removal, at constant concentration of acid (0.66 molar) and aluminium nitrate (1 molar) and at different temperatures, e.g., 25, 35, 45 and 55°C. The effect on different metal salts was determined, e.g., $V_2S_3$, NIS, CoS and $MoS_2$.

Table 7.11. The Initial and Final Weight Percent of Vanadium Removal Using Oxalic Acid at Different Temperatures With, and, Without Promoter

| Reaction Temperature | Without Promoter | | With Promoter | |
|---|---|---|---|---|
| | Initial wt % | Final wt % | Initial wt % | Final wt % |
| 25°C | 1.6 | 5.7 | 5.4 | 26.0 |
| 35°C | 1.9 | 14.0 | 2.8 | 13.5 |
| 45°C | 2.3 | 11.0 | 4.8 | 39.0 |
| 55°C | 3.4 | 16.6 | 8.7 | 39.0 |

Oxalic acid = 0.66 M
Promoter is $Al(NO_3)_3$ = 1 M
Initial = after 10 min leaching
Final = after 24 hrs leaching

Table 7.11 shows that the addition of aluminium nitrate improved the pure vanadium sulphide extraction. For example, the initial amount removed at 25°C with, and, without promoter increased from 1.6 wt% to 5.4 wt%, while the final amount increased from 5.7 wt% to 26 wt% respectively. The percent weight extraction of pure vanadium was also increased by an increase in temperature in the range 25°C to 55°C. These two conclusions are in an agreement with previous results on spent catalyst extraction.

## Catalytic Activity Tests

The catalytic activity of samples of fresh, spent and treated catalysts were established by tests on the hydrodesulphurisation of atmospheric gas oil. The flow reactor used was described in Section 6. The feed contained 2 wt % sulphur and the operating conditions were described in Section 6.

The results obtained are summarised in Table 7.12 for the catalysts described in Table 7.13. Table 7.13 also lists the wt % of V, Ni, Co and Mo calculated as remaining. Sulphur removal was measured after 2, 4, 6 and 8 h on line.

Removal of coke from the catalyst improved surface area (from 43.8 to 60.4 $m^2g^{-1}$) and activity (S removal after 2 h from 35% to 39% : Table 7.12). Spent and decoked catalyst which had been leached with acids showed the following characteristics, Without Promoter

| | | | | | |
|---|---|---|---|---|---|
| Surface area | Malonic Acid | > | Oxalic Acid | > | Acetic Acid |
| Activity (2h) | Oxalic acid | > | Acetic Acid | > | Malonic Acid |
| Activity (6h) | Malonic Acid | > | Acetic Acid | > | Oxalic Acid |
| V removal | Oxalic Acid | ~ | Malonic Acid | > | Acetic Acid |
| Ni Removal | Malonic Acid | > | Acetic Acid | > | Oxalic Acid |

The Effect of Promoter Was

| | | | | | |
|---|---|---|---|---|---|
| Surface area | Oxalic Acid | > | Malonic Acid | > | Acetic Acid |
| Activity (2h) | Oxalic acid | > | Malonic Acid | > | Acetic Acid |
| Activity (6h) | Malonic Acid | > | Oxalic Acid | > | Acetic Acid |
| V removal | Oxalic Acid | > | Malonic Acid | ~ | Acetic Acid |
| Ni Removal | Oxalic Acid | > | Malonic Acid | ~ | Acetic Acid |

Table 7.12. The Hydrodesulphurization Activity of Fresh, Spent, Decoked and Some Catalyst Samples Treated With Oxalic, Malonic and Acetic Acids of 0.66 molar for 12 h With, and Without, Promoter (1 molar)

| Ref. No. | % wt removal of Sulphur from feed After (hrs) | | | |
|---|---|---|---|---|
| | 2 | 4 | 6 | 8 |
| Fresh | 71 | 63 | 54 | 65 |
| Spent | 35 | 32 | 30 | 29 |
| Decoked | 39 | 36 | 37 | 33 |
| Oxalic acid | 57 | 30 | 28 | 29 |
| Oxalic acid + $Al(NO_3)_3$ | 47 | 46 | 45 | 46 |
| Malonic acid | 42 | 42 | 42 | 39 |
| Malonic acid + $Al(NO_3)_3$ | 44 | 48 | 48 | 47 |
| Acetic acid | 51 | 48 | 33 | 41 |
| Acetic acid + $Al(NO_3)_3$ | 40 | 35 | 34 | 32 |
| Decoked: Oxalic acid | 51 | 47 | 39 | 39 |
| Decoked: Oxalic acid + $Al(NO_3)_3$ | 51 | 50 | 48 | 45 |

Table 7.13. Wt % of Metal Remaining and the Surface Area of Fresh, Spent, Decoked and Leached Catalyst With Three Acids (0.66 molar), With and Without Aluminium Nitrate (1 molar), T = 25°C for 12 hours

| Ref. No. | Sample of Treatment | Leaching Described in Table | Pore Volume ml/g | Surface area $m^2/g$ | Wt % Remaining | | | |
|---|---|---|---|---|---|---|---|---|
| | | | | | V | Ni | Co | Mo |
| 1 | Fresh | 7.3 | 0.71 | 202.7 | 0 | 0.2 | 3.27 | 11.72 |
| 2 | Spent | 7.3 | 0.14 | 43.8 | 15.1 | 3.7 | 1.07 | 3.99 |
| 3 | Decoked | 7.3 | 0.22 | 60.4 | 16.5 | 4.1 | 1.07 | 4.2 |
| 4 | Oxalic acid | 7.9 | 0.116 | 100.2 | 12.1 | 3.6 | 1.06 | 3.3 |
| 5 | Oxalic acid + $Al(NO_3)_3$ | 7.9 | 0.31 | 125.0 | 8.2 | 1.9 | 0.78 | 3.0 |
| 6 | Malonic acid | 7.9 | 0.12 | 104.9 | 12.7 | 2.6 | 0.91 | 3.9 |
| 7 | Malonic + $Al(NO_3)_3$ | 7.9 | 0.13 | 109.9 | 12.3 | 2.7 | 0.91 | 3.9 |
| 8 | Acetic acid | 7.9 | 0.11 | 87.7 | 13.9 | 3.1 | 0.96 | 3.6 |
| 9 | Acetic + $Al(NO_3)_3$ | 7.9 | 0.04 | 84.4 | 13.4 | 3.0 | 0.91 | 3.0 |
| 10 | Decoked: oxalic acid | - | 0.26 | 57.7 | Not considered | | | |
| 11 | Decoked: oxalic + $Al(NO_3)_3$ | - | 0.46 | 110.04 | | | | |

## 8.0 DISCUSSION

As discussed in Chapter 5, leaching of a solid by a liquid involves diffusion of the liquid to the solid interface, interaction between the solid and the liquid, and diffusion of products away from the interface. If mass transfer is not the controlling process, interaction of solid and liquid may be controlled by one of several steps. These could include

i. Interaction between liquid reagent and solid to produce liquid or solid product.

ii. Dissolution of solid product to a limit dictated by the solubility of the product in solution. Either the rate of dissolution, or the solubility of the product, could dictate the amount of product in solution.

Experiments were carried out with two types of sample pure metal sulphides which were essentially non-porous (Table 7.5), and with spent catalyst which had been de-oiled but not de-coked. In the second case, the material to be leached was held inside a porous matrix (coke) which remained after leaching (see Chapter 5). For each case initial experiments were also carried out to investigate whether or not mass transfer effects controlled the rate of leaching.

### 8.1 The Kinetics of the Reactions

Measurements were made of leaching as a function of time (Figures 7.25 - 7.27, Table 7.10). The rate controlling step(s) in the process could be determined by comparison of the prediction of different rate equations (Chapter 5) with these results.

Leaching was found to involve a fast appearance of product in solution until it approached a steady state value (see Figure 8.1). Since kinetic processes will affect primarily the initial dissolution, rather than the final steady-state concentration, comparisons were drawn with initial rates. Experimental results are summarised in Tables 8.1 and 8.2.

Two comparisons may be made, i.e. with the kinetic equations predicted for a shrinking particle (pure sulphides) and for a shrinking core (spent catalyst) developed in Chapter 5. As explained there the experimental results can be applied to three equations which should allow distinction between rate control by diffusion in solution, by diffusion in pores or by chemical reaction. The application of these equations can be considered for pure sulphides and spent catalysts in turn.

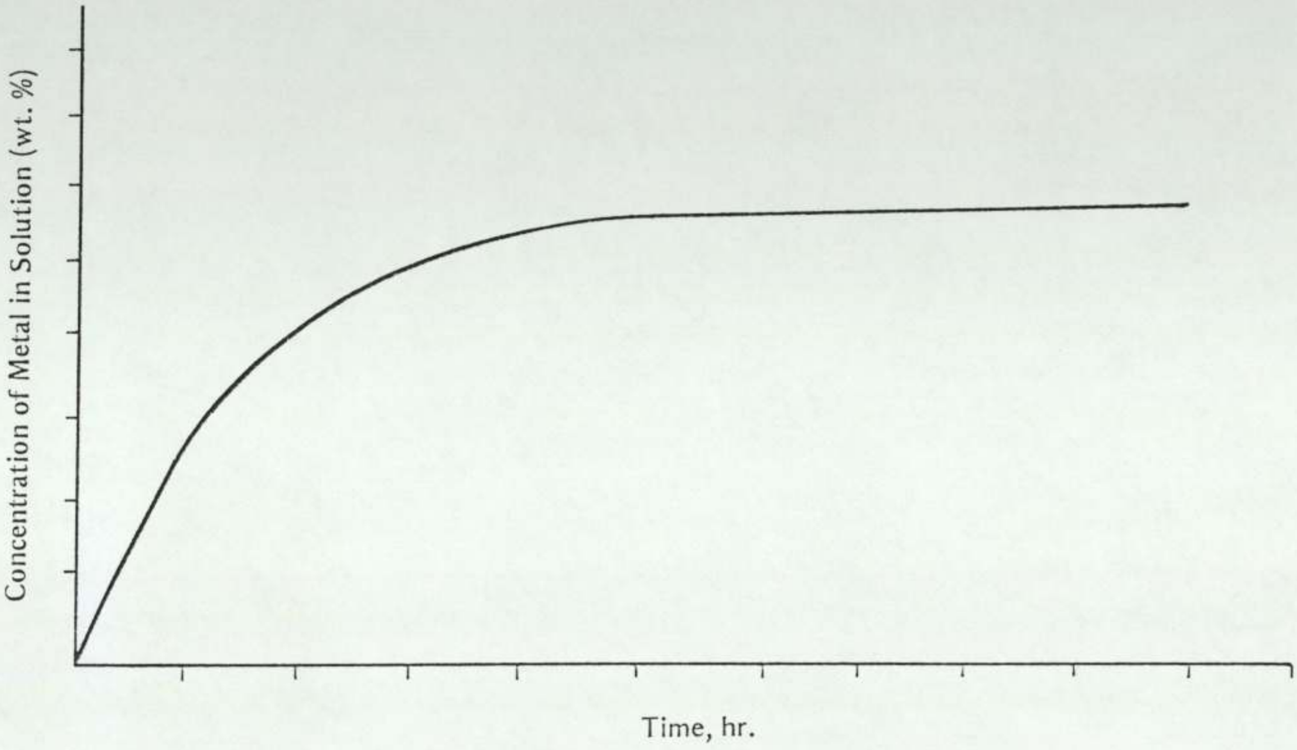

Figure 8.1. Typical plot of metal extraction in solution vs time.

Table 8.1. Rates of Reaction for V, Ni, Mo and Co Sulphides with Oxalic, Malonic and Acetic Acid with Different Temperatures

| Metal | Temp °C | Oxalic 0.66 molar wt %/min. | Malonic 0.66 molar wt %/min. | Acetic 0.66 molar wt %/min. | Oxalic Acid (.66 m) With $Al(NO_3)_3$ (1 m) wt %/min. |
|---|---|---|---|---|---|
| $V_2S_3$ | 25 | 0.33 | 0.33 | 0.15 | 2.85 |
| | 35 | 0.36 | 0.36 | 0.18 | 0.40 |
| | 45 | 0.38 | 0.40 | 0.21 | 0.40 |
| | 55 | 0.46 | 0.43 | 0.34 | 1.80 |
| NIS | 25 | 0.30 | 0.50 | 0.07 | 0.17 |
| | 35 | to | 0.65 | 0.08 | 0.18 |
| | 45 | 0.40 | 0.73 | 0.09 | 0.19 |
| | 55 | | 0.80 | 0.10 | 0.16 |
| $MoS_2$ | 25 | 0.01 | 0.008 | 0.01 | 0.04 |
| | 35 | 0.016 | 0.011 | 0.011 | 0.03 |
| | 45 | 0.02 | 0.013 | 0.014 | 0.034 |
| | 55 | 0.033 | 0.015 | 0.018 | 0.06 |
| CoS | 25 | 0.83 | 0.26 | 0.203 | 0.72 |
| | 35 | 0.90 | 0.26 | 0.225 | 1.10 |
| | 45 | 0.95 | 0.26 | 0.268 | 1.30 |
| | 55 | 0.05 | 0.26 | 0.279 | 1.40 |

Table 8.2. Rates of Reaction of spent Catalyst for V, Ni, Mo and Co After Leaching with Oxalic, Malonic and Acetic Acid, With and Without Promoter at Different Temperatures

| Metal | Temp °C | Oxalic Acid | | Malonic Acid | | Acetic Acid | |
|---|---|---|---|---|---|---|---|
| | | without promoter | with promoter | without promoter | with promoter | without promoter | with promoter |
| | | gm/min x $10^{-3}$ | | gm/min x $10^{-3}$ | | gm/min x $10^{-3}$ | |
| V | 25 | 40 | 40 | 30 | 20 | 13 | 30 |
| | 50 | 50 | 80 | 30 | 110 | 16 | 30 |
| | 75 | 70 | 160 | 30 | 220 | 20 | 70 |
| Ni | 25 | 9.1 | 120 | 70 | 100 | 25 | 70 |
| | 50 | 9.1 | 500 | 60 | 190 | 40 | 70 |
| | 75 | 15.2 | 600 | 70 | 240 | 60 | 160 |
| Mo | 25 | 50 | 160 | 10 | 10 | 10 | 50 |
| | 50 | 30 | 160 | 5.5 | 30 | 7.6 | 10 |
| | 75 | 40 | 170 | 4.9 | 340 | 9.1 | 30 |
| Co | 25 | 1.5 | 110 | 60 | 50 | 40 | 30 |
| | 50 | 2.7 | 230 | 50 | 110 | 20 | 50 |
| | 75 | 6.4 | 370 | 60 | 180 | 40 | 90 |

## 8.2 Leaching of Pure Metal Sulphides

Pure metal sulphides, were reduced in size on leaching. As a result, kinetic equations relevant to the shrinking particle (Chapter 5) should be applied.

If diffusion in the bulk was rate determining, then the leaching of all metal ions by one acid should, at a given concentration and temperature, be similar and should occur at the rate of diffusion of the acid in solution. Inspection of Table 8.1 shows that this was not the case: as a result diffusion in the liquid cannot be rate controlling.

If diffusion in pores was rate controlling, the appropriate expression (Chapter 5) is

$$\frac{t}{\tau} = 1-(1 - X_B)^{2/3} \tag{5.31}$$

If chemical reaction controls, this equation changes to

$$\frac{t}{\tau} = 1-(1 - X_B)^{1/3} \tag{5.23}$$

Attempts were made to fit the experimental results to these equations but, as shown in Figures 8.2 and 8.3, distinction between these equations is difficult.

Inspection of the characteristics of the pure solids shows that their porosity was very small Table 7.5. Hence, diffusion control seems less likely in these systems.

## 8.3 Leaching of Spent Catalysts

Spent catalysts contain a matrix of coke, which is not removed by leaching. As a result, equations pertinent to the shrinking core model should be applied (Chapter 5).

Again, if the mass transfer of acid in solution is rate-determining, the leaching of all metal ions by one specific acid under similar conditions should be similar. The data in Table 8.2 demonstrate that this is not the case. Therefore, mass transfer in the bulk solution cannot be rate controlling.

Typical plots showing the application of equations 5.18 and 5.23 to the experimental results are given in Figures 8.4 and 8.5. Again distinction between the plots is difficult. Theoretically it should be possible to widen the operating conditions to a point where a distinction can be

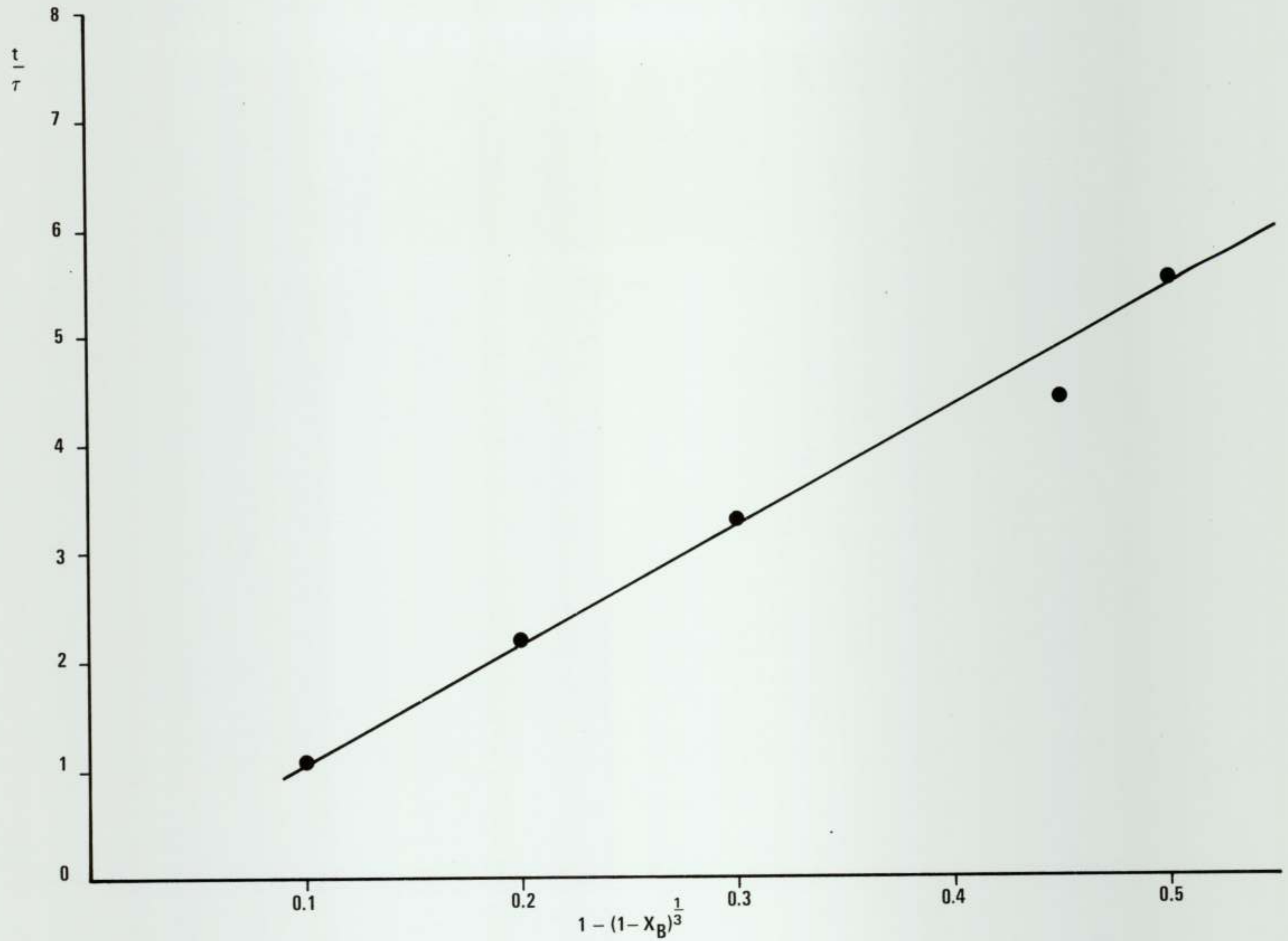

Figure 8.2. Plot of equation 5.23 to determine if chemical reaction is rate controlling for vanadium tri-sulphide removal using oxalic acid.
$T = 25^{o}C$, Acid concentration = 0.66 M, Wt. of solid = 11.68 g.

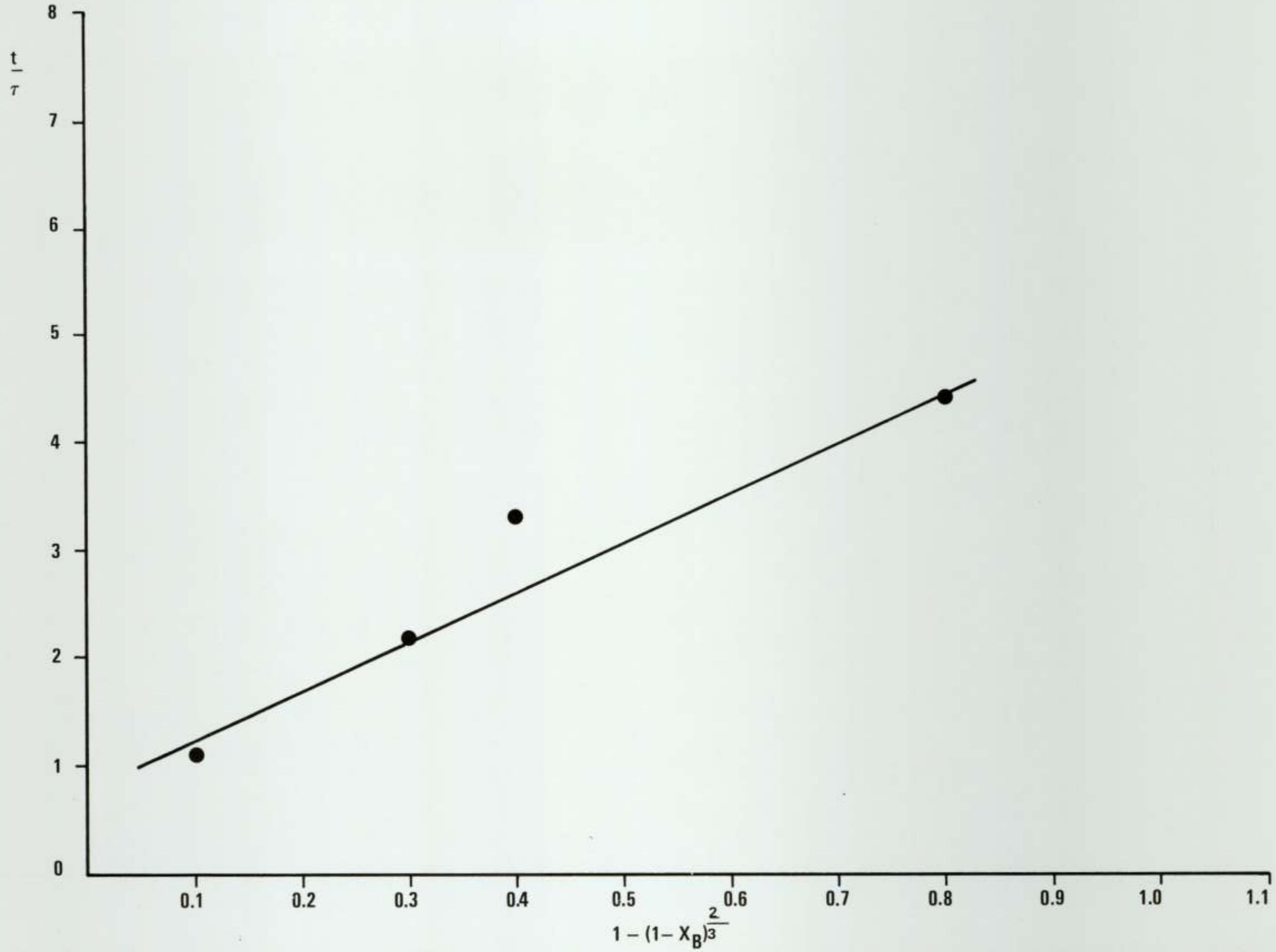

Figure 8.3. Plot of equation 5.31 to determine if diffusion is rate controlling for vanadium tri-sulphide removal using oxalic acid. T = 25°C, Acid concentration = 0.66 M, Wt. of solid = 11.68 g.

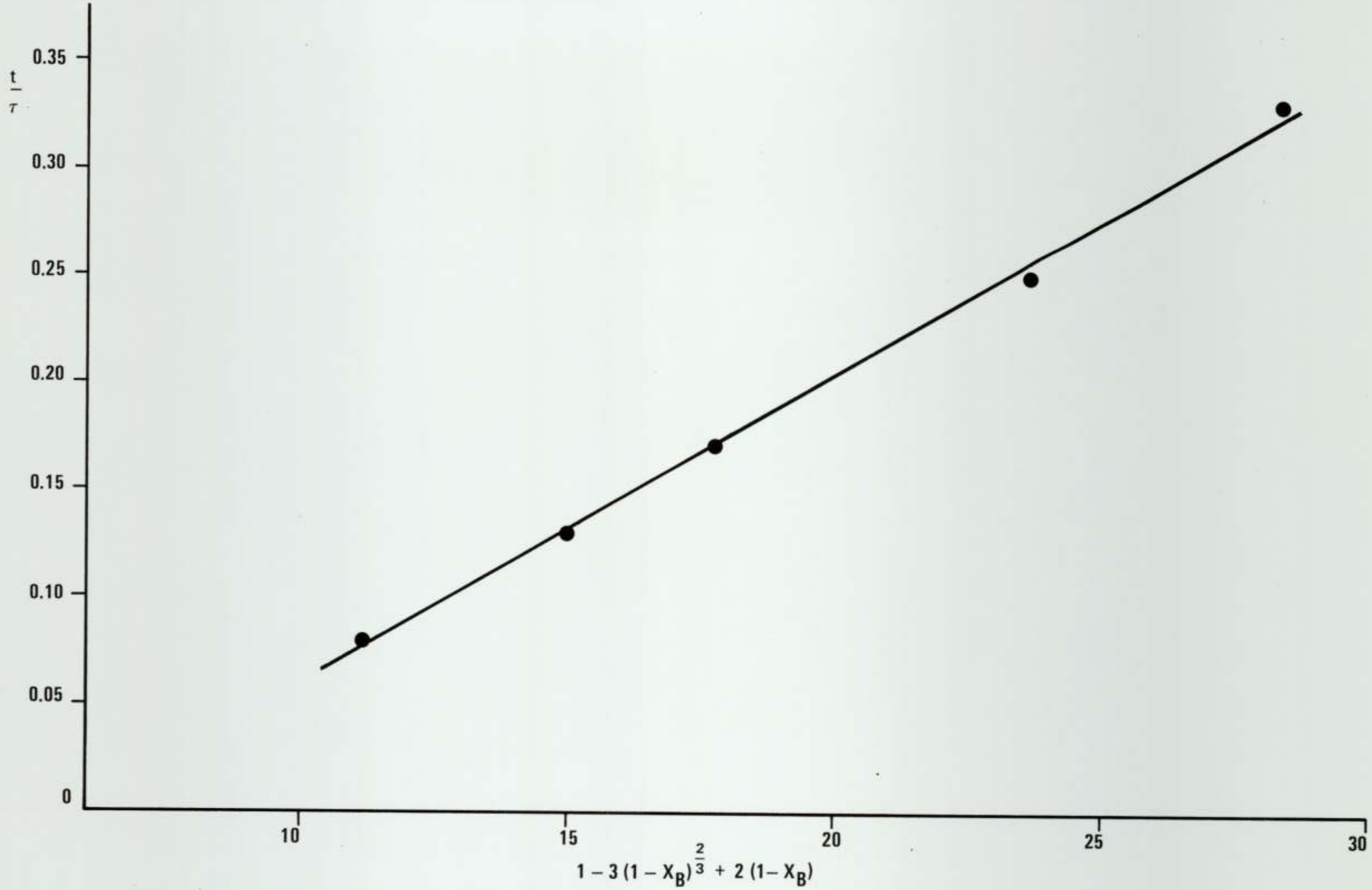

Figure 8.4. Diffusion through pores for leaching of vanadium by oxalic acid with respect to time. $T = 25^{o}C$, Acid concentration = 0.66 M, Wt. of solid = 11.68 g.

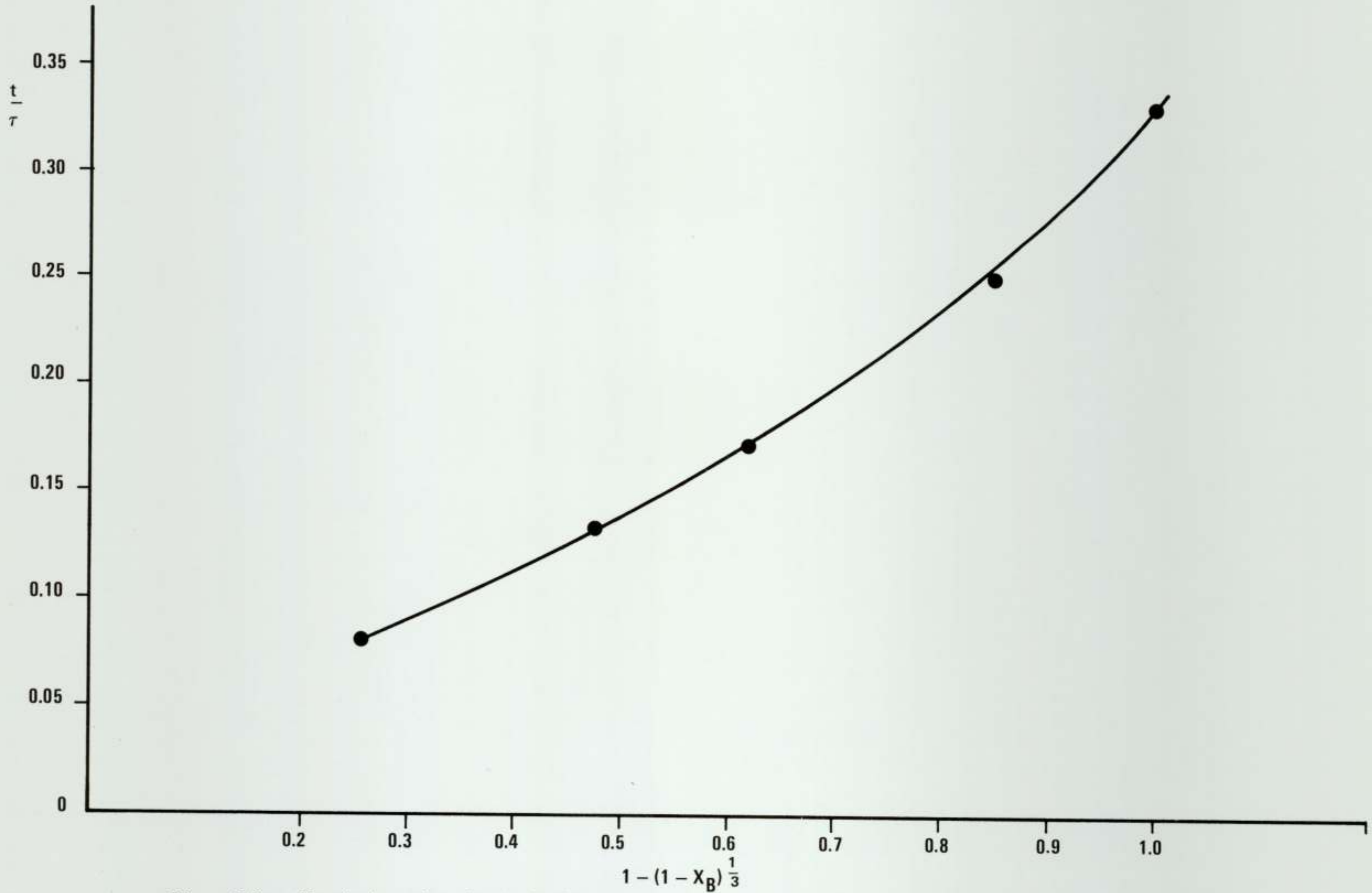

Figure 8.5. Chemical reaction plot for leaching of vanadium by oxalic acid with respect to time. $T = 25^{o}C$, Acid concentration = 0.66 M, Wt. of solid = 11.68 g.

drawn, but in an aqueous solution - limits of 0°C and 100°C are imposed. The lack of differentiation that can be achieved by operating between 25 and 75°C (Figures 8.4 and 8.5) shows that these limits are such that the rate determining step cannot be established from application of equations 5.18 - 5.23.

## 8.4 The Dependence of Leaching Rate on Temperature

The second potential method of distinguishing between rate determining steps is via the dependence of rate on temperature. If mass transfer controls, the rate can be described by Fick's Law.

$$\text{Flux } N = -D \frac{dc}{dx}$$

where the diffusion coefficient, D, obeys a pseudo-Arrhenius relationship (151)

$$D = A_1 \; e^{-Q/RT}$$

Values of Q are small (152) and, in most cases, the values of D for diffusion in aqueous systems are low ($0.5\text{-}5.0 \times 10^{-5} cm^2 s^{-1}$) and reasonably constant ($D = 10^{-4} - 10^{-5}\ cm^2 s^{-1}$(152).

If chemical reaction rates control, an Arrhenius relationship will again be expected.

$$\text{rate} = \frac{-dc}{dt} = KC_A^{\alpha}\, C_B^{\;\beta} \eta$$

where $\eta$ = effectiveness factor (153), $\alpha$ and $\beta$ are reaction orders and K, the rate constant, depends on temperature as

$$K = A\, e^{-E/RT}$$

The kinetic order of leaching was found to be zero (Figures 7.6-7.11).

Attempts were made to distinguish between chemical reaction and mass transfer by plotting log (rate of leaching) vs inverse temperature (Figures 8.6 and 8.9). In some cases a linear relationship was found to hold: in others it did not (Table 8.3). Values of the constants were found to lie between 5.2 Cal/mole.°K and 17.4 Cal/mole.°K (Tables 8.3a and 8.3b).

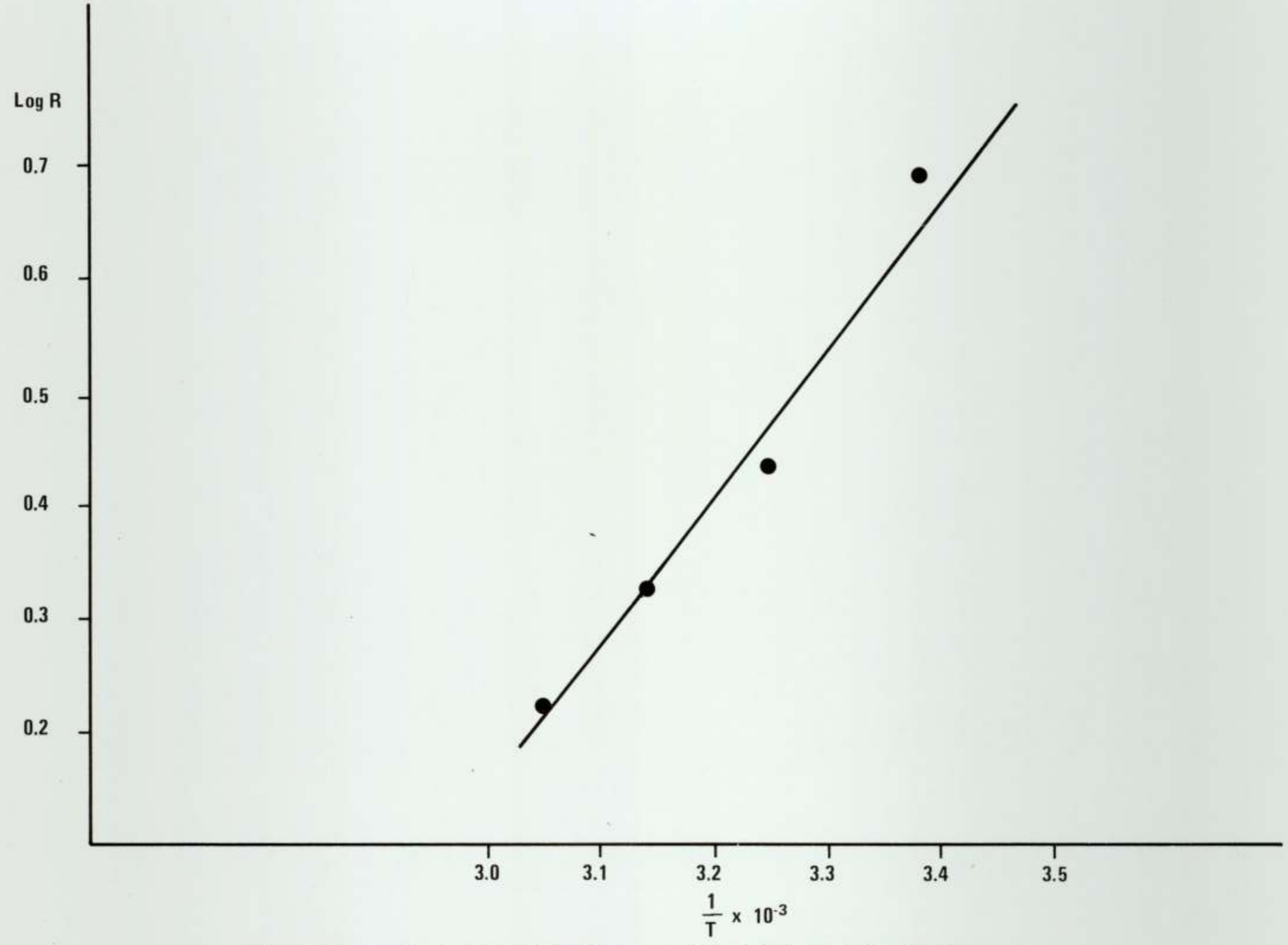

Figure 8.6. Arrhenius plot for leaching of nickel sulphide by malonic acid.
T, $^{o}C$ = 25, 35, 45, 55, Acid concentration = 0.66 M, Wt. of solid = 2.3 g.

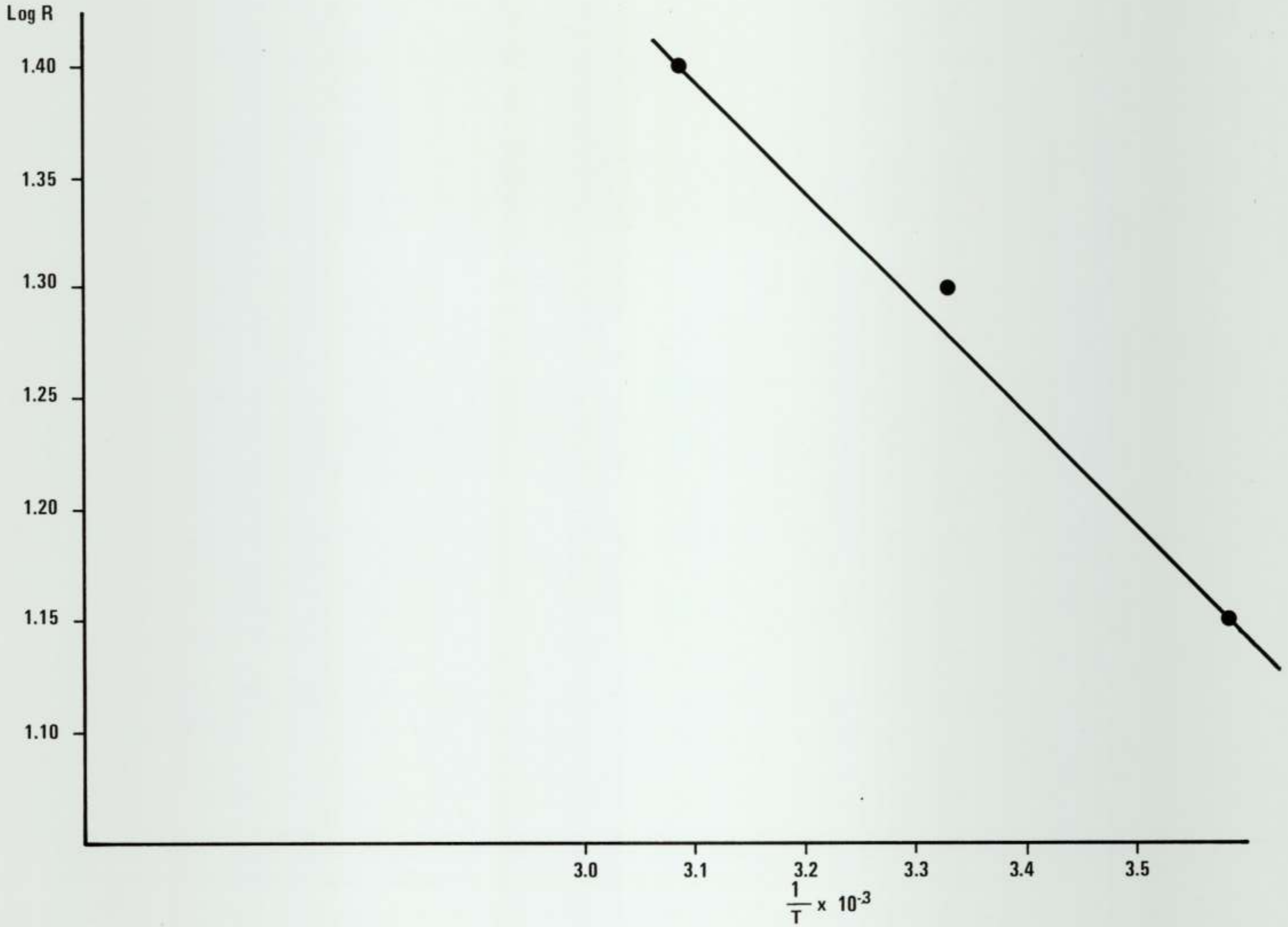

Figure 8.7. Arrhenius plot for leaching of vanadium by oxalic acid.
T, $^{o}C$ = 25, 35, 45, 55, Acid concentration = 0.66 M, Wt. of solid = 15.1 g.

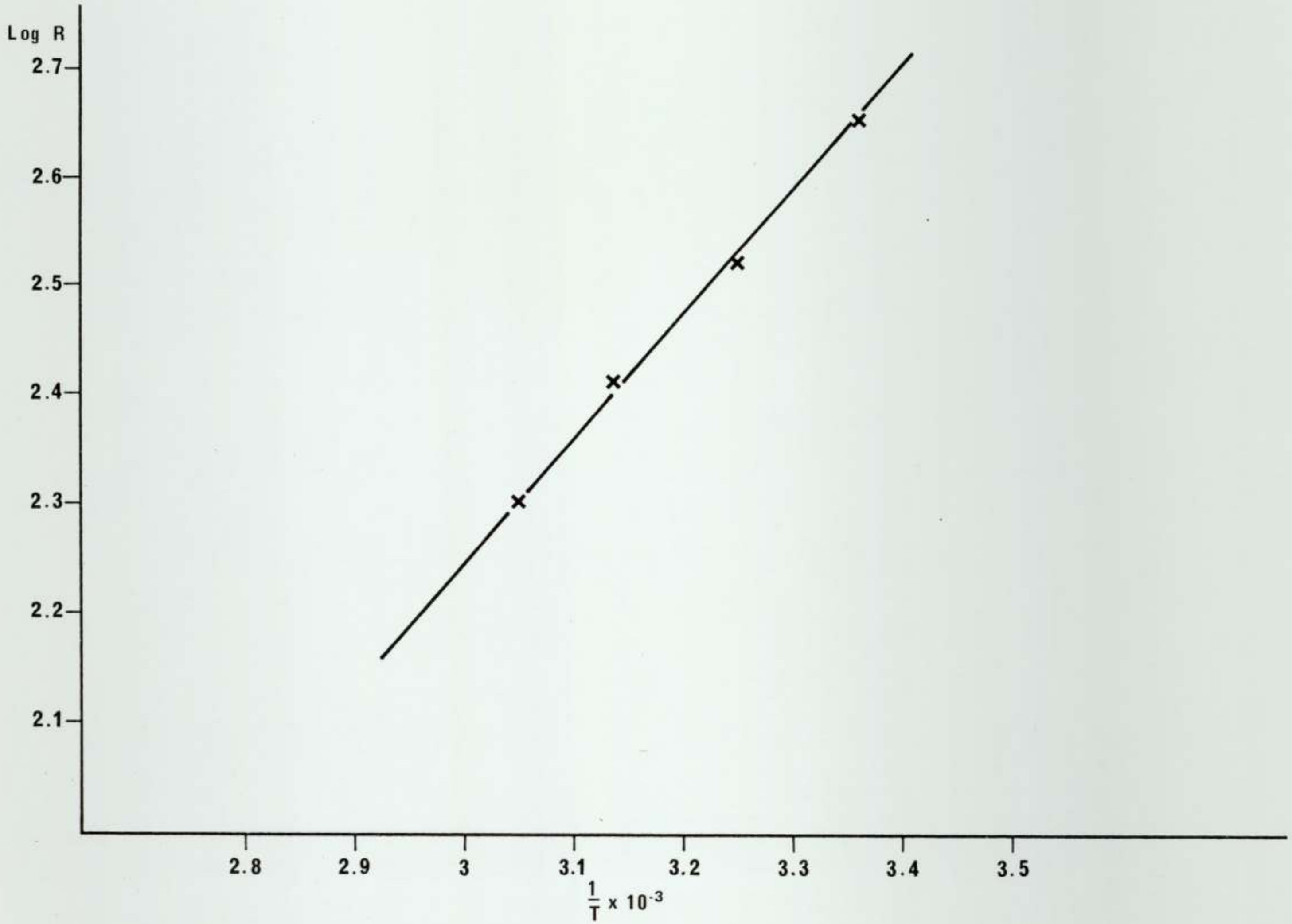

Figure 8.8. Arrhenius plot for leaching of nickel sulphides by acetic acid.
T, $^{o}$C = 25, 35, 45, 55, Acid concentration = 0.66 M, Wt. of solid = 2.3 g.

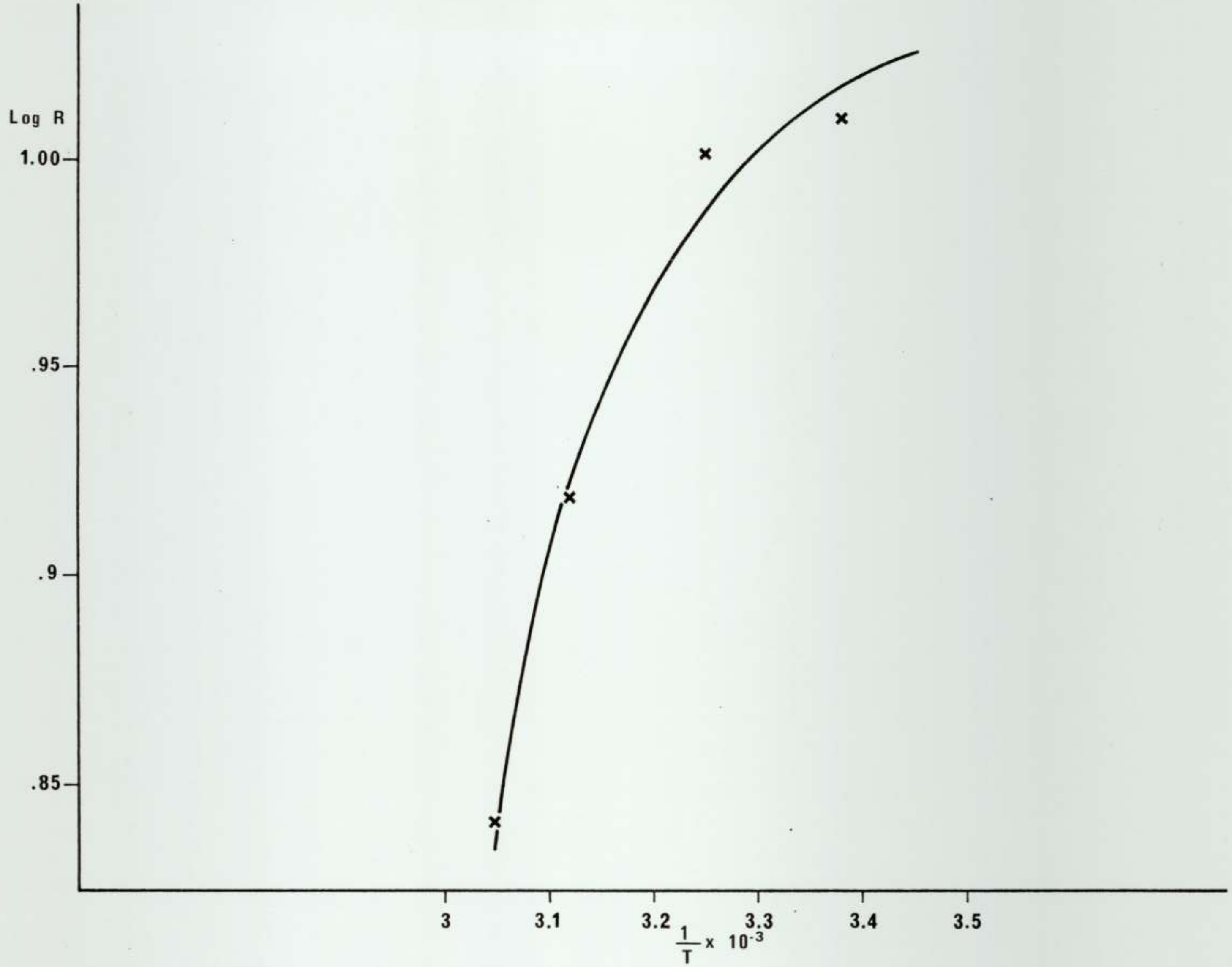

Figure 8.9. Arrhenius plot for leaching of vanadium tri-sulphides by malonic acid.
T, $^{o}$C = 25, 35, 45, 55, Acid concentration = 0.66 M, Wt. of solid = 11.68 g.

The fact that the experimental plots did not apply to all systems throws doubt on the use of temperature to distinguish the rate-determining step. Some indication of important processes can, however, be obtained from the absolute values of rates.

The data in Tables 8.1 and 8.2 show that the rate of leaching varied between 0.95 to 0.01 g/min for pure sulphides and between 1 x $10^{-3}$to 50 x $10^{-3}$ g/min.for spent catalyst. Diffusion constants in aqueous solutions are remarkably similar (152) at values between $10^{-4}$to $10^{-5}$ $cm^2s^{-1}$. Thus, it is seen that, at least in the case of spent catalysts, mass transfer control is certainly feasible.

Whilst, in view of the complexities of the process, it is not possible to identify the rate-determining steps with certainty mass transfer control would appear possible in the porous spent catalyst but less likely with pure sulphides. This would not be unexpected in the light of the characteristics of the two samples (Table 7.5).

Attention, was then directed at the steady state regime operating after longer periods of leaching (Figure 8.1).

Table 8.3a. Summary of the Relationship Between Reaction Rate and Temperature for Different Acids, With & Without Promoter, for Different Metal Sulphides Extraction

| Pure metal sulphides | Acid 0.66 molar | $\frac{1}{T}$ | E Cal/mole.°k | Oxalic Acid & promoter (1 molar) | E Cal/mole.°k |
|---|---|---|---|---|---|
| $V_2S_3$ | Oxalic acid | - | | + | 5.17 |
| | Malonic acid | - | | | |
| | Acetic acid | - | | | |
| NIS | Oxalic acid | - | | - | |
| | Malonic acid | + | 5.2 | | |
| | Acetic acid | + | 5.3 | | |
| $MoS_2$ | Oxalic acid | + | 17.4 | + | 14.6 |
| | Malonic acid | + | 10.2 | | |
| | Acetic acid | + | | | |
| CoS | Oxalic acid | - | | - | |
| | Malonic acid | - | | | |
| | Acetic acid | - | | | |

Note: (+) indicate linear relationship.
(-) indicate non-linearship.

Table 8.3b. Summary of the Relationship Between the Reaction Rates and Temperature for Different Acids, With and Without Promoter, for Different Metals in Spent Catalyst

| Metal | Reagent 0.66 molar | $\frac{1}{T}$ | E Cal/mole.°k |
|---|---|---|---|
| V | Oxalic acid | + | 5.2 |
| | Malonic acid | - | |
| | Acetic acid | - | |
| Ni | Oxalic acid | - | |
| | Malonic acid | - | |
| | Acetic acid | | |
| Co | Oxalic acid | - | |
| | Malonic acid | - | |
| | Acetic acid | | |
| Mo | Oxalic acid | - | |
| | Malonic acid | - | |
| | Acetic acid | - | |

Note: (+) indicate linear relationship.
(-) indicate not-linearship.

## 8.5 Steady State Leaching

Figure 8.1 shows that the amount of material leached from the solids first increases rapidly and then approaches a steady state. The rate of leaching during the initial stages has been found not to be informative, and attention was focused on the final steady state.

Contact between the solids and water leads to minimal leaching. Leaching only becomes appreciable once a second reagent is added to the water. This infers that the second reagent reacts with the solid to produce a product which is soluble. Preliminary attempts to identify the chemical nature of the products were not successful, and the extent of leaching was measured by determining the amount of different metal ions in solution.

It is possible that reaction between the solid and the liquid reactant produces a solid product, the dissolution of which is limited by the solubility of the product in water. Solubility limits for the expected products could not be found in the literature but the maximum amounts of product (measured as metal ion in solution) dissolved from different systems are summarized in Table 8.4. These amounts are much larger than most of the steady state values observed in leaching experiments (Tables 8.5 and 8.6). Hence, the amount of material leached in most, and perhaps in all, systems is not limited by solubility.

Table 8.4. Maximal Amounts of Product Leached From Spent Catalyst for Different Systems

| Metal Salt | Leachant Acid | T C° | Wt % Removal |
|---|---|---|---|
| V | Oxalic | 75 | 23.5 |
| | Oxalic + $Al(NO_3)_3$ | 25 | 46.0 |
| | Malonic | 50 | 19.0 |
| | Malonic + $Al(NO_3)_3$ | 75 | 38.2 |
| | Acetic | 75 | 8.9 |
| | Acetic + $Al(NO_3)_3$ | 75 | 31.6 |
| Co | Oxalic | 75 | 4.6 |
| | Oxalic + $Al(NO_3)_3$ | 75 | 47.8 |
| | Malonic Acid | 50 | 20.0 |
| | Malonic + $Al(NO_3)_3$ | 75 | 31.5 |
| | Acetic | 75 | 15.0 |
| | Acetic + $Al(NO_3)_3$ | 75 | 35.0 |
| Mo | Oxalic | 25 | 18.2 |
| | Oxalic + $Al(NO_3)_3$ | 25 | 26.0 |
| | Malonic acid | 25 | 3.1 |
| | Malonic + $Al(NO_3)_3$ | 75 | 8.6 |
| | Acetic | 25 | 8.7 |
| | Acetic + $Al(NO_3)_3$ | 25 | 23.6 |
| Ni | Oxalic | 75 | 7.9 |
| | Oxalic + $Al(NO_3)_3$ | 75 | 79.0 |
| | Malonic | 50-75 | 34-33 |
| | Malonic + $Al(NO_3)_3$ | 75 | 60.0 |
| | Acetic | 75 | 26.6 |
| | Acetic + $Al(NO_3)_3$ | 75 | 64.6 |

Table 8.5. Steady State Amount Removed for Leaching of Pure Metal Sulphides Using Different Acids, With & Without Promoters at different Temperatures

| Metal Salt | Temp °C | Oxalic Acid 0.66 molar wt % | Malonic Acid 0.66 molar wt % | Acetic Acid 0.66 molar wt % | Oxalic Acid (0.66 M) With $Al(NO_3)_3$ (1 M) wt % |
|---|---|---|---|---|---|
| $V_2S_3$ | 25 | 5.7 | 5.0 | 14.9 | 26.0 |
| | 35 | 14.0 | 10.0 | 16.2 | 13.5 |
| | 45 | 11.0 | 10.1 | 85.0 | 39.0 |
| | 55 | 16.6 | 41.4 | 90.0 | 38.8 |
| NIS | 25 | 0.20 | 1.6 | 4.8 | 4.4 |
| | 35 | 0.24 | 2.5 | 4.2 | 6.5 |
| | 45 | 0.16 | 2.1 | 6.0 | 8.2 |
| | 55 | 0.16 | 4.5 | 4.0 | 4.2 |
| $MoS_2$ | 25 | 0.52 | 0.56 | 0.52 | 28.50 |
| | 35 | 0.72 | 0.79 | 0.61 | 0.95 |
| | 45 | 1.10 | 0.93 | 0.64 | 0.86 |
| | 55 | 1.70 | 1.70 | 0.86 | 0.84 |
| CoS | 25 | 1.2 | 9.5 | 8.7 | 10.9 |
| | 35 | 1.1 | 9.7 | 10.7 | 13.0 |
| | 45 | 1.2 | 11.2 | 12.3 | 10.4 0 |
| | 55 | 1.4 | 13.1 | 21.7 | 10.6 0 |

Table 8.6. Steady State Amount Removed for Leaching of Spent Catalyst Using Different Acids, With & Without Promoters, at Different Temperatures

| Metal Salt | Temp °C | Oxalic Acid 0.66 M wt % | Malonic Acid 0.66 M wt % | Acetic Acid 0.66 M wt % | Oxalic Acid 0.66 M + $Al(NO_3)_3$= 1M wt % | Malonic Acid 0.66 M + $Al(NO_3)_3$= 1M wt % | Acetic Acid 0.66 M + $Al(NO_3)_3$= 1M wt % |
|---|---|---|---|---|---|---|---|
| V | 25 | 17.4 | 15.9 | 7.9 | 45.6 | 18.4 | 11.0 |
| | 50 | 22.4 | 19.0 | 8.5 | 27.5 | 28.5 | 11.7 |
| | 75 | 23.5 | 14.5 | 8.9 | 22.1 | 38.2 | 31.8 |
| Ni | 25 | 3.3 | 29.5 | 15.1 | 48.4 | 31.8 | 20.1 |
| | 50 | 5.8 | 34.1 | 21.5 | 78.9 | 35.2 | 26.4 |
| | 75 | 7.9 | 33.0 | 26.6 | 79.0 | 59.9 | 64.6 |
| Mo | 25 | 18.2 | 3.10 | 8.7 | 25.7 | 3.4 | 23.6 |
| | 50 | 13.0 | 1.99 | 3.9 | 11.7 | 3.0 | 02.8 |
| | 75 | 5.4 | 1.45 | 4.2 | 4.3 | 8.6 | 12.6 |
| Co | 25 | 0.7 | 16.4 | 14.2 | 29.3 | 17.5 | 13.3 |
| | 50 | 2.7 | 19.5 | 12.2 | 47.0 | 18.4 | 14.3 |
| | 75 | 4.6 | 18.0 | 14.9 | 47.8 | 31.7 | 35.0 |

### Accessibility of Metal Salts in the Spent Catalyst.

Some estimate may be obtained of the accessibility of different metals within the spent catalysts. Analysis of a catalyst gives the amount of metals present but does not give a measure of their accessibility, since clearly a monolayer of metal salt can be leached more quickly than the same amount of salt in a multilayer deposit.

If the chemical reaction controls the rate of leaching, then the rate of metal salt reaction should be proportional to the surface area of the deposit. It is possible to calculate rate of leaching/unit surface area for the pure salts. Assuming that this is similar in the case of the compounds in the spent catalyst, some estimate can be obtained of the surface area of the different salts in the catalyst. These values are summarised in Table 8.7

This can only provide a rough estimate, since it is assumed that the rate-controlling step is similar in both cases. In fact, it appears more likely that the rate of chemical reaction controls the leaching of pure compounds, while mass transfer in the pores controls the leaching of spent catalysts.

However, it is of scientific interest, and supportive of the experimental techniques, that all three leachants give approximately the same estimate for the surface areas of the different metal salts (Table 8.7).

Table 8.7. The Approximate Surface Areas of Different Metal Salts Available for Leaching

| Leachant acid | Metal ion | Pure Samples | | Spent Catalyst | |
|---|---|---|---|---|---|
| | | Rate of Leaching wt % $\text{min}^{-1}$ | Rate of Leaching wt % $\text{min}^{-1}\text{m}^{-2}\text{g}$ | Rate of Leaching wt % $\text{min}^{-1}$ x $10^{-3}$ | Estimated Surface Area $\text{m}^2\text{g}^{-1}$ |
| Oxalic | V | 0.33 | 0.046 | 40.0 | 0.87 |
| | Ni | 0.35 | 0.28 | 9.1 | 0.032 |
| | Co | 0.83 | 0.64 | 1.5 | 0.07 |
| | Mo | 0.01 | 0.002 | 50.0 | 2.5 |
| Malonic | V | 0.33 | 0.046 | 30.0 | 0.65 |
| | Ni | 0.5 | 0.4 | 100.0 | 0.175 |
| | Co | - | - | 60.0 | - |
| | Mo | 0.008 | 0.0019 | 10.0 | 5.20 |
| Acetic | V | 0.15 | 0.021 | 13.0 | 0.62 |
| | Ni | 0.07 | 0.073 | 25.0 | 0.34 |
| | Co | 0.203 | 0.02 | 40.0 | 2.0 |
| | Mo | 0.01 | 0.002 | 10.0 | 5.0 |

## 8.6 Leaching by Acids

It is helpful to consider acid leaching in the context of pure metal sulphides in which the chemical nature and the structure of the solids are well defined. In such systems, the leaching reactions can be expected to be of the overall form e.g.:

$$MoS_2 + 4CH_3COOH \dashrightarrow Mo(-OOC.CH_3)_4 + 2H_2S \qquad (8.1)$$

or

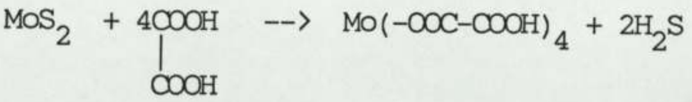

$$MoS_2 + 4\begin{array}{c}COOH\\ |\\ COOH\end{array} \dashrightarrow Mo(-OOC-COOH)_4 + 2H_2S \qquad (8.2)$$

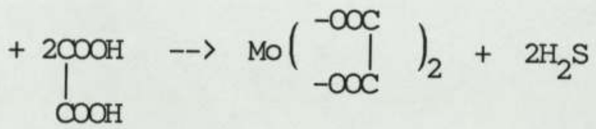

$$+ 2\begin{array}{c}COOH\\ |\\ COOH\end{array} \dashrightarrow Mo\left(\begin{array}{c}-OOC\\ |\\ -OOC\end{array}\right)_2 + 2H_2S \qquad (8.3)$$

In fact such reactions in aqueous systems can be expected to proceed in two stages

$$MoS_2 + 4H^+ \longrightarrow 2H_2S + Mo^{4+} \quad (8.4)$$

$$Mo^{4+} + 4CH_3COO^- \longrightarrow Mo(OOCCH_3)_4 \quad (8.5)$$

which will be controlled by the ionisation constants of the acids, by the production of metal ions (reaction 8.4) and by the production of the metal complex (reaction 8.5). The dissociation of the acids by removal of one ($K_1$) or two ($K_2$) hydrogen ions is reported in Table 8.8, as one of the stability constants for the formation of different complexes. These values reflect the formation of the complex by

$$K_3 = \frac{[\text{M complex}]}{[M^{x+}]\,[\text{ligand}]}$$

Values reported are best values found for lower valency metal ions. The organic acids are generally mild reducing agents, and it is not expected that major oxidation would occur.

It is shown that reaction 8.5 will proceed to form the complex in all cases except, possibly, for reaction with acetic acid. Values of $K_3$ are so large that, if the metal ion is produced, it will rapidly be converted to the metal complex.

The amount of product in solution (Table 8.4 and 8.5) is much less than the amount expected if all the acid reacted. Although the dissociation of the organic acids is not large (Table 8.8), both $H^+$ and acid$^-$ should be removed as they are formed via reactions 8.4 and 8.5. Hence, it is unlikely that the dissociation of the acid limits the amount of product.

It seems likely therefore, that the leaching from the pure sulphides is limited by reaction 8.4, the production of metal ions from the sulphides. Ionisation constants for these sulphides could not be located, but the heats of formation of the solids give some indication of their relative stability. These values ($MoS_2$ = -55.52 kcal mole$^{-1}$: NiS = -19.6 kcal mole$^{-1}$: CoS = -19.8 kcal mole$^{-1}$: $V_2S_3$ = -227 kcal mole$^{-1}$ (154) indicate that the extent of ionisation can be expected to be very different between the four sulphides, as reflected in the extent of leaching observed (Table 8.5).

Table 8.8. Dissociation Constants and Stability Constants for Acids and their Metal Complexes

| Metal ion | Acid | T | Dissociation Constants | | Stability Constant |
|---|---|---|---|---|---|
| | | °C | $K_1$ | $K_2$ | $K_3$ (mole/liter) |
| -- | acetic | | $1.76 \times 10^{-5}$ | - | - |
| $Co^{2+}$ | | | | | 5 |
| $Ni^{2+}$ | | | | | 5 |
| $MoO_2^{2+}$ | | | | | - |
| $VO^{2+}$ | | | | | $1.99 \times 10^3$ |
| -- | oxalic | | $5.9 \times 10^{-2}$ | $6.4 \times 10^{-5}$ | - |
| $Co^{2+}$ | | | | | $2 \times 10^3$ |
| $Ni^{2+}$ | | | | | $6.3 \times 10^3$ |
| $MoO_2^{2+}$ | | | | | 39.8 |
| $VO^{2+}$ | | | | | $3.16 \times 10^6$ |
| -- | malonic | | $1.49 \times 10^{-2}$ | $2.03 \times 10^{-6}$ | - |
| $Co^{2+}$ | | | | | $1 \times 10^3$ |
| $Ni^{2+}$ | | | | | $2 \times 10^3$ |
| $MoO_2^{2+}$ | | | | | 25 |
| $VO^{2+}$ | | | | | $1.56 \times 10^5$ |

Spent catalyst represents a more complex problem, because the sulphide deposits are held within a porous carbon matrix and a porous catalyst pellet and also because the sulphides deposited on the catalyst cannot be expected to be of similar chemical composition. Non-stoichiometric sulphides are known to be formed during catalysis (2, 157) and the extended surface area may encourage partial oxidation of each sulphide during storage. The porous matrix should allow greater surface area of deposit and, as a result, enhance leaching rate, but limitation of access by reagent to the sulphide will partly counter this. In addition local areas of highly concentrated product solution could be trapped inside the matrix to limit further dissolution.

Given these uncertainties, and particularly because conversion of sulphides to ions (reaction 8.4) appears to be controlling, little quantitative information on the systems can be gained without knowledge of the nature of the deposits and their ionisation.

## 8.7 The Role of Promoter

It was observed that the addition of aluminium nitrate to the acid leachant led to enhanced leaching (Table 7.6). Since it seemed unlikely that $Al(NO_3)_3$ is a leachant in its own right, attention was directed to the possibility that interaction between the nitrate and the acid would lead to the production of a new leachant e.g.

$$3CH_3COOH + Al(NO_3)_3 \rightarrow 3HNO_3 + Al(OOCCH_3)_3$$

With this concept in mind, the pH of 0.66 M oxalic acid, 1M $Al(NO_3)_3$ and a 1:1 mixture was measured and a solution of nitric acid was prepared to the same pH (0.64). As shown in Table 7.7, leaching with nitric acid was less selective than with oxalic acid or oxalic acid/aluminium nitrate and resulted in the extraction of more material than oxalic acid but less than the mixture.

If the formation of nitric acid is important in the action of the promoter, it should be possible to generate the acid from other nitrate salts. Therefore, studies were made of leaching by oxalic acid mixed with different salts (Table 7.7). Ammonium nitrate did not result in enhanced leaching, probably as a result of the failure of the ammonium ion in solution to complex with the sulphide. Indeed, the degree of leaching with or without oxalic acid was of the same order of magnitude, although the selectivity of the leaching changed. Pure nitric acid gave enhanced leaching, but the extraction was very non-selective. Mixtures of aluminium sulphate and oxalic acid did not enhance leaching to the same degree as the corresponding nitrate system, reflecting the stronger bonding in aluminium sulphate and the lower tendency to form sulphuric acid.

Since the production of nitric acid cannot entirely explain the effect of the promoter (Table 7.7), a synergistic effect must occur in the oxalic acid/aluminium nitrate system, Oxalic acid alone is a mild reducing agent, and it was decided that the role of the nitrate may be to oxidise sulphides to a form which is more easily attacked by oxalic acid. Leaching experiments were therefore, carried out in which the deposit was partially or fully oxidised. With a fully oxidised catalyst, the promoter was found to have no effect on the efficiency of leaching (Table 8.9). Leaching with $H_2O_2$ gave leaching rates of similar order to those observed with $Al(NO_3)_3$/oxalic acid mixtures. Thus it would appear that one important role of the promoter is to partially oxidise the sulphide deposits, in order to facilitate attack by oxalic acid. Formation of nitric acid by reaction between the acid and the promoters may also contribute to the enhanced leaching.

The best explanation of these results would seem to be with the reactions that can occur before reaction with oxalic acid. In the absence of promoters, decomposition or hydration of sulphides may be expected to a limited extent eg.

$$NiS \longrightarrow Ni^{2+} + S^{o} + 2e^{-}$$

$$NiS + 4H_2O \longrightarrow Ni^{2+} + SO_4^{2-} + 8H^{+} + 8e^{-}$$

Such reactions have been observed to occur with sulphides such as $Ni_3S_2$, CuS, $Fe_{1-x}S$ etc (153). In the presence of an oxidising agent, sulphate production becomes more important eg.

$$NiS + 2O_2 \longrightarrow NiSO_4$$

and the metal ions tend to move to a higher valency. This allows greater solubility (154) and should favour attack by oxalate.

In agreement with this, the oxidised catalyst samples in which the S content was reduced from 8.34 % wt. to 3.86 % wt. by production of sulphate (Table 8.9) showed no increase in leaching on addition of promoter.

The nature of the complex formed by oxalate attack on the oxidised species may be expected to vary with the concentration of different species on the catalyst. Species such as $[VO(\text{oxalate})_2]^{2-}$ and mixed Ni/V/oxalate species have been observed under differing conditions (155). Accurate identification of the products of reactions was beyond the scope of the present study but certainly the nature of the products obtained by leaching would be of considerable interest for further study.

The level of material extracted after 24 h also requires consideration. These amounts are not dictated by solubility, nor by the availability of oxalic acid and/or promoter (Section 7.2.1.1). It would seem that the level of extraction to be achieved is dictated by leaching passiva-

Table 8.9. The Effect of Promoter on Leached Catalyst of Oxide Form With Oxalic Acid (0.66 molar), at Room Temperature at Steady State.

| Reagent | Metal<br>Wt % removal<br>V | Ni | Co | Mo |
|---|---|---|---|---|
| Oxalic acid | 42 | 44 | 50 | 47 |
| Oxalic acid + + $Al(NO_3)_3$, 1 Molar | 40 | 44 | 53 | 51 |

tion. If attack on the sulphides results in complexes which may be slow to dissolve, product would slowly build up on the surface until it reached a level that could not be penetrated by the leaching reagent. At this point, leaching would slow down to a rate dictated by the (slow) removal of protective product and the resulting (fast) attack of exposed sulphide by the leaching agent.

If this is the case, the amount of material leached would be expected to increase with the surface area of the sulphides. For a given surface area, a given amount of sulphide will react before the protective layer accumulates, so that the bigger the surface area, the greater the product which will be dissolved before protection is achieved. In agreement with this, the higher surface area spent catalysts were indeed leached more effectively than the lower surface area metal sulphides.

## 8.8 The Efficiency of Leaching Acids

The formation of metal ions, probably in the higher valency state, has been shown to control the extent of leaching. As a result differences may be expected in the rate of leaching of different metal salts.

However, differences in leaching efficiencies were also observed between acids. Since the formation of metal-acid soluble complexes does not appear to control leaching, it is more probable that the ionisation of the acid, leading to attack on sulphides and formation of metal ions

$$NiS + 2H^+ \longrightarrow Ni^{++} + H_2S$$

dictates at least in part the relative efficiency of the three acids.

Attempts were therefore, made to relate leaching efficiencies with ionisation constants. Such concepts have to be applied to the period before the passivation layer is built-up because leaching after this time reflects only the removal of part of the passivating layer and relatively fast attack on the exposed sulphide.

Given that formation of the metal ion is followed by formation of a soluble metal salt, ionisation constants alone would not dictate leaching. However, the relative efficiency of oxalic, malonic and acetic acid leaching would be expected to reflect the ionization constants.

As a result the relative leaching efficiencies of the three acids were compared with the relative ionization constants (Table 8.7) as shown in Table 8.10. The relative ionization clearly reflects the relative leaching although, as would be expected, the relationship is non-linear.

Table 8.10. The Relative Efficiency of Leaching With Three Acids With the Relative Ionization Constants for Pure Metal Sulphides at T=25°C,Conc. of Acid=0.66M at Steady Stat

| Metal | Oxalic Acid Final wt % Removal A | A/B ratio | Ionization Constant Ratio | Malonic Acid Final wt % Removal B | Ionization Constant ratio | B/C ratio | Acetic Acid Final wt % Removal C |
|---|---|---|---|---|---|---|---|
| V | 5.7 | 1.14 | 4.0 | 5.0 | 847 | 0.34 | 14.9 |
| Co | 1.2 | 0.79 | 4.0 | 9.5 | 847 | 1.1 | 8.7 |
| Mo | 0.52 | 0.93 | 4.0 | 0.52 | 847 | 1.1 | 0.52 |
| Ni | 0.2 | 0.13 | 4.0 | 1.6 | 847 | 0.33 | 4.8 |

## 8.9 The Activity of Leached Catalysts

The hydrodesulphurisation activity of leached and fresh catalysts was measured as described in Chapter 6. The results are summarised in Table 8.11. These demonstrate that the full activity of the fresh catalyst was never recovered with leached catalyst, but that the closest approximation was obtained by leaching with oxalic acid plus promoter.

It would be expected that catalytic activity would decrease with the amount of Ni and V remaining on the catalyst and with decreasing surface area and pore volume. As shown by Figures 8.10 and 8.11, activity was found to be a function of surface area and pore volume, but there was no regular trend of activity with the Ni and V content of the catalysts. This is an interesting finding, in that it would indicate that metals do not poison the catalyst but their main role as deactivants is to block off the surface - either by fouling the surface or by blocking pores. Leaching to remove the fouling/blocking agent allows access to the catalyst surface area and increases activity.

Oxalic acid/promoter and malonic acid/promoter were the most effective leachants despite the fact that some Co and Mo was also removed from the catalyst (Table 8.11). The percent weight removal of Co and Mo from both treated samples ranged from 76% - 73% and 75% - 68% respectively with respect to fresh catalyst. The leached catalyst thus contained a Co:Mo ratio of (0.3:0.7) which is much less than the ratio in the fresh catalyst (3:12). Despite this the hydrodesulphurization activity of leached catalyst approached that of the fresh catalyst. This could be related to the ability of acids used in the regeneration process for metal leaching to help in redispersing the active metal components of the catalyst during the treatment.

The results also show that, although different reagents were used for metals leaching, the activity of the leached catalyst did not reflect the nature of leaching reagent.

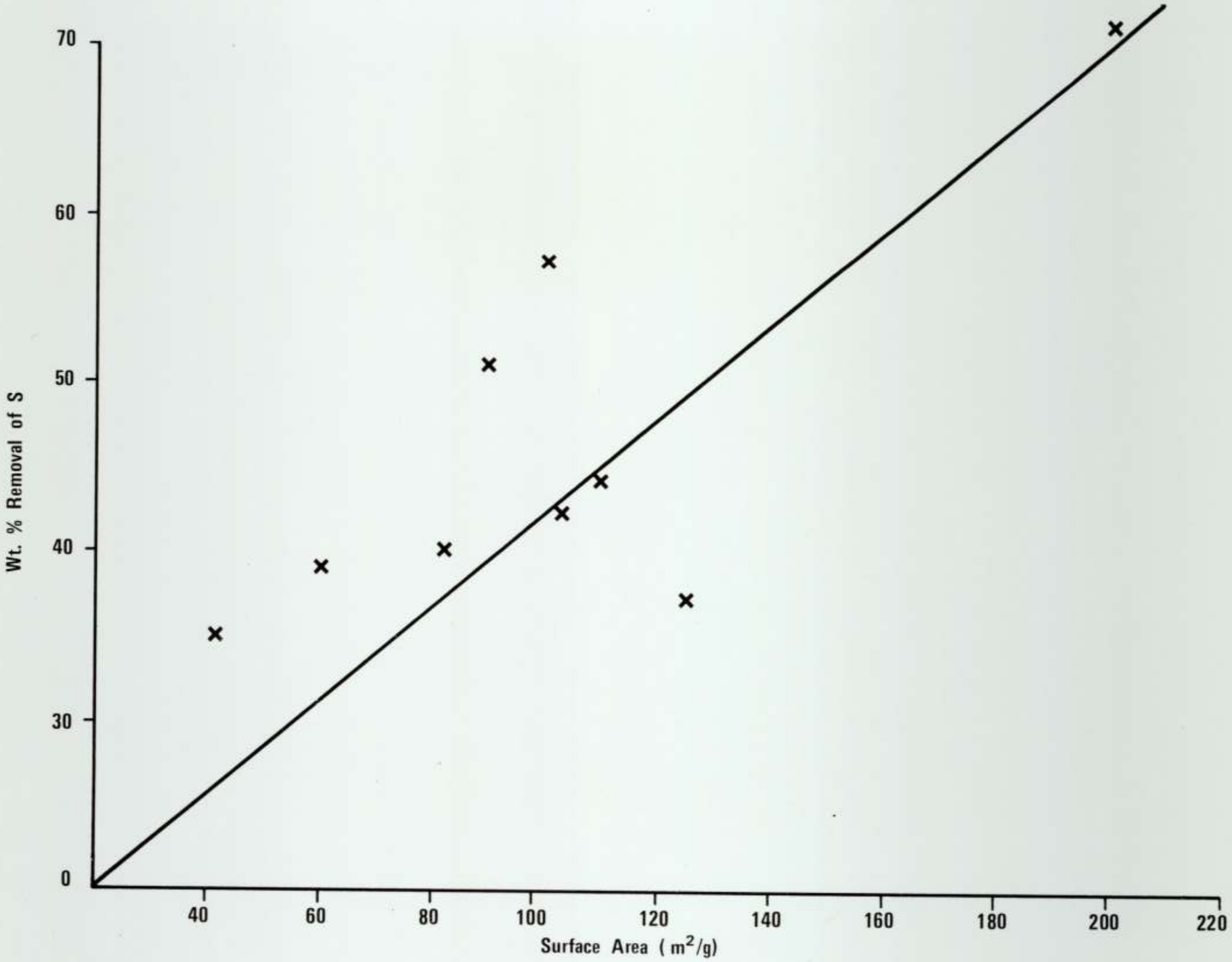

Figure 8.10. The relation between sulphur percent removal with surface area.

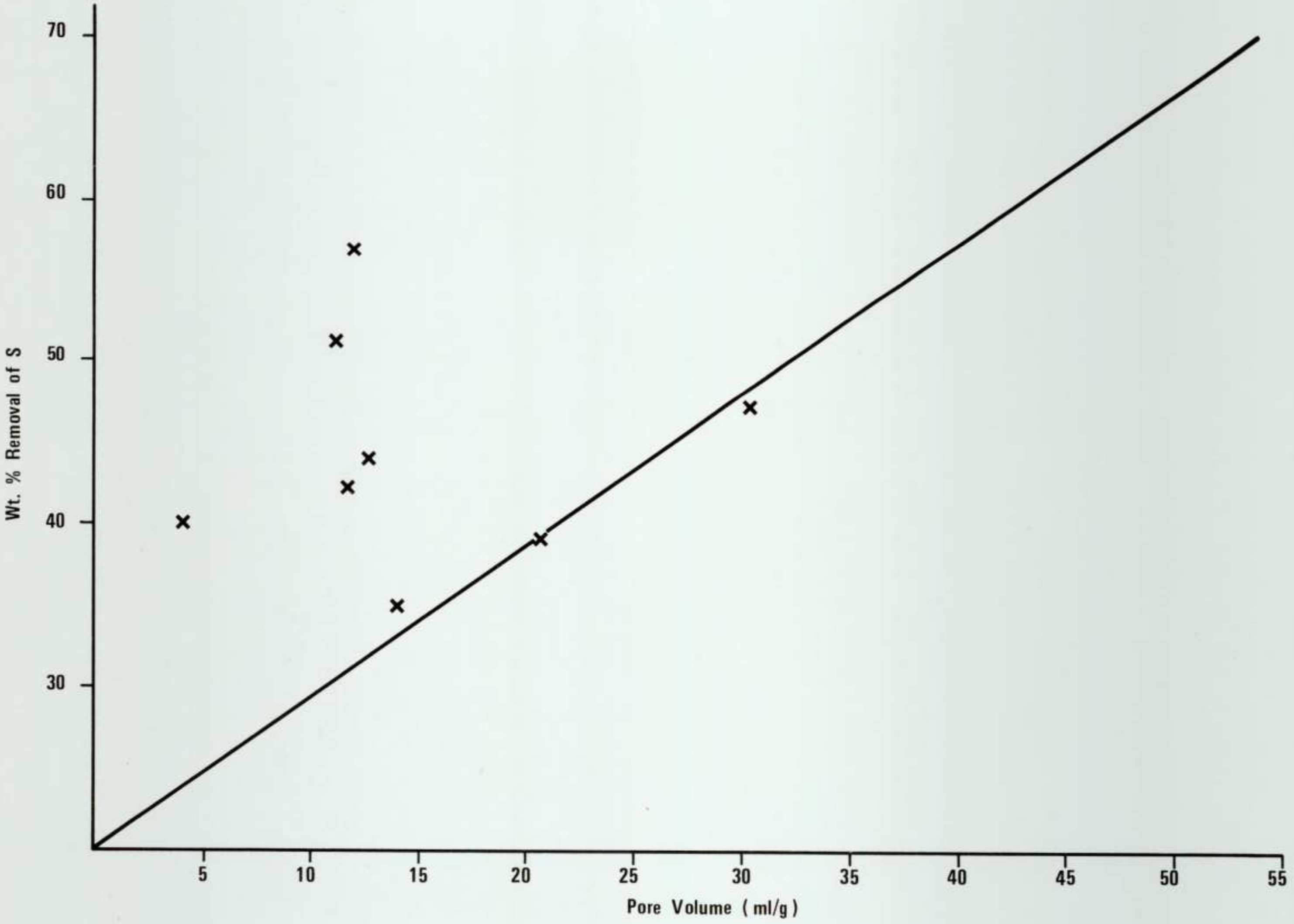

Figure 8.11. The relation between sulphur percent removal with pore volume.

Table 8.11. The Relation Between wt % removed of Sulphur at Steady State and Other Properties for Fresh, Spent, Decoked and Treated Samples with Different Acids (0.66 molar), With and Without Promoter (1 molar) at 25°C.

| Sample | Wt % of V Remaining | Wt % of Ni Remaining | Wt % of Mo Remaining | Wt % of Co Remaining | Surface Area $m^2/g$ | Pore Volume ml/g | Wt % Removed of Sulphur after 6 hrs |
|---|---|---|---|---|---|---|---|
| Fresh | 0.0 | 0.2 | 11.72 | 3.27 | 202.7 | 0.710 | 54 |
| Spent | 15.1 | 3.7 | 3.99 | 1.07 | 43.8 | 0.140 | 30 |
| Decoked | 16.5 | 4.1 | 4.20 | 1.07 | 60.4 | 0.220 | 37 |
| Oxalic acid | 12.1 | 3.6 | 3.30 | 1.10 | 100.2 | 0.116 | 28 |
| Oxalic acid +$Al(NO_3)_3$ | 8.2 | 1.9 | 3.00 | 0.80 | 125.0 | 0.307 | 45 |
| Malonic acid | 12.7 | 2.6 | 3.90 | 0.90 | 104.9 | 0.121 | 42 |
| Malonic acid + $Al(NO_3)_3$ | 12.3 | 2.7 | 3.90 | 0.90 | 109.9 | 0.127 | 48 |
| Acetic acid | 13.9 | 3.1 | 3.60 | 0.9 | 87.7 | 0.106 | 33 |
| Acetic acid + $Al(NO_3)_3$ | 13.4 | 3.0 | 3.00 | 0.93 | 84.4 | 0.038 | 34 |

## Conclusions

The major conclusions arising from this investigation are as follows:

1. Either oxalic, malonic or acetic acid can be used to regenerate hydrodesulphurization catalyst by the removal of deposits of poisonous metal sulphides such as vanadium and nickel. The effectiveness of an acid for selective removal of V and Ni appears to depend upon the stability constant of complex formation and the ionization content of the acid. Thus for example oxalic acid with the highest stability constant was the best for vanadium removal. Acid concentration in the range 0.33-1.0 Molar had little effect on the degree of metal sulphides extraction. However, the degree of leaching was increased by an increase in temperature in the range 25-75°C.
2. The process of metal sulphides extraction was more effective when a promoter (aluminium nitrate) was added to the acid reagent, as a result of a synergistic effect. The optimum concentration for promoter ranged from 0.1-0.5 molar.
3. Because aluminium sulphate and ammonium nitrate were ineffective as promoters, and from separate tests using nitric acid for leaching, the role of promoter was postulated to involve formation of nitric acid during the process, which increased the efficiency of metal sulphides leaching and oxidized the sulphides. The oxidized products were leached more easily.
4. The formation of a passive layer on the catalyst surface during the reaction limited the amount of metal sulphides removed by leaching.
5. Sulphide catalyst can be regenerated by extraction of metal salts of vanadium and nickel prior to coke burning and still retain its hydrodesulphurization activity. This activity was retained even though the acid treatment removed part of the main active metal constituents (e.g. oxalic acid with promoter removed 73% and 75% respectively). The HDS was regenerated up to an activity of 83.3% of that for fresh catalyst.
6. It was found that contaminated metals do not poison the catalyst but block-off the surface, either by fouling the surface or by blocking pores. This is of relevance to the regeneration process selected.

7. The rate determining step in pure metal sulphides leaching appeared to be the rate of chemical reaction as indicated by their small porosity. Spent catalyst leaching (prior to decoking) appeared to be controlled by liquid diffusion in the pores.

The minor conclusions are:

1. Oxalic and malonic acid with the addition of promoter were the most effective leachants as demonstrated from HDS activity measurements.
2. The efficiency of leaching by an acid appears to be related to its ionization constant.
3. The optimum time for metal sulphides extraction from spent catalyst was in most cases approximately 12 hrs. The amount of material leached appeared to increase rapidly with time but then approached a steady state value.
4. The use of pure metal sulphides for identifying the individual steps in leaching assisted in providing information for identification of the kinetics of the process. Further studies on pure metal oxides will be useful in view of the postulated leaching mechanism.
5. From pure metal sulphide leaching experiments a rough prediction was possible for surface areas of the different metal salts for the purpose of estimating the accessibility of metal salts in the spent catalyst.

Recommendations for Further Work

1. A comparative study should be carried out on leaching from the oxide form of atmospheric hydrodesulphurization catalyst after burning off the coke.
2. An investigation could be made into the nature of the products formed by leaching of metal sulphides from spent catalyst using oxalic acid.
3. Application of new selective reagents can be investigated to give optimum, selective removal of contaminated metal deposits. Selection will depend on the ionization constants of the acid and the stability constant of the complex formed.
4. A study should be carried out of the effect of using different promoters upon metal sulphides and oxide removal from spent catalyst.
5. A process could be developed for regeneration of ARDS catalysts by selective metals removal prior to de-oiling of the spent catalyst for the assessment of process costs.

6. It would be worthwhile to investigate the effect of different parameters (including temperature, pressure, gas flowrate, oxygen content and the presence of steam) upon the efficiency of decoking ARDS catalysts.
7. The effect on activity and mechanical strength of repeated regeneration by the preferred process should be investigated.
8. A mathematical model could be developed for the leaching out of metal sulphides from catalyst particles. The purpose would be to quantify the effects of various parameters e.g. particle size, surface area and pore volume. The regeneration of catalyst particles with a similar degree of de-activation but different diameters could be studied experimentally and the results compared with the model.
9. Finally the preferred process for metal sulphides removal should be investigated on a pilot scale.

# APPENDIX 1

## 1.1 Determination of Compacted Bulk Density (C.B.D.)

### Scope

Determination of the weight of a known volume of catalyst, whereby a container of known volume is filled with catalyst by tapping.

### Principle

The compacted bulk density (C.B.D.) is the weight per unit volume (g/ml) of the compacted catalyst.

### Apparatus

- P.V.C. container (cylindrical), 200 ml. capacity, 5.3 cm dia., 9.5 cm deep.
- Drying oven, operating temperature 110°C.

### Pretreatment

Take approximately 300 ml of sample to be tested, using a sample splitter. Dry at 110°C for 1 hour and allow to cool in a desiccator. Samples of which the loss on ignition is lower than 3% need not be predried.

### Procedure

- Weigh the container of known volume to the nearest 0.1 gram (a). (Volume of the container is determined by weighing it whilst filled with water at 20°C and by weighing it empty).
- Fill the container with pretreated sample until nearly full. Tap the container with a spatula and tap the container itself on the table at the same time.
- Fill again and repeat tapping.
- Repeat filling and tapping until container is full and level is constant.
- Wipe off excess of sample with a straight-edge spatula leaving the container filled flush with the top.
- Weigh the filled container to the nearest 0.1 gram (b).

Calculation

$$\text{C.B.D. (g/ml)} = \frac{\text{(b-a) grams}}{\text{container volume (ml)}}$$

## 1.2 Side Crushing Strength

### Scope

The side crushing strength of catalyst particles of average length (5-10 mm) is determined as an average of the values for 40-50 particles.

### Principle

The crushing strength of individual particles is determined by placing them one by one on a holding plate between two vertical plates. One of the plates is held stationary while the other moves automatically, slowly pressing the particle with increasing force until it is crushed. The pressure at the crushing point is registered automatically. The side crushing strength of each particle is reported as force per unit length. The crushing strength of the sample is calculated as the average of the values for 40-50 particles.

### Apparatus

- Muffle furnace with temperatures up to 500°C
- Pair of tweezers and brush
- A tablet crushing strength measuring apparatus capable of applying pressures up to 300 Newton.

### Pretreatment

Using a sample splitter, take an amount of the sample to be tested containing approximately 50 particles. Calcine the sample for 1 h at 550°C, then cool in a desiccator.

### Procedure

Place the particle between the plates of the crushing instrument on the holder. Start the instrument and allow it to crush the particle. Read the printed value of the force required to crush the sample and record it. Repeat the same procedure for other particles of the sample up to 50 particles.

### Calculation

The average side crushing strength of the catalyst sample is found from:

$$\text{Average Side Crushing Strength} = \frac{\text{Side Crushing Strength (Newton)}}{\text{Length (mm)}}$$

$$\underset{\text{(N/mm)}}{\text{Average Side Crushing Strength}} = \frac{\text{Average Side Crushing Strength}}{4.45}$$

## 1.3 Determination of Surface Area

### Scope

Total surface area of a catalyst is determined by Brunauer-Emmet-Teller (BET) method (using flow technique).

### Reagents

- Nitrogen
- Helium gas
- Liquid nitrogen

### Apparatus

- Adsorption apparatus (Quantasorb)
- Sample tubes
- Dewar flasks
- Linear mass flow controller
- Recorder

### Procedure

1. Take a catalyst sample (0.1 g) in the sample tube. Fix it in the sample holder in the Adsorption Unit (in the pretreatment position). Put the heating mantle around the sample tube and clamp it. Pass nitrogen (20 $cm^3$/min) through the sample tube.
2. Switch on the Qantasorb UNIT and flow controller.
3. Put liquid nitrogen in the Dewar flask around the trap in the right hand side of the unit. Adjust the temperature control-knob until the temperature reaches 400°C. Keep it under these conditions (temperature 400°C, nitrogen flow rate 20 $cm^3$/min) for 90 min and switch on the recorder.
4. Allow the sample tube to cool to room temperature. Transfer it to the adsorption position (at the front panel of the unit) and pass

nitrogen through the sample by opening the valve at the top of the Quantasorb Unit. Set the attenuation at 32 (Quantasorb) and bridge current at 150 mA. Set the recorder span at 5 and chart speed at 0.5 cm/min. Put the by-pass valve to the by-pass position. Open the helium cylinder and helium valve in the Quantasorb. Adjust the helium flow control valve in the flow controller to get flow rate of 18 $cm^3$/min. Adjust the nitrogen flow control valve until the flow rate of $N_2$ is 2 $cm^3$/min.

Open the by-pass valve (at the top) to the sample position and allow the gas mixture (10% $N_2$ in He) to pass through the sample. Wait for 30 min until a steady base line is observed in the recorder. Zero the integrator reading in the counter. Put the polarity switch in the adsorption position (up). Immerse the sample tube in liquid nitrogen.

A peak will appear in the recorder due to adsorption. The adsorption is complete and the recorder pen has returned to the base line, and the reading becomes constant. Note down the integrator reading. Zero the integration counts and change the polarity switch to the desorbtion position (down). Bring the base line to the original position. Remove the liquid nitrogen flask from the sample.

5. Desorption of nitrogen takes place and a peak appears in the recorder. When the recorder pen returns to the base line and the integrator reading becomes constant, note down the reading.
6. Withdraw 2.5 $cm^3$ of $N_2$ in a gas syringe from the OUT position in the Quantasorb and inject it into the carrier stream in the IN position. Watch the calibration peak and note down the calibration counts when the reading becomes constant.
7. Turn the valve at the top of the unit to the by-pass position.
8. Make another mixture containing 12.5% $N_2$ in helium. (Increase the nitrogen flow rate to 2.5 $cm^3$/min and decrease helium flow rate to 17.5 cc/min.).
9. Repeat steps 4 to 8.
10. Make another mixture containing 15% $N_2$ in helium. (Nitrogen flow rate 3 $cm^3$/min and helium flow rate 17 $cm^3$/min.)
11. Repeat steps 4 to 8.
12. Shut down the unit as follows:
    - Switch off the recorder.

- Switch off the Quantasorb unit.
- Switch off the flow control unit.
- Close the $N_2$ and the cylinders.
- Close the $N_2$ and helium valves in the Quantasorb Unit.

13. Find the accurate weight of the catalyst in the sample tube

## Calculation

The volume of nitrogen desorbed at various nitrogen partial pressures is calculated as follows:

$$\text{Volume of } N_2 \text{ desorbed, cm}^2 = \frac{\text{Digital counts for desorption}}{\text{Digital counts for calibration}} \times 2.5$$

Calculate $\frac{P}{V(P_o - P)}$ for each nitrogen partial pressure

Plot $P/V(P_o-P)$ against $P/P_o$ and find the slope of the straight line. Calculate the monolayer volume, $V_m$, from the slope and the intercept of the line.

$$V = \frac{1}{\text{Slope + Intercept}}$$

(intercept is normally zero since the line usually passes through the origin)

Calculate the monolayer volume at STP

$$V_m \text{ (at STP)} = V_m \text{ (at room temperature)} \times \left( \frac{273}{273 + t} \right)$$

$$\text{Surface area, m}^2/\text{g} = \frac{4.356 \times V_m \text{ (at STP)}}{\text{sample weight}}$$

## 1.4 Pore Volume ($N_2$ method) and Average Pore Diameter

### Scope

Pore volume and average pore diameter of a catalyst is determined by nitrogen adsorption.

## Principle

By measuring the volume of nitrogen adsorbed at a relative pressure of 0.98, the pore volume is calculated using the following equation:

$$V_{pore} = \frac{P \times V_{ads}}{RT} \times V_m \qquad (1)$$

where

$P$ is the ambient pressure (1 atm);

$V_{ads}$ is the volume of nitrogen adsorbed per gram catalyst;

$T$ is the room temperature in degrees Kelvin;

$V_m$ is the molar volume of liquid adsorbate (34.7 $cm^3$ for $N_2$); and

$R$ is the gas constant (82.1 ml atm. $deg.^{-1}$ $mole^{-1}$).

Assuming that cylindrical pores constitute the nature of the entire surface, the average pore diameter can be calculated using the following equation:

$$d = \frac{4\ V_{pore}}{S} \times 10^4 \text{ Angstroms} \qquad (2)$$

where

$V_{pore}$ is the pore volume per gram catalyst ($cm^3$) and

$S$ is the surface area ($m^2/g$)

## Procedure

The experimental set up and experimental procedure for measuring the volume of nitrogen adsorbed are the same as described under surface area measurement. The sample is pretreated by heating at 400°C for 1 h in flowing nitrogen (20 ml $min^{-1}$) to free the sample from air and moisture. It is cooled to room temperature and allowed to equilibrate with nitrogen-helium gas mixture containing 98% ($P/P_o = 0.98$). It is then cooled to liquid nitrogen temperature and the volume of adsorbed nitrogen is measured.

Calculation

The pore volume is calculated using equation (1) and average pore diameter is calculated using equation (2). An example of data tabulation, pore volume and average pore diameter calculations from adsorption data is shown below.

Sample I.D: A 333 Sample Wt: 0.09870 g

Temperature: 24°C

| $P/P_o$ | Digital counts for adsorption | Digital counts for calibration | Calibration volume ml | Vol of nitrogen adsorbed ml/g |
|---|---|---|---|---|
| 0.98 | 6147 | 406 | 2.5 | 383.5 |

$$\text{Volume of nitrogen adsorbed} = \frac{6147}{406} \times 2.5 = 37.85 \text{ ml}$$

$$\text{Volume of nitrogen adsorbed } (V_{ads}) \text{ per gram catalyst} = \frac{37.85}{0.0987} = 383.5 \text{ ml}$$

$$\text{Pore volume } (V_{pore}) = \frac{383.5 \times 1 \times 34.7}{82.1 \times 297}$$

$$= 0.546 \text{ ml/g catalyst}$$

Average Pore Diameter

$$d = \frac{4 \times V}{S} \quad 10^4 \text{ A}^\circ$$

$$V = 0.546 \text{ ml/g catalyst}$$

$$S = \text{m}^2/\text{g cat} = 187 \text{ m}^2/\text{g}$$

$$d = \frac{4 \times 0.546}{187} \times 10^4 \text{ A}^\circ$$

$$d = \underline{116.8 \text{ A}^\circ}$$

## 1.5 Determination of Pore Size Distribution by Nitrogen Adsorption

### Scope

Determination of pore size distribution is determined by nitrogen adsorption-desorption isotherm measurements.

### Apparatus

- Adsorption unit (Quantasorb)
- Flow control accessory
- Dewar flasks
- Sample tubes
- Recorder

### Reagents

- Nitrogen gas (high purity grade)
- Helium gas (high purity grade)
- Liquid nitrogen

### Procedure

The experimental apparatus and operating procedure for measuring adsorption-desorption are the same as described under surface area measurement. The $N_2$ adsorption-desorption volumes are measured at various relative pressures ($P/P_o$ from 0.3 up to 0.98) using nitrogen-helium mixtures of varying compositions. The volume of nitrogen desorbed ($V_{des}$) is plotted against $P/P_o$ to obtain the desorption isotherm.

### Calculations

Starting with the desorption branch of the isotherm, the volume of gas desorbed (V in $cm^3$) at several intervals of $P/P_o$ is determined down to a relative pressure of 0.3. The Kelvin radius ($r_k$) and the pore radius ($r_p$) are calculated using the following equations.

$$r_k = \frac{4.146}{\text{Log } P_o/P}$$

$$r_p = r_k + t$$

The value of t is obtained from Table 1. The volume of liquid desorbed ($V_{liq}$) at any interval is calculated from the volume of gas desorbed ($V_{gas}$) using the relationship:

$$V_{liq} = \frac{\Delta V_{gas} \, P}{273 \times 2.37}$$

The mean values $r_p$ and $r_k$ in each interval are used along with $V_{liq}$ and $\Delta t \sum A$ are used to calculate the mean volume of pores ($V_p$ in $cm^3$) with mean radius $r_p$ using the following equation.

$$V_p = \left[\frac{\bar{r}_p}{\bar{r}_k}\right]^2 \{V_{liq} - \Delta t \sum A\}$$

The surface area A is calculated using the equation:

$$A = \frac{2 \, V_p}{\bar{r}_p} \times 10^4$$

Data Treatment

- Fill in data sheets similar to the attached.
- Plot the cumulative pore volume against the mean pore radius $r_p$.
- Plot $\Delta V_p/\Delta r_p$ against $r_p$ to obtain differential pore size distribution.

Table 1. Adsorbed Layer Thickness at Various Relative Pressures

| $P/P_o$ | t,A | $P/P_o$ | t,A | $P/P_o$ | t,A | $P/P_o$ | t,A |
|---|---|---|---|---|---|---|---|
| .3 | 5.6 | .62 | 7.7 | .75 | 9.1 | .87 | 11.5 |
| .35 | 5.9 | .64 | 7.8 | .76 | 9.2 | .88 | 11.9 |
| .40 | 6.2 | .66 | 8.0 | .77 | 9.4 | .89 | 12.2 |
| .425 | 6.3 | .67 | 8.1 | .78 | 9.5 | .90 | 12.7 |
| .45 | 6.5 | .68 | 8.2 | .79 | 9.7 | .91 | 13.1 |
| .475 | 6.6 | .69 | 8.3 | .80 | 9.9 | .82 | 13.7 |
| .50 | 6.8 | .70 | 8.5 | .81 | 10.1 | .93 | 14.4 |
| .52 | 6.9 | .71 | 8.6 | .82 | 10.3 | .95 | 16.2 |
| .54 | 7.0 | .72 | 8.7 | .83 | 10.5 | .96 | 17.3 |
| .56 | 7.2 | .73 | 8.8 | .84 | 10.7 | .97 | 19.2 |
| .58 | 7.3 | .74 | 8.9 | .85 | 1.0 | .98 | 22.1 |
| .60 | 7.5 |  |  | .86 | 11.2 | .99 | 27.8 |

## 1.6 Determination of Sulphur Using the Shroninger Method

### Scope

The concentration of sulphur in organic compounds can be determined by the Shroninger method.

### Principle

Sulphur in organic compounds can be determined by burning the organic sample in an oxygen gas atmosphere in a 1 l flask that contains 1 N NaOH and hydrogen peroxide.

$$RSR + O_2 \text{ ------> } SO_2 + CO_2 + H_2O$$

$$NaOH + SO_2 \text{ ------> } Na_2SO_3$$

$$H_2O_2 + Na_2SO_3 \text{ ------> } Na_2SO_4 + H_2O$$

Sodium sulphate can be determined quantitatively by precipitation as lead sulphate from a nitric acid solution containing isopropyl alcohol that is added to reduce the stability of the precipitate. The precipitate is filtered off using 0.45 Um millipore filter paper and redissolved in a measured quantity of standard EDTA solution. The excess EDTA is back titrated with a standard solution of zinc chloride using Erichrome Black T as an indicator.[1]

Apparatus

Shroninger instrument used for burning the sample.

- o 1 l Erlenmeyer flask quick fit
- o Platinum net
- o 0.45 m μ filter paper
- o Filtering set
- o Oxygen gas
- o Graduate cylinder 10 ml, 100 ml

Reagents

- o 1 N NaOH
- o 30% $H_2O_2$
- o Ammonia solution
- o 1 M lead acetate solution
- o 0.1 M EDTA solution
- o 0.05 M $ZnCl_2$ solution
- o Erschrome Black T indicator-grind 0.2 gm of this compound firmly in a mortar with 50 g of potassium chloride
- o 0.45 μ in, millipore filter paper
- o 0.1 μ $Na_2SO_4$ solution

Procedure

1. Weigh a filter paper; cut in special form.
2. Add a known weight of the sample (10-50 mg) to the filter paper and tie it.
3. Fix the sample between the leaves of the platinum net.
4. Put 10 ml of 1 N NaOH solution and 3 ml of $H_2O_2$ solution in a clean Erlenmeyer flask.
5. Fill the flask with oxygen and stop it with the platinum net that is holding the sample.
6. Put the flask, with the platinum net, in the Shroninger burning device.
7. After the sample is completely burned, leave it for 30-120 min until all the fumes disappear.
8. Add 5 ml concentration $HNO_3$ to the flask and shake.
9. Add 50 ml isopropyl alcohol.
10. Introduce 5 ml of 1 M lead acetate solution.
11. Allow to stand for 15 min for complete precipitation.

12. Filter the precipitate through 0.45um millipore filter paper.
13. To the precipitate add a known volume of EDTA solution sufficient to dissolve it, followed by 10 ml of concentrated ammonia solution to dissolve the precipitate.
14. Add 0.2 g of Erichrome Black T indicator and titrate with a zinc chloride solution until the colour changes from blue to violet.

### Calculation

$$S\% = 1/3 \; \frac{\text{(Vol. of 0.1 MEDTA - 1/2 vol. of 0.05M } ZnCl_2 \times 9.606 \times 100}{\text{Wt. of sample (mg)}}$$

## 1.7 ICAP-OES Simultaneous Analysis of Trace Metal Fe, Mg, Cu, Ca, Si and As in the Catalyst

### Scope

This method is used for the simultaneous determination of multi trace elements in an $Al_2O_3$-based catalyst.

### Procedure

The following steps were used to prepare the samples:

1. About 0.1 g of the samples are weighed in 100 ml beaker.
2. 2 ml concentrated super pure $H_2SO_4$ is added to the beaker. The samples are heated at 200°C. A white ppt appeared on $H_2SO_4$ treatment.
3. Then two 2ml portions of concentrated HCl is added and heated on the hot plate till the white ppt disappears.
4. The final solution was made to 50 ml in a volumetric flask by adding deionized water.
5. For Si determination, a sample (about 100 mg) was fused for 2 h with 300 mg $Na_2CO_3$ and 200 mg boric acid in a platinum crucible in a muffle furnace at 1000°C. After cooling, the fused mixture was dissolved in about 2 ml conc. HCl by heating and then transferred and washed to 50 ml with deionized water in a volumetric flask.

### Calculation

The system is calibrated for concentration by developing a matrix into the microprocessor using two standards with a low and high concentration range for each required analytical element.

The signal for each atomic spectral line is corrected for its background, and the net signal of intensity is recorded. The microprocessor prints out the concentration of each element in a sample.

## 1.8 Analyses of Distribution Profile of Elements in Catalyst Pellets by Rapid Electron Scanning Method

### Scope

Analysis by scanning represents the method for estimating relative concentrations of different elements in a selected number of points across the diameter of catalyst pellets. These relative concentrations are plotted in the form of a continuous curve representing a distribution profile of relative concentrations of individual elements.

### Principle

When electron beams interact with a solid specimen, characteristic x-rays are produced that are used both for qualitative and quantitative analysis. X-ray intensity at a selected X-ray line of element wavelengths is related to the concentration of this element. Therefore, the number of X-ray counts within a chosen time interval is proportional to the concentration of the element in the analysed area. When a sample moves along an X or Y axis, the X-ray intensity for a selected number of points (areas) can be estimated, and a distribution profile of the relative concentration of elements can be calculated.[2]

### Reagents

- Embedding resin (acrylic moulding powder No. 13121).
- Grinding materials (Si/C paper grade 220 and 600).
- Polishing material (alumina FF).
- Carbon rods
- Argon - methane (90% - 10%).

## Apparatus

- Mounting unit (Metaserv).
- Grinding machine (Metaserv).
- Polishing machine (Metaserv).
- SEM coating unit (Polaron).
- Scanning Electron-Microprobe Analyser (Cabex).
- PDP-11 computer analytical programs (SCAN, SCAHP).
- HP Plotter.

## Procedure

**Sample Preparation.** Catalyst pellets are embedded in acrylic resin and ground by SiC paper (grade 220 and 600) without solvent. Programmed pellets are polished by FF alumina with limited solvent application under continuous check of optical microscope. Polished samples are coated with 30 um thick layer of carbon in a vacuum of about $10^{-2}$ torr.

**Analysis.** A camebax WDS system with two inclined spectrometers (TAP, PET and LIF crystals) is used for analysis at 15 kV of accelerating voltage and $1.10^{-7}$ A of sample current. The PDP-11 computer with SCAN programs (Cameca) is applied for performance of analysis. Requested shift on X axis and/or Y axis is entered into the program as well as size of scanned area (entered in relative numbers 1-5). Preselected counting time is usually 3-5 sec. An analysis can be performed in "points" (about 0.1 $\mu m^2$) when the electron beam is focussed on the sample , or in area (corresponding to several $\mu m^2$) when electron beam is defocussed. X-ray intensities obtained for each analysed point are stored on det. floppy disc. 2 elements can be analysed by 2 spectrometers simultaneously.

**Plotting.** An HP-Plotter, operating under SCAHP Program (Cameca) is used for plotting the results. The scale factor for Y-axis is chosen as well as graduations for X-axis. X-axis graduations are subsequently recalculated for the real distance estimated from X or Y stage movement.

## References to Appendices

1. Musleh, F. M. and Awayes, R., Method CAL-W-11, Central Analytical Laboratory, KISR.
2. Korb, J., Method CAL-P-08, Central Analytical Laboratory, KISR.

# NOMENCLATURE

| | |
|---|---|
| A, B | Reactants |
| b | Stoichiometric coefficient for reacting substabce B |
| C | Constant for energy of adsorption |
| $C_{Al}$ | Concentration of A for liquid, mol/cm$^3$ |
| $C_{As}$ | Concentration of A for solid, mol/cm$^3$ |
| $\frac{dc}{dt}$ | Rate of reaction, g/s |
| $\frac{dc}{dx}$ | Concentration gradient of c in x direction, mole/cm. |
| d | Average pore volume, ml/g |
| $\frac{dN}{dt}$ | Rate of diffusion of a reactant, g/s |
| D | Pore diameter, A° |
| D | Diffusion coefficient, cm$^2$/s |
| $D_o$ | Frequency factor |
| $d_p$ | Diameter of particle, cm |
| $D_e$ | Effective diffusion coefficient of liquid reactant in the ash layer, cm$^2$/s |
| E | Activation energy, cal/mole.°K |
| K | Chemical rate constant |
| $K_l$ | Mass transfer coefficient in liquid phase, cm/s |
| $K_s$ | First order reaction rate constant based on unit surface, cm/s |
| M.wt. | Molecular weight, g/mole |

| | |
|---|---|
| N | Flux , mole/cm$^2$. s |
| N | Force, Newtons |
| $N_A$ | Moles of component A |
| $N_B$ | Moles of component B |
| $N_m$ | Total number of gas molecules, cc/sTp |
| P | Ambient pressure, atm. |
| $P/P_o$ | Pressure ratio, mm |
| Q | Activation energy, cal/mol.°K |
| $Q_A$ | Flux of material A through surface of any radius r |
| $Q_{Ac}$ | Flux of A through reaction surface |
| $Q_{As}$ | Flux of A through exterior surface of particle |
| R | Radius of particle, cm |
| R | Universal gas constant , Cal. /mole. °K |
| $r_e$ | Radial position within a particle (equivalent radius of pore), cm |
| $S_{ex}$ | Exterior surface, cm$^2$ |
| S | Surface area, m$^2$/g |
| S% | Sulphur percent |
| t | Time of leaching, s |
| T | Room temperatue, °K |
| V | Volume of solid particle, cm$^3$ |
| V | Volume of gas adsorbed at $P/P_o$, ml |
| $V_{ads}$ | Volume of nitrogen adsorbed per gram catalyst, cm$^3$ |
| $V_m$ | Molar volume of liquid adsorbate, cm$^3$ |
| $V_{pore}$ | Pore volume, ml/g |

| | |
|---|---|
| $X_B$ | Fractional conversion |
| Y | Mole fraction |

## Greek Symbols

| | |
|---|---|
| $\alpha$, $\beta$ | Order of reaction for component A and B respectively. |
| $\theta$ | Diffraction angle |
| $\rho_B$ | Molar density, mole/cm$^3$ |
| $\sigma$ | Surface tension of mercury, 484 dynes/cm |
| $\eta$ | Effectiveness factor |
| $\tau$ | Time for complete conversion of a single solid particle, s |
| $\mu$ | Velocity, cm/s |

## References

1. L. L. Hegedus and R. W. McCabe. Catalyst Poisoning, in "Catalyst Deactivation", (Eds. B. Delmon and G. F. Froment), Elsevier, Amsterdam, p. 471, 1980.
2. C. H. Bartholomew, P. K. Agarwal, and J. R. Katzer. Sulphur Poisoning of Metals, in "Advances in Catalysis" vol. 31, p. 135, 1982.
3. D. L. Trimm. Catalyst Design for Reduced Coking (review), Appl. Catal. 5, p. 263, 1983.
4. C. H. Bartholomew. Carbon Deposition in Steam Reforming and Methanation, Catal. Rev. Sci. Eng. 24, p. 67, 1982.
5. S.T. Sie. Catalyst Deactivation by Poisoning and Pore Plugging to Petroleum Processing, In "Catalyst Deactivation", (B. Delmon and G. F. Froment, Eds), Elsevier, Amsterdam, p. 545, 1980.
6. G. F. Huttig. Disc. Farad. Soc. 8, p. 215, 1950.
7. A. E. B. Presland, G. L. Price, and D. L. Trimm. Prog. in Surface Science 3, 63, 1972.
8. M. Moayeri and D. L. Trimm. Reorganisation of Nickel under Steam Reforming Conditions. Farad. Soc. Trans. 73, p. 1245, 1977.
9. W. M. Gitzen. Alumina as a ceramic material. Amer. Cer. Soc., Columbia, 1970.
10. S. E. Wanke. Models for sintering of supported metal catalysts, in "Progress in Catalyst Deactivation (J. L. Figueiredo, ed), p. 315, 1982.
11. B. Delmon and P. Grange. The role of chemical transformations of solids in ageing and deactivation of catalysts, in "Progress in Catalyst Deactivation (J. L. Figueiredo, ed), p. 231, 1982.
12. J. R. Rostrup-Nielsen. Catalytic Steam Reforming, in "Catalysis Science and Technology" vol. 5, p. 245, 1983.
13. A. Stanislaus and K. Al-Dolama. Effect of Thermal Treatment on the Concentration and Distribution Profiles of Molybdenum, Cobalt, and Nickel in Co-Mo/$Al_2O_3$ and Ni-Mo/$Al_2O_3$ catalysts. J. Catal. 101, p. 536, 1986.
14. S. Gultekin and E. Hamad. Catalyst Deactivation the Arabian Journal for Science and Engineering vol. 26, No. 1, pp. 59-65, 1986.

15. F. M. Dautzenberg and J. C. De Deken. Reactor Developments in Hydrotreating and Conversion of Residues. Catal. Rev. Sci. Eng., 26(3 & 4), p. 421, 1984.
16. W. J. Rossi, B. S. Deighton and A. J. Macdonald. Get More Light Fuel from Resid. Hydrocarbon Processing, p. 105, May 1977.
17. L. Hadley-Coates and J. J. Casares Long. Residual-Oil Upgrading. An overview of available technologies. The Arabian Journal for Science and Engineering, 11, p. 3, 1985.
18. J. R. Murphy, E. L. Whittington and C. P. Chang. Review ways to upgrade resids. Hydrocarbon Processing, p. 119, September 1979.
19. D. P. Teichman, A. G. Bridge and E. M. Reed. Building to handle more resid. Hydrocarbon Processing, p. 105, May 1982.
20. D. H. Shaw and Others. Recent Developments in Oil Refining. 11th World Petroleum Congress, 4RP8, p. 345, August 1983, London.
21. M. Hus. Visbreaking Process has Strong Revival, Oil and Gas Journal, pp. 109-120, April 1981.
22. A. Rhoe and C. de Blignieres. 'Visbreaking: a Flexible process', Hydrocarbon Processing, pp. 131-135, January 1979.
23. G. L. Yespen and J. H. Jenkins. 'Visbreak by Crude Unit Revamp', Hydrocarbon Processing, pp.117-120, September 1981.
24. R. Hournac, J. Kuhn and M. Notarbartolo. 'Visbreaking: More Feed to FCC', Hydrocarbon Processing, pp. 97-102, December 1979.
25. R. De Biase and J. D. Elliott. Coking Process Reflects Trends, Innovation, Oil and Gas Journal, pp. 81-88, April 19, 1982.
26. N. P. Lieberman. Time for Coking Cycle Can be Routinely Halved, Oil and Gas Journal, p. 39-44, August 29, 1983.
27. D. P. DiElsi, D. J. Miller and N. R. Cox. A Modern Delayed Coker Pilot Plant, Energy Progress, 3, No. 4, pp. 193-196, 1983.
28. J. G. Ditman. Deasphalt to Get Feed for Lubes, Hydrocarbon Processing, pp. 110-113, May 1973.
29. A. Billon and Others. SDA Key to Upgrading Heavy Crudes, Oil and Gas Journal, pp. 43-48, January 24, 1977.
30. J. M. Pazos, L. Aquino and J. Panchano. Upgrading of High Metals Venezuelan Residua, Preprints of the American Chemical Society, 26 No. 2, pp. 456-463, 1981.

31. D. A. Viloria and Others. Solvent Deasphalt Boscan Crude, Hydrocarbon Processing, pp. 109-113, March 1977.
32. S. C. Spencer. Petroleum Coke, Report No. 72, SR1, Process Economics Program, October 1971.
33. R. A. Busch and Others. Coke Heavy Stocks, then Treat, Hydrocarbon Processing, pp. 136-142, September 1979.
34. J. B. Rush. Twenty Years of Heavy Oil Cracking, Chemical Engineering Progress, pp. 29-32, December 1981.
35. J. A. Finneran, J. R. Murphy and L. W. Schneider. Application of Heavy Oil Cracking in a Fuels Refinery, American Institute of Chemical Engineers Symposium Series, 69, No. 135, pp. 69-70, 1973.
36. A. K. Logwinuk and D. L. Caldwell. Application of ART to Heavy Oil Processing, Chemical Economy and Engineering Review, 15 No. 3, pp. 31-36, 1983.
37. D. B. Bartholic and R. P. Haseltine. New Process Cleans up FCC Feed, Oil and Gas Journal, pp. 89-92, June 1, 1981.
38. P. M. Geren. Commercialization of the Asphalt Residual Treating (ART) process, Energy Processing, pp. 48-52, July-August 1982, Canada.
39. S. J. Yanik. Latest Data on Gulf HDS Process, Hydrocarbon Processing, pp. 97-104, May 1977.
40. G. R. Ondish and A. J. Suchanek. Potential for Gulf Residual HDS in Upgrading Very Heavy Crudes, Ist International Conference on the Future of Heavy Oils and Tar Sands, paper 78, June 1979, Canada.
41. W. C. Langhout, C. Guwerkerk and K. M. A. Pronk. New Process Hydrotreats Metal-Rich Feed Stocks, Oil and Gas Journal, pp. 120-126, December 1980.
42. A. G. Bridge and Others. Chevron Isomax Processes Desulfurize Arabian Heavy Residual, American Institute of Chemical Engineers Symposium Series, 69, No. 135, pp. 102-104, 1975.
43. A. G. Bridge, G. D. Gould and J. F. Berkman. Residua Processes Proven, Oil and Gas Journal, pp. 85-98, January 19, 1981.
44. M. A. Christ, G. N. Shah, and L. G. Sherman. Broad Range of Resids Upgraded, Oil and Gas Journal, pp. 95-102, May 28, 1979.
45. F. Stolfa, R. H. Jensen and C. W. Selvidge. Low Sulfur Residual Fuels by RCD Isomax, American Institute of Chemical Engineers Symposium series, 69, No. 135, pp. 105-106, 1973.

46. J. G. Sikonia and Others. Hydrocracking's Role in Resid. Schemes, Oil and Gas Journal, pp. 126-135, November 2, 1981.

47. M. Skripek. Upgrading Heavy California Crudes to Low-Sulphur Syncrude by the Unicracking/HDS Process, Ist International Conference on the Future of Heavy Oils and Tar Sands, paper 79, June 1979, Canada.

48. J. R. Murphy and S. A. Treese. HDS + HOC = High Resid Conversion, Oil and Gas Journal, pp. 135-142, June 25, 1979.

49. A. Billion and Others. More Ways to Use Hydrocracking. Hydrocarbon Processing, pp. 122-128, May 1978.

50. B. M. Moyse. Chemical Economy and Engineering Review, 14, pp. 10-16, 1982.

51. R. M. Eccles. H-Oil, a Flexible Process for Maximum Distillate Yield from Vacuum Residues, Erdol and Kohle-Erdgas - Petrochemie, 34, No. 6, pp. 256-258, 1981.

52. R. M. Eccles, A. M. Gray and W. B. Livingston. New Resid Conversion Scheme Set for Louisiana Refinery, Oil and Gas Journal, pp. 121-129, April 1982.

53. M. S. Rakow and M. Calderon. The Dynacracking Process-an Update, Chemical Engineering Progress, pp. 31-36, February 1981.

54. J. Sosnowski, D. W. Turner and J. Eng. Upgrading Heavy Crude to Clean Liquid Products, Chemical Engineering Progress, pp. 51-55, February 1981.

55. R. P. Van Driesen and L. L. Fornoff. Bottom of the Barnol Upgrading Economics, Energy Progress, 2, pp. 47-52, 1982.

56. J. G. Sikonia and C. L. Hemler. The Aurabon Process: New Way to Upgrade Tars and Heavy Crudes, Energy Processing, pp. 16-20, July-August 1980, Canada.

57. J. G. Sikonia and C. L. Hemler. The Aurabon Process: New Way to Upgrade Tars and Heavy Crudes: Product Processing, Ist International Conference on the Future of Heavy Oils and Tar Sands, Paper 72, June 1979, Canada.

58. D. J. Patmore, C. P. Khulbe and K. Belinko. Residuum and Heavy Oil Upgrading with the CANMET Hydrocracking Process, Preprints of the American Chemical Society, 26, No. 2, pp. 431-439, 1981.

59. A. E. Silva, H. K. Rohrig and A. R. Dufresne. CANMET Process Going in to Montreal Refinery, Oil and Gas Journal, pp. 81-88, March 26, 1984.

60. R. Bearden and C. L. Aldridge. Novel Catalyst and Process to Upgrade Heavy Oils, Energy Progress, 1, pp. 44-48, 1981.

61. A. M. Edelman, and C. R. Lipuma. Developments in Thermal and Catalytic Cracking Processes for Heavy Feeds. 10th World Petroleum Congress, 4, p. 167, 1979.

62. A. Rohe and C. de. Blignieres. Visbreaker Design Considers Trade-off Between Gasoline Yield and Residue Stability Among Variables Considered: Conversion, Rate of Reaction and Type of Quench, Hydrocarbon Processing, p. 131, January 1979.

63. W. F. Bland, R. L. Davidson. Petroleum Processing Hand Book, McGraw Hill, 1967, U.S.A.

64. B. C. Gates, J. R. Katzer and G. C. A. Schuit. Chemistry of Catalytic Processes, McGraw Hill, Ch. 4, 1979, New York.

65. T. Ohtsuka. Catalyst for Hydrodesulfurization of Petroleum Residua, Catal. Rev. Sci., Eng., 16, p. 291, 1977.

66. J. J. Elliot and M. T. Melchior. KIRK - Othmer Encyclopedia of Chem. Tech. 3rd Ed.; vol. 17, John Willey and Sons, p. 119, 1982, New York.

67. B. C. Gates, J. R. Katzer and G. C. A. Schuit. "Chemistry of Catalytic Processes", McGraw Hill, Ch. 5, 1979, New York.

68. O. Weisser and S. Landa. "Sulphide Catalysts, Their Properties and Applications", Pergamon Press, 1963, Oxford.

69. McColla. Applied Industrial Catalysis, Vol. 1, p. 70, 1983.

70. J. C. Vlugter and P. Van T. Spijiker. Catalysts for Hydrocracking of Distillates and Residuums, 8th World Petroleum Congress, vol. 4, Applied Science Publisher, p. 159, 1971, London.

71. T. Ohtsuka, Y. Hasegawa and N. Takanari. Bull. Jpn. Pet. Inst., 10, 14, 1968.

72. F. E. Massoth. Characterization of Molybdena Catalyst. Adv. Catal., 27, p. 265, 1978.

73. B. Delmon. In Proceedings of the Climax Third International Conference on Chemistry and Uses of Molybdenum (H. F. Barry and P. C. H. Mitchell, eds.), Climax Molybdenum Co., Ann Arbor, p. 73, 1979, Michigan.

74. P. Ratnasamy and S. Sivasanker. Structural Chemistry of Co-Mo-Alumina Catalysts. Catal. Rev. Sci. Eng. 22, p. 401, 1980.

75. H. Topsoe. In Surface Properties and Catalysis by Non-metals. Reidel, Dordrecht, p. 326, 1983.

76. W. K. Hall. In Proceedings of the Climax Fourth International Conference on Chemistry and Uses of Molybdenum (H. F. Barry and P. C. H. Mitchell, eds.), Climax Molybdenum Co., Ann Arbor, p. 224, 1982, Michigan.

77. G. C. A. Schuit and B. C. Gates. Chemistry and Engineering of Catalytic Hydrodesulfurization. AICHEJ, 19, p. 417, 1973.

78. R. Mone. "Preparation of Catlysts I (B. Delmon, P. A. Jacobs and G. Poncelet, Eds), Elsevier, p. 381, 1976, Amsterdam.

79. P. Grange. Catalytic Hydrodesulfurization. Catal. Rev. Sci. Eng., 21, p. 135, 1980.

80. B. Delmon, P. Grange, P. Gajardo and F. Delannay. C. R. Hebd. Seances Acad. Sci., Ser. C, 288, p. 391, 1979.

81. N. P. Martinez, P. C. H. Mitchell and P. Chiplunker. In Proceedings Climax Second International Conference on the Chemistry and Uses of Molybdenum, (P. C. H. Mitchell, Ed), p. 164, 1977, London.

82. G. Delvaus, P. Grange and B. Delmon. X-ray Photoelectron Spectroscopic Study of Unsupported Cobalt-Molybdenum Sulfide Catalysts. J. Catal. 56, p. 99, 1979.

83. P. Canesson, B. Delmon, G. Delvus, P. Grange and J. M. Zabala. The Origin of Synergy Between $MoS_2$ and $CO_9S_8$ in Hydrotreating Catalysts. In Proceedings of the 6th International congress on Catalysis (G. C. Bond, P. B. Wells and F. C. Tompkins, Eds), Chemical Society, p. 927, 1977, London.

84. De Beer, V. G. H. J. and G. C. A. Schuit. The $CoO-MoO_3$-y-$Al_2O_3$-Catalyst, Influence of the Support, A. Review. In "Preparation of Catalysts" (B. Delmon, P. A. Jacobs and G. Poncelet, Eds), Elsevier, p. 343, 1976, Amsterdam.

85. A. L. Farragher and P. Cossee. Catalytic Chemistry of Molybdenum and Tungsten Sulfides and Related Ternary Compounds. In Proceedings of the 5th International Congress on Catalysis (J. W. Hightower, ed.), p. 1301, 1972, Amsterdam.

86. Hagenbach, G. Ph. Courty and B. Delmon. J. Catal., 31, p. 264, 1973.

87. F. E. Massoth and G. Muralidhar. In Proceedings of the Climax Fourth International Conference on Chemistry and Uses of Molybdenum (H. F. Barry and P. C. H. Mitchell, eds.), Climax Molybdenum Co., Ann ARbor, p. 343, 1982, Michigan.

88. Y. Okatmoto, T. Imanaka and S. Teranishi. Comments on "Stabilization Effect of Co for Mo Phase in Co-Mo-/$Al_2O_3$ Hydrodesulfurization Catalysts Studied with X-ray Photoelectron Spectroscopy". J. Catal., 54, p. 452, 1978.

89. F. Massoth. Comments on the State of Dispersion of Molybdena on Sulfided Co-Mo-$Al_2O_3$ Catalysts. J. Catal., 50, p. 190, 1977.

90. H. Topsoe and B. S. Clausen. Importance of Co-Mo-S Type Structure in Hydrodesulfurization. Catal. Rev. Sci. Eng., 26, p. 395, 1984.

91. H. Topsoe and B. S. Clausen. Active Sites and Support Effects in Hydrodesulfurization Catalysts. Applied Catalysis, 273, p. 25, 1986.

92. H. Topsoe, B. S. Clausen, R. Candia, C. Wivel and S. Morup. In situ Mossbauer Emission Spectroscopy Studies of Unsupported and Supported Sulfided Co-Mo Hydrodesulfurization Catalysts: Evidence for and Nature of a Co-Mo-S Phase. J. Catal., 68, p. 433, 1981.

93. O. Soensen, B. S. Clausen, R. Candia and H. Topsoe. HREM and AEM Studies of HDS Catalysts: Direct Evidence for the EDGE Location of Cobalt in Co-Mo-S. Appl. Catal., 13, p. 363, 1985.

94. P. J. Denny and M. V. Twigg. Factors Determining the Life of Industrial Heterogeneous Catalysts. Catalyst Deactivation Ed. Delmon, B. and Froment, G. F. Elsevier, Scientific Publication Co., 1980, Amesterdam.

95. S. T. Sie. Catalyst Deactivation By Poisoning and Pore Plugging in Petroleum Processing. In "Catalyst Deactivation", (B. Delmon, G. F. Froment Eds.) Elsevier Scientific Publ. Co., p. 545, 1980, Amsterdam.

96. F. M. Dautzenberg, S. E. George, C. Ouwerkerk and S. T. Sie. Symp. Advances in Catalystic Chemistry, 1982, Salt Lake City.

97. F. M. Dautzenberg et al. Catalyst Deactivation Through Pore Mouth Plugging During Residue Desulfurization. ACS Symp. Ser., 65, p. 254, 1978.

98. M. F. Oxenreiter, C. G. Frye, G. B. Hoekstra and J. M. Sroka. Paper presented at the Japanese Pet. Inst., November 30, 1972.

99. W. F. Arey, N. E. Blackwell and A. D. Reichie. Advances in Desulfurization of Residual Reactions and Asphalts. 7th World Petroleum Congress, p. 167, 1967, Mexico.

100. F. A. Audibert and P. Duhaut. Residual Reduction by Hydrotreatment. Paper presented at the 35th Midyear Meeting of the American Petroleum Institute Division of Refining, p. 992, May 13-15, 1970, Houston.

101. M. Sato, N. Takayoma, S. Kurita and S. Kwan. Nippon Kagaku Zasshi, 92, p. 834, 1971.

102. N. Todo et al. Kogyo Kagaku Zasshi, 74, p. 563, 1971.

103. M. Inoguchi et al. Bull. Jpn. Pet. Inst., 13, p. 153, 1971.

104. D. S. Thakur, M. G. Thomas. Catalyst Deactivation in Heavy Petroleum and Synthetic Crude Processing: A Review, Applied Catalysis, 15, pp. 197-225, 1985.

105. P. W. Tamm, H. F. Harnsberfer and A. G. Bridge. Effects of Feed Metals on Catalyst Aging in Hydroprocessing Residuum. Ind. Eng. Chem. Process. Des. Dev., 20, p. 262, 1981.

106. J. Wei and R. G. Wei. Metal Deposition Profiles in Hydro-Demetallation. Chem. Eng. Comm., 13, p. 251, 1982.

107. R. Agarawal and J. Wei. Hydrodemetalation of Nickel and Vanadium Porphyrins Intraparticle Diffusion. Ind. Eng. Chem. Proc. Des. Dev., 23, p. 515, 1984.

108. P. N. Hannerup and A. C. Jacobsen. A Model For the Deactivation of Residue HDS Catalysts. ACS Div. Petrol. Chem., 28, p. 576, 1983.

109. A. C. Jacobson, P. N. Hannerup, B. H. Cooper. J. Bartholdy and A. Nielsen. Paper presented at the AICHE Meeting, March 1983, Houston.

110. A. C. Jacobson, In "Surface Properties and Catalysis by Non-Metals (J. P. Bonnelle, Ed), Reidel Publishing Company, p. 305, 1983.

111. R. Galiasso et al. Deactivation of Hydrodemetallization Catalyst by Pore Plugging. Fuel, 62, p. 817, 1983.

112. J. M. Bogdanor and H. F. Rase. Characteristics of a Commercially Aged Ni-Mo/$Al_2O_3$ Hydrotreating Catalyst: Component Distribution, Coke Characteristics, and Effects of Regeneration. Ind. Eng. Chem., Prod. Ref. Dev. 25, p. 220, 1986.

113. H. Beuther and B. K. Schmid. Reaction Mechanism and Rates in Residue HDS. Proceedings 6th World Petrol. Congr., p. 297, Section III, 1963.

114. H. Beuther, O. A. Larson and A. J. Perrotta. The Mechanism of Coke Formation on Catalysts. J. Stud. Surf. Sci. Catal, 6, p. 271, 1980.
115. J. E. Wukasch and H. F. Rase. Some Characteristics of Deposits on a Commercially Aged, Gas-Oil Hydrotreating Catalyst. Ind. Eng. Chem. Prod. Res. Dev., 23, p. 558, 1982.
116. D. L. Trimm. The Formation and Removal of Coke from Nickel Catalyst. Catal. Rev. 16, p. 155, 1977.
117. J. M. Pazos, J. C. Gonzalez and A. J. Salazar. Effect of Catalyst Properties and Operating Conditions on Hydroprocessing High Metals feeds. Ind. Eng. Chem. Process. Des. Dev., 22, p. 653, 1983.
118. S. S. Shih, P. N. Angevine, R. H. Heck and S. Sawruk. Catalyst Assessment for Upgrading Short-Contact Time SRC to Low Sulfur Boiler Fuels. Preprints ACS, Div. Fuel Chem., 25, p. 152, 1980 and ACS Symp. Ser. 156, p. 175, 1981.
119. J. P. Dickie and T. F. Yen. Macrostructures of Asphaltic Fractions by Various Instrumental Methods. Anal. Chem., 39, p. 184, 1967.
120. A. M. Henke. Gulf's residual HDS process. Oil and Gas Journal, 68, p. 97, April 1970.
121. J. G. Speight. The Desulphurization of Heavy Oils and Residua, Marcel Dekker Inc., 1981, New York.
122. R. A. Flinn, H. Beuther and B. K. Schmid. Now You can Improve Residue Treating. Petrol. Refiner., Ao, p. 139, 1961.
123. B. G. Silbernagel and K. L. Riley. Heavy Feed Hydroprocessing Deactivation: The Chemistry and Impact of Vanadium Deposits. In "Catalyst Deactivation", B. Delmon and G. F. Froment (Eds.), p. 313, 1980, Elsevier, Amsterdam.
124. A. Nielsen, B. H. Cooper and A. C. Jacobson. Composite Catalyst Beds for Hydroprocessing of Heavy Residua. Preprints, ACS, Div. Petrol. Chem., 26, p. 440, 1981, Denmark.
125. K. E. Hastings, L. C. James and W. R. Mounce. Demetallization Cuts Desulfurization Costs, Oil and Gas Journal, 73, p. 122. June 1975.
126. E. L. Moorehead et al. Heavy Oil Upgrading: An Overview of Feed Reactivities and Catalyst Selection, Ketjen Catalysts Symposium, Paper No. H-7, 1986, Amersfoort, The Netherlands.
127. I. Naka. Fundamental Aspects of Desulfurization-Demetallization Reactions and Catalyst Deactivation Residuum Hydroprocessing, Ketjen Catalysts Symposium, Paper No. H-8, 1986, The Netherlands.

128. J. C. Plumail, Y. Jacquin, G. Martino and H. Toulhoat. Effect of the Pore Size Distribution on the Activities of Alumina Supported Co-Mo Catalysts in the Hydrotreatment of Boscan Crude, Preprints, ACS, Div. Petrol. Chem., 28, p. 562, 1983.

129. G. J. Stlegel, R. F. Tischer and L. M. Polinski. Hydroprocessing of Solvent-Refined Coal: Effect of Catalyst Properties, Preprints, ACS, Div. Petrol. Chem., 28, p. 562, 1983.

130. Y. T. Shah and J. A. Paraskos. Ind. Eng. Chem. Proc. Des. Dev., 20, p. 470, 1981.

131. L. M. Polinski, G. J. Stiegel and L. Saroff. Use of Fundamental Concepts in Catalyst Aging to Increase Catalyst Utilization During Coal Liquefaction, Steam Reforming and Other Carbon-Forming Reactions, Ind. Eng. Chem. Proc. Des. Dev. 20, p. 470, 1981.

132. D. S. Mitchel, Rafael, A. G. Bridge, and J. Jaffe. Catalyst Rejuvenation with Oxalic Acid. U.S. Patent 3,791,989, 1974.

133. J. F. P. Le Page, P. Baumgartner, and D. Duhaut. Process for Regenerating Catalysts Used for Hydrotreating Hydrocarbons. British Patent 1,245,358, 1971.

134. D. R. Farrell and J. W. Ward. Method for Rejuvenating Hydroprocessing Catalysts. U.S. Patent 4,089,806, 1978.

135. H. Beuther and R. A. Flinn. Technique for Removing Metal Contaminants from Catalysts, Ind. Eng. Chem., Vol. 2, No. 1, p. 53, 1963.

136. J. O. Hernandez. On the Use of Spent Hydrodesulphurization Catalysts. Presented before the American Chemical Society, Kansas city meeting, Sept. 12-17, 1982.

137. B. G. Silbernagel; R. R. Mohan; G. H. Singhal. Regeneration of Spent Hydrodesulphurization Catalysts Employing Presulphiding Treatment and Heteropoly Acids. U.S. Patent 4,272,400, 1981.

138. R. R. Mohan, B. G. Silbernagel and G. H. Singal. Regeneration of Spent Hydrodesulphurization Catalysts with Heteropoly Acids and Hydrogen Peroxide. U.S. Patent 4,268,415, 1981.

139. W. R. Coons; G. V. Nelson; and G. C. Wray. Regeneration of Catalysts Used in Residual Oil Hydroprocessing. U.S. Patent 3,565,820, 1971.

140. A. Anderson. Removing Contaminants from Silica-Based Cracking Catalysts. U.S. Patent 3,173,882, 1977.

141. E. H. Burke; J. S. Yoo; J. A. Karch and J. Yuan Sun. Catalyst Demetallization with a Reductive $SO_2$ Wash. U.S. Patent 4,243,550, 1981.

142. P. Ganguli. Regeneration of Spent Catalysts from Coal Liquefaction and Petroleum Residua Processing Operations. 17th IECEC Proceedings, pp.825-830, 1982.

143. J. H. Everston. Hydrocarbon Research Inc. Regeneration of Metals Contaminated Hydrocarbon Process Catalyst. U.S. Patent 3,240,208, 1983.

144. IOKA, Masatada; Shimizu, Toshiharu. Regeneration of Spent Catalyst for Hydrogenation of Heavy Oil. (Chiyoda Chemical Engineering and Construction Co. Ltd), Jpn. Kokai Tokkyo Koho, 79,101,794, 1979.

145. O. F. Poezd, Lipkinol, B. A., Sutyrin, A. M. Maslova. Regeneration of a Spent Catalyst for Hydrofining of Petroleum Raw Material, U.S.S.R. 825,136, 1981.

146. P. J. Marcantonio. Leaching Metals from Spent Hydroprocessing Catalysts with Ammonium Sulfate. U. S. Patent 4,554,138, 1985.

147. A. Arteaga, J. L. G. Fierro, P. Grange and B. Delmon. Co/MO HDS Catalyst: Simulated Deactivation and Regeneration. Role of Various Regeneration Parameters. Catalyst Deactivation (B. Delmon and G. F. Froment, Eds.), p. 59, September 29 to October 1, 1987, Antwerp, Belgium.

148. A. Arteaga, J. L. G. Fierro, F. Delannay and B. Delmon. Simulated Deactivation and Regeneration of an Industrial CoMo/$\gamma$-$Al_2O_3$ Hydrodesulphurization Catalyst. Applied Catalysis, Elsevier Science Publishers B. V., 26, pp. 227-249, 1986.

149. Klusacek, Karel, Davidova. HDS Catalyst Regeneration: Coke Burning-Off by Air in a Shallow Bed. Chemical Eng. Sci. 40 (9):1717-1721, 1985.

150. O. Levenspiel. Chemical Reaction Engineering. John-Wiley & Sons, Inc., Second Edt., 1972, U.S.A.

151. G. H. Geiger and D. R. Poirier. Transport Phenomena in Metallurgy, Adison-Wesley Publishing Co., Morris Cohen Ed., 1973.

152. C. N. Satterfield. Mass Transfer in Heterogenous Catalysis. Robert E. Krieger publishing Co., 1980.

153. S. Wadsworth. Rate Processes of Extractive Metallurgy. A Division of Plenum Publishing Co., 1979, Salt Lake.

154. R. C. Weast. Hand book of Chemistry and Physics, 65th Edition, Chemical Rubber Co., 1984/1985.

155. B. F. G. Johnson. Inorganic Chemistry of the Transition Elements, Vol. 5. A specialist periodical report, The Chemical Society, 1977, London.

156. A. Stanislaus and M. Halabi. Catalyst Characterization, Hand book, Petroleum Division, Kuwait Institute for Scientific Research, 1984, Kuwait.

157. O. Weisser and S. Landa. Sulphide Catalysts, Their Properties and Applications. Pergamon Press, 1973, Oxford.